

NON-ISOTHERMAL POLYMERIZATION OF STYRENE

NON-ISOTHERMAL POLYMERIZATION OF STYRENE

by

Luis Miramontes Vidal,  
B.Sc. (Ingeniero Quimico)

A Thesis  
Submitted to the Faculty of Graduate Studies  
in Partial Fulfilment of the Requirements  
for the Degree  
Master of Engineering.

McMaster University

May 1976

DEDICATION

*A Amparo, por on apoyo, por todo lo que  
dejó atrás, y sobre todo, por su amor.*

*To Amparo, for her support, for everything  
she left behind and most of all, for her love.*

MASTER OF ENGINEERING (1977)  
(Chemical Engineering)

McMASTER UNIVERSITY  
Hamilton, Ontario.

TITLE: NON-ISOTHERMAL POLYMERIZATION OF STYRENE.

AUTHOR: LUIS MIRAMONTES VIDAL,  
B.Sc. (Ingeniero Quimico) UNAM, Mexico.

SUPERVISOR: Professor A.E. Hamielec.

NUMBER OF PAGES: x , 114.

## ABSTRACT

The non-isothermal polymerization of styrene under runaway chemically initiated reactions was studied. A system of multiple initiators was used. The experiments were performed in an insulated batch reactor. Experimental temperature and pressure profiles with respect to time were obtained and used to evaluate a mathematical model at high temperatures. Molecular weights and conversion measured by gel-permeation chromatography (GPC) provided further evidence about the adequacy of the model. The behaviour of a non-isothermal polymerization is fully discussed, including such phenomena as depropagation, gel-effect and dead-end polymerization.

## ACKNOWLEDGEMENTS

The author wishes to express his gratitude to:

Dr. A.E. Hamielec, for the marvellous opportunity to work with him and for the benefit of his experience

Professor Jorge Ludlow L. (University of Mexico), for his guidance, help, and mainly for being such a remarkable friend.

McMaster University, for the financial support provided.

Mexico's Consejo Nacional de Ciencia y Tecnologia (CONACYT), for the complementary financial support.

My fellow graduate students, M.Y. Ilahie and L.H. Garcia-Rubio, who provided friendship, discussions and help whenever needed.

Dr. Jesus Guzman, Rafael Fernandez and Lilia Miramontes, for some very special favours.

Mr. David Lowe, for his eagerness to help.

Mrs. Peggy Johnstone, for her excellent typing and kindness.

Those who bother to read this work.

## TABLE OF CONTENTS

	Page No.
Scope and Contents.	ii
Acknowledgements.	iii
List of Figures.	vi
Nomenclature.	viii
1. Introduction.	1
1.1 General Characteristics.	1
1.2 Problems with Stability During Polymerization.	4
1.3 Kinetic Studies under Non-Isothermal Conditions. Literature Survey.	9
2. Theory.	12
2.1 Free Radical Polymerization.	12
2.2 Gel Effect.	17
2.3 Dead-End Polymerization.	20
2.4 Degradation and Depropagation.	22
2.5 Thermodynamics of Polymerization.	24
2.5.1 Effect of Pressure on Rate of Polymerization.	24
2.5.2 Thermodynamics of Equilibrium Polymerization.	27
2.5.3 Thermodynamics of Polymer Solutions.	33
3. Mathematical Model Development.	37
3.1 Reaction.	37
3.2 Rate of Polymerization.	40

	Page No.
3.3 Rate of Heat Generation.	42
3.4 Gel Effect Corrections.	43
3.5 Molecular Weights and Molecular Weight Distribution.	44
4. Experimental.	46
4.1 Description of the Reactor.	46
4.2 Choice of Reactants and Conditions.	49
4.3 Experimental Techniques.	52
4.4 Analysis.	58
5. Results and Discussion.	62
5.1 Temperature.	62
5.2 Conversion.	74
5.3 Molecular Weight Development.	80
5.4 Pressure Development.	88
6. Conclusions.	96
Appendices	
A1 Physical Properties of Styrene and Polystyrene.	98
A2 Review of Pressure Relief Systems.	100
A3 Heat Transfer Coefficient for Reactor.	103
A4 Limiting Conversion as Function of Glass Transition Temperature.	108
Bibliography.	111



## LIST OF FIGURES

- Figure 1.1 Rate of heat generation versus time.
- Figure 2.1 Propagation, depropagation and equilibrium constants versus temperature.
- Figure 2.2 Conversion versus temperature. Reaction paths.
- Figure 4.1 Reactor.
- Figure 4.2 Temperature profiles. Thermocouples at points ① and ②.
- Figure 4.3 Temperature profiles for heat transfer coefficient determination.
- Figure 4.4 GPC calibration curve.
- Figure 5.1 Effect of different initiators on the temperature profile.
- Figure 5.2 Average temperature profile and its 95% confidence intervals.  $P_i = 50$  psig.
- Figure 5.3 Temperature profile for  $P_i = 0$  psig.
- Figure 5.4 Temperature profile for  $P_i = 100$  psig.
- Figure 5.5 Temperature profiles for Points ② and ④,  $P_i = 0$  psig.
- Figure 5.6 Temperature profiles for Points ① and ⑤,  $P_i = 50$  psig.
- Figure 5.7 Conversion versus time for average temperature profile at  $P_i = 50$  psig.
- Figure 5.8 Conversion versus time,  $P_i = 0$  psig.
- Figure 5.9 Conversion versus time,  $P_i = 100$  psig.
- Figure 5.10 Average number molecular weight versus conversion.
- Figure 5.11 Average weight molecular weight versus conversion.
- Figure 5.12  $k_t/k_{t_0}$  versus conversion.
- Figure 5.13 Effect of amount of initiator on the temperature profile.
- Figure 5.14 Initiator concentration versus reaction time.
- Figure 5.15 Pressure versus time,  $P_i = 0$  psig.
- Figure 5.16 Pressure versus time,  $P_i = 50$  psig.

List of Figures (Continued)

- Figure 5.17 Pressure versus time,  $P_1 = 100$  psia.
- Figure 5.18 Temperature profile, experiment 32.
- Figure 5.19 Pressure profile, experiment 32.
- Figure 5.20 Pressure as function of temperature and conversion.
- Figure A2.1 Huff's algorithm.
- Figure A2.2  $Y$  versus  $L/D$ .
- Figure A3.1 Reactor's composite walls.
- Figure A4.1 Polymerization temperature versus limiting conversion.

## NOMENCLATURE

a	activity.
AH	Diels-Alder adduct.
$A_i$	Arrhenius Frequency Factor for $i^{\text{th}}$ rate constant.
$A_s$	Area of liquid-vapor interface, $\text{cm}^2$ .
$C_p$	Heat capacity, $\text{cal/g mol } ^\circ\text{K}$ .
$D_z$	Slope of GPC calibration curve.
$E_i$	Energy of activation for $i^{\text{th}}$ rate constant, $\text{cal/g mol}$ .
f	Initiator Efficiency.
$\Delta G$	Gibbs free energy, $\text{cal/g mol}$ .
h	Dispersion factor, dimensionless
$\Delta H_p$	Heat of polymerization, $\text{cal/g mol}$ .
$\Delta H_v$	Heat of vaporization, $\text{cal/g mol}$ .
I	Initiator.
$k_d$	Initiator decomposition rate constant.
$k_{d_p}$	Depropagation rate constant.
$K_e$	Equilibrium constant.
$k_{f_m}$	Transfer to monomer rate constant.
$k_{f_{AH}}$	Transfer to Diels-Alder Adduct rate constant.
$k_i$	Thermal initiation rate constant.
$k_p$	Propagation rate constant.
$k_t$	Termination rate constant.
M	Monomer.
$\bar{M}_i$	Average Molecular Weight, number (n) or weight (w).
$M_m$	Monomer molecular weight.
$M_p$	Molecular weight at peak.

Nomenclature (Continued)

N	Avogadro number.
P	Pressure, lb/in <sup>2</sup> .
Q	Heat, removed (r) or generated (g), cal/sec lt.
R	Gas constant cal/g mol °K.
r	number of monomeric units in the polymer chains.
R <sub>IC</sub>	Rate of chemical initiation.
R <sub>IT</sub>	Rate of thermal initiation.
$\bar{r}_i$	Average chain length, number or weight.
R <sub>p</sub>	Rate of Polymerization, g mol/lt sec.
R <sub>v</sub>	Rate of evaporation.
ΔS	Entropy of polymerization, cal/g mol °K.
SK	skewing factor, dimensionless.
t	Time, seconds.
T	Temperature, °K.
T <sub>A</sub>	Maximum adiabatic temperature.
T <sub>C</sub>	Ceiling temperature.
T <sub>g</sub>	Glass transition temperature.
T <sub>gm</sub>	Glass transition temperature of the monomer.
T <sub>gs</sub>	Glass transition temperature of the solution.
T <sub>g∞</sub>	Glass transition temperature of the polymer with ∞ molecular weight.
T <sub>R</sub> =T <sub>B</sub>	Oil bath temperature
UA	Heat transfer coefficient times wetted area.
V	Volume, lt.
v <sub>i</sub>	Molar volume, lt/g mol.
w(r)	Fraction of polymer chains of length r.
x	Conversion.

## Greek letters

- $\alpha$  Difference between the volume expansion coefficient in the melt state and in the glassy state.  
 $\sim 2.94 \times 10^{-4} \text{ } ^\circ\text{K}^{-1}$  for polymers.  
 $\sim 1 \times 10^{-3} \text{ } ^\circ\text{K}^{-1}$  for all small molecules
- $\beta$  Dimensionless parameter.
- $\sigma$  Solubility parameter ( $\text{cal/cm}^3$ )<sup>1/2</sup>
- $\epsilon$  Volume contraction, dimensionless.
- $\theta$  Contribution of the chain end to the free volume  $\sim 80 \text{ } \text{Å}^3$
- $\mu$  Chemical potential.
- $\rho$  Density g/lt.
- $\tau$  Dimensionless parameter.
- $\phi$  Volume fraction, dimensionless.
- $\chi$  Interaction parameter, dimensionless.

## 1. INTRODUCTION

### 1.1 General characteristics

Commercial polymerizations of styrene were started in the 1930's by Dow and BASF. Styrene-based polymers contributed about 15% of the total polymers produced in the World. Production of polystyrene is only smaller than that for polyethylene and poly(vinyl-chloride). Most of the polystyrene homopolymers, which are about 62% of all styrene polymers, are produced in bulk, mainly in batch reactors. Since 1968 the number of processes in active use were as follows:

TABLE 1.1 Number of Processes in Use for Styrene Polymerization

<u>process type</u>	<u>Batch</u>	<u>CSTR</u>	<u>Tubular</u>
Bulk	57	28	7
Suspension	5	3	1
Emulsion	12	2	0

Modern plants are huge<sup>(1)</sup>, producing over 450,000 ton/year; using reactors with volumes as large as 50,000 gal<sup>(2)</sup>, with individual unit capacities up to  $10^5$  ton/year. It is estimated that plants producing less than 200,000 ton/year will become obsolete in the near future. Costs have been decreasing from 37¢/kg in 1955, to 15¢ in 1974. The present higher prices are due to the step change in the price of crude oil. Styrene polymers are relatively cheap, hard, rigid, transparent, with brilliance, mold very easily, have good electric properties, are

easy to color, are inert to many chemicals. Brittleness and low softening temperature, along with some weatherability and ultra-violet sensitivity problems limit their uses.

Commercial polymerizations are conducted mostly by free radical mechanism, either with chemical or thermal initiation or both; anionic and cationic polymerizations are very limited in industrial production. Those polymerizations are usually made above  $T_g$ , the glass transition temperature and therefore complete conversion can be obtained. The styrene homopolymers find their applications below  $T_g$ , which means they are in a glassy state.

Molecular weights of commercial interest are in the range 40,000 to 180,000 for the number average molecular weight  $\bar{M}_n$  and 100,000 to 400,000 for the weight average molecular weight  $\bar{M}_w$ , but polymers with  $\bar{M}_n$  as low as 10,000 are widely used as waxes. It has been shown elsewhere<sup>(3)</sup> that it is possible to obtain any desired combination and values of molecular weights by manipulating several variables: temperature (and temperature programming)<sup>(4,5)</sup>, time of reaction<sup>(6)</sup>, amount of initiator and combinations of initiators with different half-lives<sup>(7)</sup>. To get complete conversion it is usual to use temperatures as high as 280°C; these are the usual temperatures in extruders. This step involves a devolatilization.

Although the viscosities are very high, around  $10^6$  cp, as it is a non-Newtonian shear thinning fluid, the reaction mixture can be handled using specially designed equipment, and sometimes the rate of heat

transfer can overcome the rate of heat generation by using higher temperatures. Methods of fabrication are reviewed elsewhere<sup>(1,8,9,10,11)</sup> and the readers are encouraged to read these publications to obtain a broader perspective. It must be stressed that the most critical variable in styrene polymerization is the temperature. An adequate control of temperature is imperative, otherwise hot spots, runaways and pressure buildup can occur.



## 1.2 Problems with Stability During Polymerization

The main problem during a batch, bulk polymerization is the control of temperature. This problem arises from the poor mixing when conversion is high and the medium very viscous. Temperature can vary appreciably with respect to space (hot spots) or with respect to time (peaking and runaways). Temperature variations affect the molecular weights and the molecular weight distribution (MWD), through the accompanying increase in rate of polymerization ( $R_p$ ). The usual effect is a broadening of the molecular weight distribution, but other inhomogeneities can occur. At the end, we must remember that the physical properties of the final product are going to be determined by the polymerization history. In general, the physical properties are related to the molecular weight as:

$$\text{physical property} = A - \frac{B}{\bar{M}_i} ; B > 0 \quad (1)$$

where  $\bar{M}_i$  is the average molecular weight, either number or weight. Some properties are better related to one of the molecular weights. A and B are constants, specific to a property.

Usually in batch, bulk polymerizations, the polymer-monomer mixture is discharged from the reactor when conversion is between 30-60% and the final product is obtained either by a semi-adiabatic polymerization in "ad-hoc" reactors or by removal of the residual monomer either by flashing it or in an extruder reactor.

In the event of power failure, i.e. loss of temperature control if the conversion is low, two methods are widely used: a) quenching the reaction by addition of a chain stopper, and b) venting.

Several papers have been published in the area of vent relief systems<sup>(12,13,14,15,54)</sup>. However, there is a gap between the theory and the criteria used for the design of pressure relief systems. This is due to the fact that kinetics of polymerization at high temperatures and conversions are poorly understood. Venting the polymerization medium usually means losing the charge. If the conversion is high, the runaway reaction could be contained within the reactor. In general, the most pessimistic event would occur when the reaction runs away near zero conversion and the full vapor pressure of monomer is exerted on the reactor walls.

A runaway reaction is one which causes the temperature profile  $T(t)$  of the reaction, to exhibit two characteristics<sup>(16)</sup>:

$$\frac{dT}{dt} \gg 0 \quad (2a)$$

$$\frac{d^2T}{dt^2} > 0 \quad (2b)$$

The first expresses the very fast temperature rise in a very short period of time (for example, more than 1.5°C/sec; while the second one gives the characteristic upward concavity associated with runaway reactions.

Biesenberger and coworkers<sup>(16,17,18,19)</sup> recently discussed the behaviour of polymerizations under thermal ignition phenomena. Thermal ignition is defined as the phenomenon that satisfies equations (2a) and

(2b) and has an extreme sensitivity to variations in the system parameters. It is characterized by the sharp transition from isothermal to runaway behaviour. It is better known in Chemical Reaction Engineering as parametric sensitivity or instability.

These studies used several simplifications that are questionable, i.e. neglecting gel-effect, thermal initiation, chain transfer to monomer and depropagation or degradation reactions. Biesenberger, Capinpin and Sebastian<sup>(16)</sup> pointed out that it is impossible to conduct isothermal polymerizations in constant temperature baths if the temperature of the cooling medium ( $T_R$ ) is controlled rather than the reaction temperature. This agrees with some results reported by Balke<sup>(20)</sup>.

Sebastian and Biesenberger<sup>(19)</sup> in their study of the effects of initiator mischarge and control malfunctions on the behaviour of a batch reactor provided qualitative ways of understanding the boundaries of stability for abnormal situations in reactors.

It should be noted that in a real reactor, even under the worst possible conditions, a polymerization will never proceed in a pure adiabatic manner. There will be only peaking in temperature to some extent, it can be moderate or extreme. We should remember that some of the heat released will go to monomer evaporation and at higher temperatures to polymer degradation; these two phenomena will be discussed later. In addition, even if the coolant fluid is not circulating there will be heat losses through the reactor walls all the time. Another effect frequently overlooked is that, at high conversions as the rate of polymeri-

zation decreases very fast, so does the rate of heat generation. Figure 1.1 shows the latter effect.

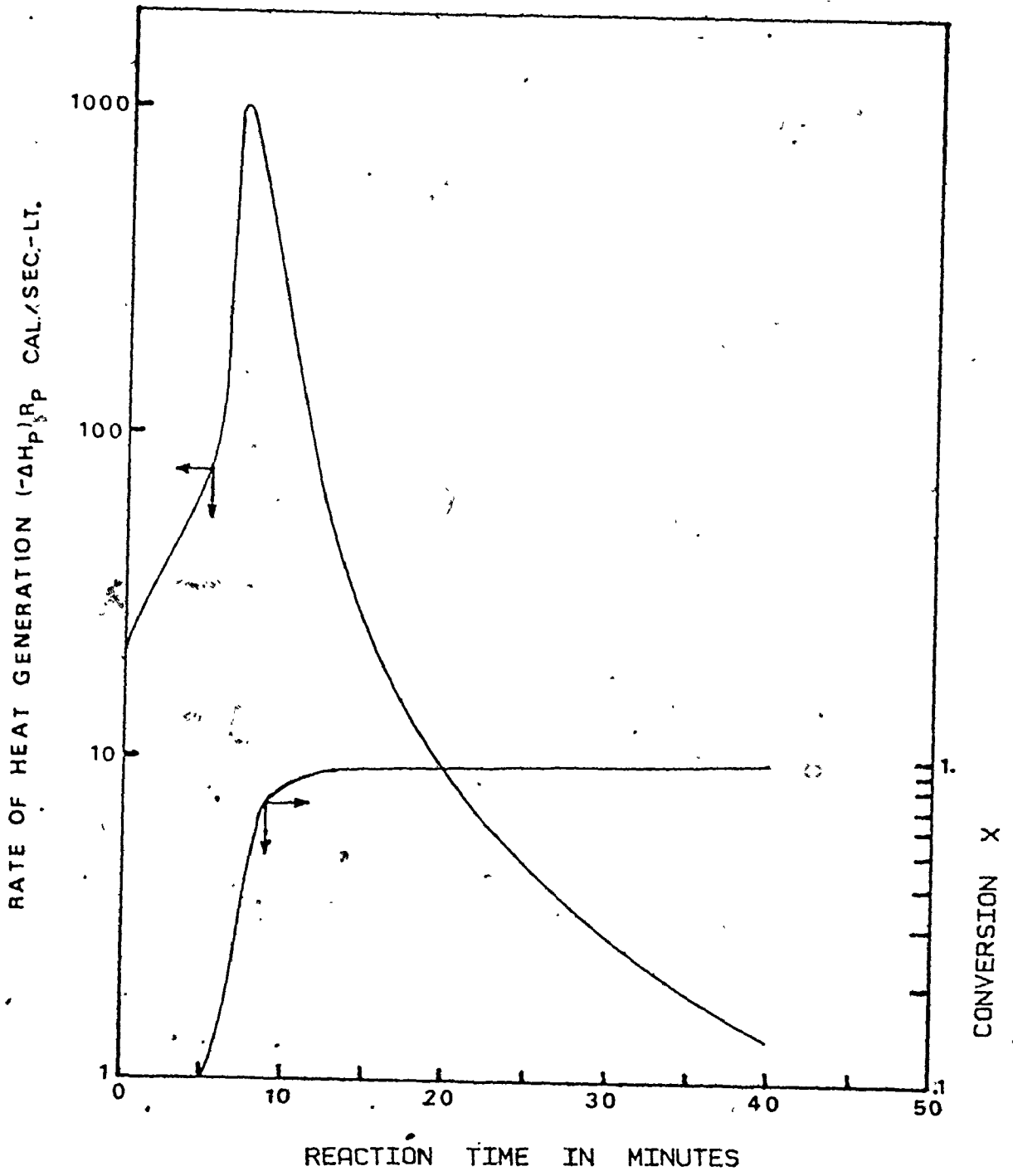


Figure 1.1 : Rate of heat generation versus time.

### 1.3 Kinetic Studies under Non-isothermal Conditions - Literature Survey.

Most of the kinetic data published in the literature were obtained with isothermal measurements. The kinetic rate constants are thus determined at different temperature levels to obtain an Arrhenius equation. This expression would permit the evaluation of the corresponding rate constants at any temperature for isothermal or non-isothermal polymerizations. The use of these constants is restricted to the temperature interval within which the isothermal determinations were made, with possibly some extrapolation. The following assumptions were used by Gordon<sup>(57)</sup> in his early proposal to study polymerizations in adiabatic mode:

1. The law of mass action holds.
2. The Arrhenius expressions are valid.
3. The heat released is due exclusively to the propagation reaction.
  - a) no physical or chemical changes occur with contributions to the total heat balance.
  - b) this secondary change, if any, does not affect the kinetics of reaction.
4. The heat of reaction is independent of temperature.
5. The heat capacity of the system is independent, both of temperature and composition. The heat capacities of monomer and polymer are within the same range.
6. The system is closely enough adiabatic.

There are serious limitations to these assumptions:

- a) Assumption 2 cannot be verified separately, its validity has to be assumed.
- b) Under different experimental conditions, assumption 3 might not be valid. This point will be discussed extensively in Chapter 6.
- c) Assumptions 4 and 5 are definitely invalid. Although the heat capacity and the heat of polymerization both vary in a slight form, the so-called thermal character  $((-\Delta H_p)/C_p)$  varies in a more dramatic form. Table 1.2 shows several values for these three physical properties.

TABLE 1.2 Dependence of Heat of Polymerization and Heat Capacity with respect to Temperature.

Temperature (°C)	$(-\Delta H_p)$ (cal/g mol)	$C_p$ (Cal/g mol°K)	thermal character (°K)
0	16200	41.15	394
100	17380	46.15	377
200	17960	51.15	351
300	18060	56.15	322

- d) The notion of an adiabatic system is an idealization, since even the best insulating materials have a non-zero thermal conductivity. Hence, assumption 6 does not hold, but in some large reactors it could be a good approximation<sup>(12)</sup>.

In this study, some of the above assumptions will be used as they stand and the deviations from the rest will be accounted for, either by theory or by an empirical correction. Although Gordon<sup>(57)</sup> proposed the

use of adiabatic polymerizations a long time ago; very few papers have been published on this topic. See, for example, Tonoyan et al<sup>(55)</sup> and Biesenberger et al<sup>(16,17,18,19,50)</sup>. The principal aim of this study is to provide information about the polymerization kinetics at high temperatures. A model which predicts both the conversion history and the molecular weight development during a non-isothermal polymerization will be evaluated.



## 2. THEORY

### 2.1 Free Radical Polymerization

The polymerization of styrene has attracted a great deal of attention from researchers. In fact, there is more information available on polystyrene than on any other polymer. Extensive reviews have been published<sup>(9,21)</sup>. A review of the basic theory of free radical polymerization will be presented here.

#### 2.1.1 Free Radical Reactions

Free radical polymerization consists of three basic reactions:

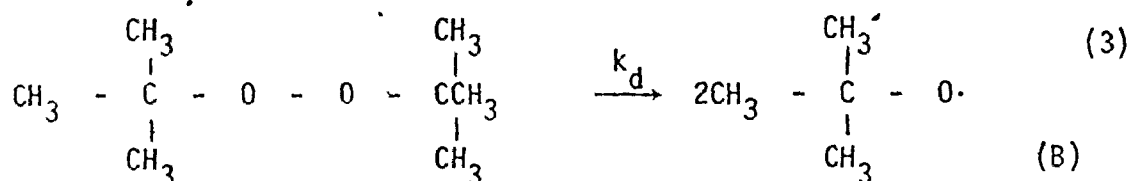
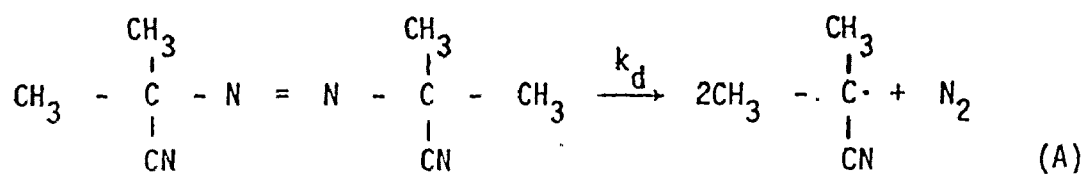
I. Initiation, II. Propagation, and III. Termination. The kinetic scheme is very complicated and several assumptions are made:

1. The reactivity of free radicals is independent of their chain length. For example, a single rate constant for the propagation reactions will characterize all the steps at all times.
2. The average chain length is large.
3. All free radical concentrations are at steady state.

#### I. Initiation

##### a) Chemical Initiation

Consider an initiator such as AIBN or DTBP, both of which follow a first-order decomposition:



Species (A) and (B) will be symbolized as  $R_c$

The rate of decomposition is thus expressed as:

$$\frac{d[I]}{dt} = -k_d[I] \quad (4)$$

assuming an isothermal decomposition, equation (4) can be integrated to:

$$[I] = [I]_0 \exp(-k_d t) \quad (5)$$

where  $[I]_0$  is the initial concentration of initiator and  $k_d$  is its first order decomposition constant. As a polymerization proceeds, the accompanying volume decrease causes an actual increment in the initiator concentration; equation (5) then will become:

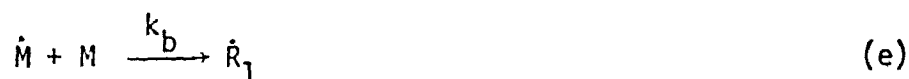
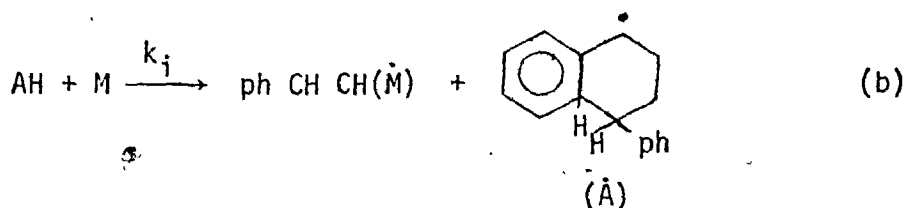
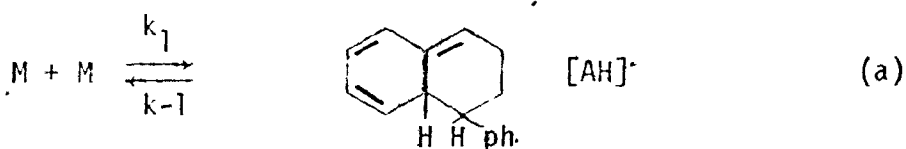
$$[I] = [I]_0 \frac{\exp(-k_d t)}{(1 + \epsilon x)} \quad (6)$$

#### b) Thermal Initiation

Styrene is one of the few monomers able to undergo thermal initiation. Since the mechanism involves free radicals, styrene must react with itself to produce free radicals. Thermal polymerizations of styrene have

been extensively studied by Hui<sup>(22)</sup> in the range (100-200°C) and by Husain<sup>(23)</sup> in the 200-230°C range. George<sup>(21)</sup> and Husain<sup>(23)</sup> have provided literature reviews on this topic.

The mechanism for thermal initiation which has most support involves monoradicals<sup>(72)</sup>.



where: M = monomer

$\dot{R}_1$  = free radical with one monomer unit

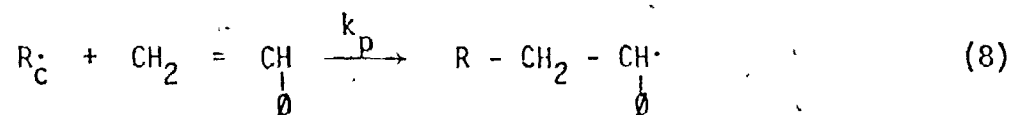
AH = Diels Alder adduct.

In addition to polymer, acyclic and cyclic oligomers are found.

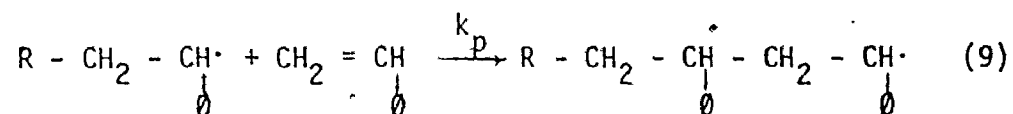
Thermal and chemical initiation effects are additive, as it was shown by Seha and Suab<sup>(26)</sup>.

## II. Propagation

The radical  $R\cdot$  react readily with monomer.

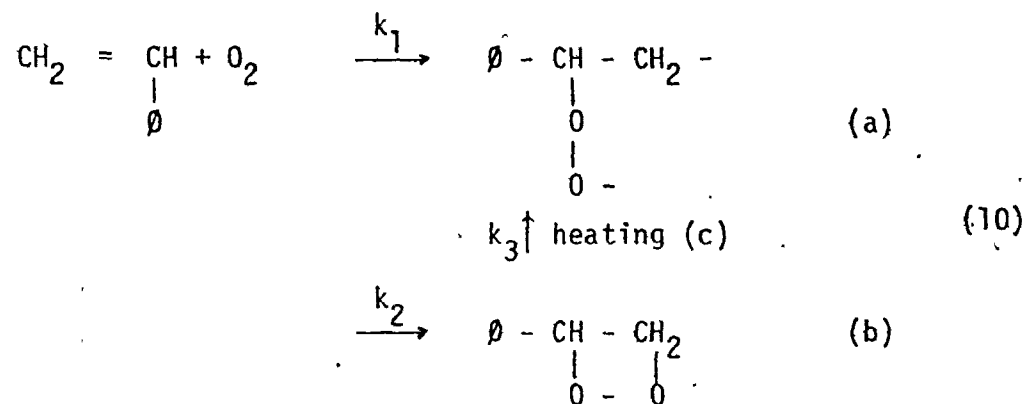


The radical has been transferred and once this condition is set, the system could go on with unlimited repetition, this is the propagation step:



and so on.

Studies were made by Staudinger and coworkers (24,25) and they concluded that the most favored mechanism of propagation would lead to a head-to-tail structure. Although the presence of oxygen during the polymerization would lead to a less stable polymer, the following reactions have to be mentioned:



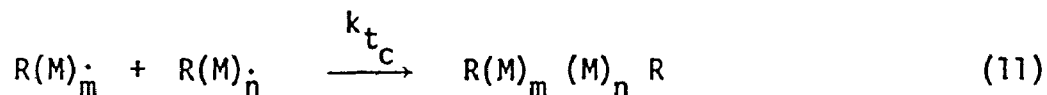
reaction (10a) will be favored at temperatures higher than 150°C; while reaction (10b) will take place at temperatures lower than 150°C. Reaction

(10a) is a propagation step. That path (10c) is possible has been shown by Husain<sup>(23)</sup>. However, the reactions (10a - 10c) will not be considered in the present kinetic treatment, as far as the production of stable small molecule byproducts could not be measured quantitatively.

### III. Termination.

Termination can occur either by combination of two long chain radicals or by disproportionation, in which hydrogen transfer results in the formation of two molecules with one of them saturated and the other with an unsaturated end group.

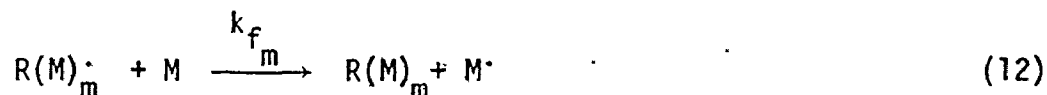
For polystyrene the main termination mechanism is by combination and only this mechanism will be considered in this study:



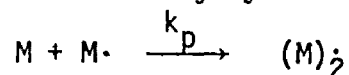
The termination rate constant will be represented from here on as

$$k_t \quad (k_t = k_{t_c})$$

Although chain transfer reactions do not affect the free radical population, they could be considered as a special termination reaction case. Transfer to monomer and to some byproduct molecules are important during styrene polymerization.



followed immediately by reaction (9).



It is emphasized that both  $k_p$  and  $k_t$  are independent of molecular weight.

## 2.2 Gel Effect

A "conventional" polymerization system is one whose rate of polymerization is first order with respect to monomer concentration and half order with respect to initiator concentration. This behavior seems to be more the exception than the rule for most vinyl polymerizations. Styrene does experience a gel-effect.

With increasing conversion, the reaction medium becomes more and more viscous. This increase in viscosity slows the diffusion of polymer chains. The termination reactions become diffusion controlled and gel effect takes place. The gel effect onset is characterized by a deviation in the rate of polymerization from the conventional behavior. This deviation is present as a rapid auto-acceleration in the rate of polymerization, followed by a faster and dramatic fall in rate as monomer is almost depleted and/or the mixture approaches the glass transition temperature<sup>(28)</sup>. There is general agreement that the reactions most affected by the increase in viscosity are the termination reactions. There are several interpretations for this phenomenon; two of the most accepted ones are reviewed elsewhere<sup>(27)</sup>, and briefly presented here.

- a. The first interpretation regards the termination between two polymeric chain radicals as a three step process:
  - i) Two chain radicals diffuse together. This stage is known as translational diffusion.
  - ii) Once these radicals are close enough, rearrangement of the

chains will occur; so that the reactive radical ends are close and properly oriented for the reaction to take place. This is known as segmental diffusion.

iii) The termination would occur.

If the termination steps were controlled by segmental diffusion, the termination rate constant would be chain length dependent, violating one of the assumptions made.

b) The concept of polymer entanglements is founded in the idea that above a certain chain length, the critical chain length, polymer molecules are long enough to become entangled among themselves.

Of course, the diffusion rate is much lower for an entangled molecule. There would then be two radical populations, the population of entangled chains and the population of unentangled chains.

A formulation based on this theory was presented by Cardenas<sup>(27)</sup>. This researcher worked out his model using as an example the polymerization of methylmethacrylate for two temperature levels and comparing his results with those reported by Balke<sup>(20)</sup>. Regardless of a fairly good fit, two of the parameters used are so highly correlated that when the writer tried them for a third temperature level, the new parameters obtained were not consistent with the previous ones. No simple dependence of the parameters with respect to temperature was observed. Therefore, the application of that model is restricted to the two temperature levels for which values of the parameters were obtained and no generalization is in sight unless further developments are available in theory.

In general, the several interpretations are complex and very often present serious mathematical complications. An empirical approximation will be discussed later in Section 3.4.

The severity of gel effect decreases with temperature<sup>(23)</sup>.



### 2.3 Dead End Polymerization

Dead end polymerization is a term to indicate an initiator-limited polymerization. This term was first proposed by Tobolsky<sup>(29)</sup> when studying the polymerization of styrene at moderate temperatures and using a variety of initiators. However, Tobolsky and coworkers<sup>(29,30)</sup> neglected the occurrence of gel-effect, thermal initiation and, most important, their polymerizations were done below the glass transition temperature for polystyrene. It is then not surprising that they confounded the effects. As shown experimentally by Hui<sup>(22)</sup> and theoretically by Dainton and Ivin<sup>(31)</sup>, even at 100°C the reaction will go to completion, given enough time. Tobolsky et al<sup>(30)</sup> were able to get an analytical solution of the rate expression, by neglecting the gel-effect and thermal polymerization. They took the volume shrinkage into account. They proposed this scheme as a tool to predict the efficiency ( $f$ ) and kinetic data ( $k_d$ ) for a given initiator if the limit conversion and the ratio  $k_p/k_t^{1/2}$  is known for a certain monomer. O'Driscoll and White<sup>(32)</sup> showed that if thermal polymerization is accounted, the scheme of Tobolsky cannot be used; but failed to account for the occurrence of gel-effect phenomena.

Tadmor and Biesenberger<sup>(33)</sup> attempted to obtain a general expression. They arrived at an expression in which dead end polymerization and thermal polymerization are mutually exclusive.

More recently, Biesenberger and coworkers<sup>(17,19)</sup> have suggested that in a runaway reaction, dead end polymerization always takes place. A complete discussion will be made in Chapter 5.

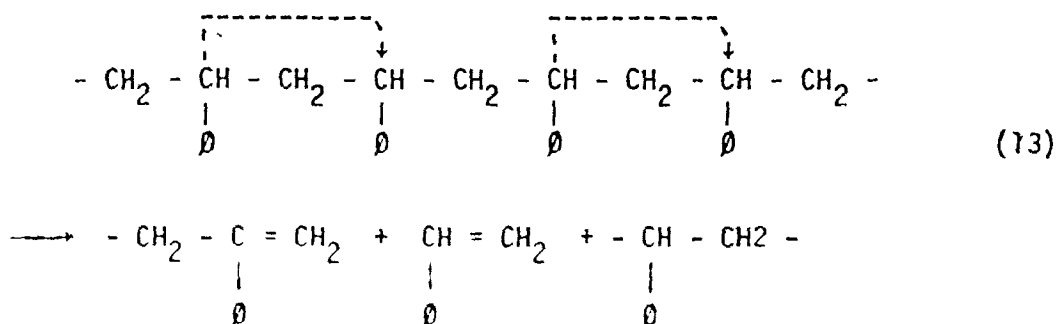
#### 2.4 Degradation and Depropagation

Polystyrene molecules can be broken down or degraded to smaller molecules by various means. They can be broken at random into fragments of different sizes and eventually could go to regeneration of monomer. In fact polystyrene is one of the few polymers that yield a significant amount of monomer when degraded. Another mechanism involves the release of monomeric units from a polymeric chain end. Extensive research has been done in this area and the reader is referred to the excellent books of Mardosky<sup>(34)</sup>, Jellinek<sup>(35)</sup> and Reich and Stivala<sup>(36)</sup>.

Staudinger and coworkers<sup>(24,25)</sup> during their studies of polystyrene degradation found the degradation products to be mainly monomer, dimer and trimer, with the amount of monomer being by far the greatest. When the degradation is conducted at atmospheric pressure or higher, the amount of monomer released is around 65%. They found a great variety of dimers and trimers, unsaturated and saturated. There is general agreement that the degradation of polystyrene takes place in two stages:

- a. An initial sudden drop in molecular weight, due to a random scission reaction, at the beginning. This chain breaking process is responsible for a substantial decrease in molecular weight.
- b. A gradual decrease in molecular weight, due to unzipping of monomer units from the end of the polymeric chain. This reaction would occur simultaneously and after stage (a).

Staudinger<sup>(25)</sup> proposed a chain depropagation reaction mechanism as follows:



There are similar reactions for the formation of dimers, trimers, etc.

The same reaction can be represented as<sup>(31)</sup>:



The mathematical treatment is very complex<sup>(35)</sup> and no adequate data is available. In this study only the unzipping or depropagation reaction will be considered, as represented by equation (14).

In addition, the random degradation process is chain length dependent and as such it would invalidate the assumption that the kinetic rate constants are chain length independent.

## 2.5 Thermodynamics of Polymerization

For a polymerization to occur, two conditions must be satisfied: i) that under the polymerization conditions, the free energy would decrease. The extent to which the polymerization will proceed is a function of the magnitude of the decrease; and (ii) that a mechanism is available. A great deal of research has been done on the second condition. A review of some thermodynamic aspects of polymerization reactions will be presented here.

It is interesting to indicate at this stage, that polymerization is a chemical aggregation process. A similar situation exists for physical aggregation processes, i.e. crystallization. Solid, liquid and freezing point are analogues of polymer, monomer and ceiling temperature. This analogy has permitted the thermodynamic analysis of polymerization to be done in a simple manner.

### 2.5.1 Effect of pressure on polymerization reactions.

There is a significant shrinkage, i.e. reduction of volume during polymerization, due to the fact that polymers have higher densities than the monomers from which they are produced. Of course, this suggests the use of pressure during polymerization. There are several papers on this topic. See, for example, the literature cited by Weale<sup>(37)</sup>.

The rate constants for free radical reactions: 3, 7, 9, 11 and 12 vary, according to Evans and Polanyi<sup>(38)</sup> as:

$$\frac{\partial(\ln k)}{\partial P} = - \frac{\Delta V^*}{RT} \quad (15)$$

where  $k$  is any rate constant and  $\Delta V^*$  is the volume change that occurs when a transition state is formed from the reacting molecules.  $\Delta V^*$  for  $k_d$  is likely to be positive, whereas it will be negative for  $k_p$  and  $k_t$ . But, as  $k_t$  becomes diffusion controlled and diffusion is retarded under pressure, due to increased viscosity of the medium, the net effect on  $k_t$  will be balanced. It is widely accepted that the increment in rate of polymerization is due mainly to the acceleration of the propagation reaction. For styrene, the value of  $\Delta V^*$  for  $k_p$  is  $-13.4 \text{ cm}^3/\text{mol}$ . Therefore equation(15) becomes:

$$\ln\left(\frac{k_p}{k_{p_0}}\right) = \int_{P_0}^P \frac{-\Delta V^*}{RT} dP \quad (16)$$

where  $k_{p_0}$  is the propagation rate constant at pressure equal to one atmosphere and  $k_p$  is the propagation rate constant at any pressure. After integration of equation (16) the actual increase of  $k_p$  for the extreme conditions found in the experimentation ( $305^\circ\text{C}$  and  $130 \text{ psig}$ ) was found to be less than 0.19%.

A maximum increment of 0.19% in the rate of polymerization under the conditions described, can be easily neglected.

There is some controversy about the effect of pressure on the molecular weights. While Zhanov et al<sup>(40)</sup> suggest that there is no variation, Norrish and coworkers<sup>(41,42)</sup> indicated an increase in the polymer molecular weights. In Section 3.5 the expressions for molecular

weights are presented. However, a brief analysis can be made at this point.

As  $k_p$  increases, so does the rate of polymerization  $R_p$ ; bearing in mind that  $\Delta V^*$  for the transfer to monomer reaction is negative ( $\Delta V^* = -11$ ),  $k_{f_m}$  will increase with pressure. Therefore, as  $k_p$  also increases, the parameter  $\tau$  will decrease a small amount. The parameter  $\beta$  will also decrease. Decrements in  $\tau$  and  $\beta$  will lead to actual increases in  $\bar{M}_n$  and  $\bar{M}_w$ , the molecular weights. So, an increase in molecular weights is to be expected with respect to pressure. This increase would be very slight under the pressure conditions at which the present study was conducted and no attempt to account for it was made.

### 2.5.2 Thermodynamics of Equilibrium Polymerization

The corresponding rates for equations (9) and (14) are:

$$k_p [M] [R\cdot] \quad (17)$$

and  $k_{d_p} [R\cdot] \quad (18)$

And the rate of polymerization can be expressed as:

$$R_p = k_p [M] [R\cdot] - k_{d_p} [R\cdot] \quad (a)$$

$$= (k_p [M] - k_{d_p}) [R\cdot] \quad (b) \quad (19)$$

where  $k_p$  and  $k_{d_p}$  vary with temperature as expressed by Arrhenius expressions:

$$k_p = A_p \exp(-E_p/RT) \quad (a)$$

$$k_{d_p} = A_{d_p} \exp(-E_{d_p}/RT) \quad (b) \quad (20)$$

and  $E_p - E_{d_p} = \Delta H_p \quad (21)$

$\Delta H_p$  is the enthalpy change for the overall reaction and it is a large quantity, as  $E_{d_p}$  is several times larger than  $E_p$ . Then,  $k_{d_p}$  will be negligible when compared with  $k_p[M]$  at low temperatures, but it will grow very fast with increasing temperatures.

There will be a temperature for which the rate  $R_p = 0$ , this temperature is called the ceiling temperature  $T_c$ . At this temperature:

$$k_p[M] = k_{d_p} \quad (22)$$



and hence 
$$K_e = \frac{k_p}{k_{dp}} \quad (23)$$

so that 
$$[M]_e = K_e^{-1} \quad (24)$$

where  $[M]_e$  is the equilibrium monomer concentration at the ceiling temperature in (g mol/lit)

Therefore: 
$$\Delta G^0 = \Delta H_p^0 - T\Delta S^0 = -RT \ln K_e \quad (a)$$

$$\Delta G^0 = RT \ln [M]_e = \Delta H_p^0 - T_c \Delta S^0 \quad (b) \quad (25)$$

and 
$$T_c = \frac{\Delta H_p^0}{\Delta S^0 + R \ln [M]_e} \quad (26)$$

The ceiling temperature  $T_c$  has been defined as the temperature at which the Gibbs free energy of propagation changes from a negative value to a positive one, passing by zero. This scheme is reported by Joshi and Zwolinski<sup>(43)</sup> and by Reich and Stivala<sup>(36)</sup>.

Although the criterion of the ceiling temperature provides the thermodynamic condition for a limit conversion to exist, there is experimental evidence that under certain conditions, no complete conversion can be reached. Horie et al<sup>(28)</sup>, based on the Free Volume Theory, established that a diffusion-controlled reaction will stop, due to transition of the system, at the glass transition temperature of the mixture, from a viscous liquid to a glassy state. A brief outline of this theory and a graph supporting it are presented in Appendix A4.

$\Delta S^0$  is the entropy change for  $[M]_e = 1 \text{ mol liter}^{-1}$  and can be calculated as:

$$\Delta S^0 = R \ln \left( \frac{A_p}{A_{d_p}} \right) \quad (27)$$

or as:

$$\Delta S^0 = \Delta S^0_{\text{monomer}} - \Delta S^0_{\text{polymer}} \quad (28)$$

by means of a semiempirical group contribution method. The behavior of  $k_{d_p}$ ,  $k_p$  and  $K_e$  for styrene is shown in Figure 2-1. Figure 2-2 shows the equilibrium or limiting conversion vs. temperature locus, indicating  $T_C$ ,  $T_A$ ,  $T_R$  and the actual reaction paths for this study's experiments. The need to include a depropagation term in the kinetic model is obvious and furthermore, it is supported by the experimental results.

Since polymerization is accompanied by a diminution in volume ( $\Delta V < 0$ ), an increase in pressure causes an increase in free energy in favour of polymerization. This is more clearly expressed by the relationship:

$$\frac{d(\Delta G^0)}{dP} = \Delta V \quad (29)$$

The ceiling temperature  $T_C$  (or  $\Delta G^0 = 0$ ) is raised by an increase in pressure and also by an increase in monomer, initiators and free radical concentrations. The change of  $T_C$  with pressure is given by the Clausius-Clapeyron equation<sup>(43,44)</sup>

$$\frac{dT_C}{dP} = T_C \frac{\Delta V}{\Delta H} \quad (30)$$

and after integration:

$$\ln T_C = \ln T_C^0 + \frac{\Delta V \Delta P}{\Delta H} \quad (31)$$

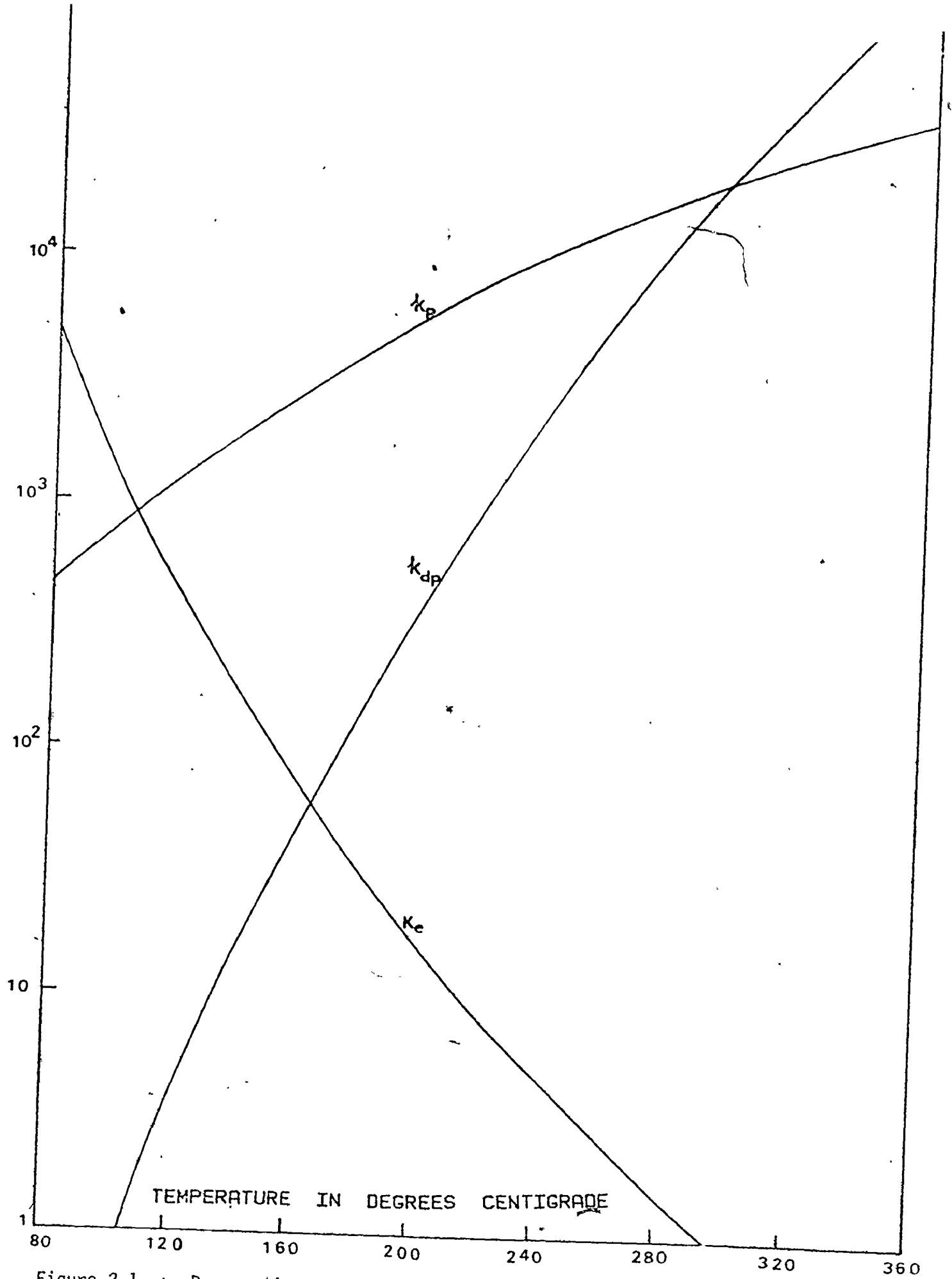


Figure 2.1 : Propagation, depropagation and equilibrium constants versus temperature

CONVERSION X AS FUNCTION OF  
REACTION TEMPERATURE IN DEGREES CENTIGRADE

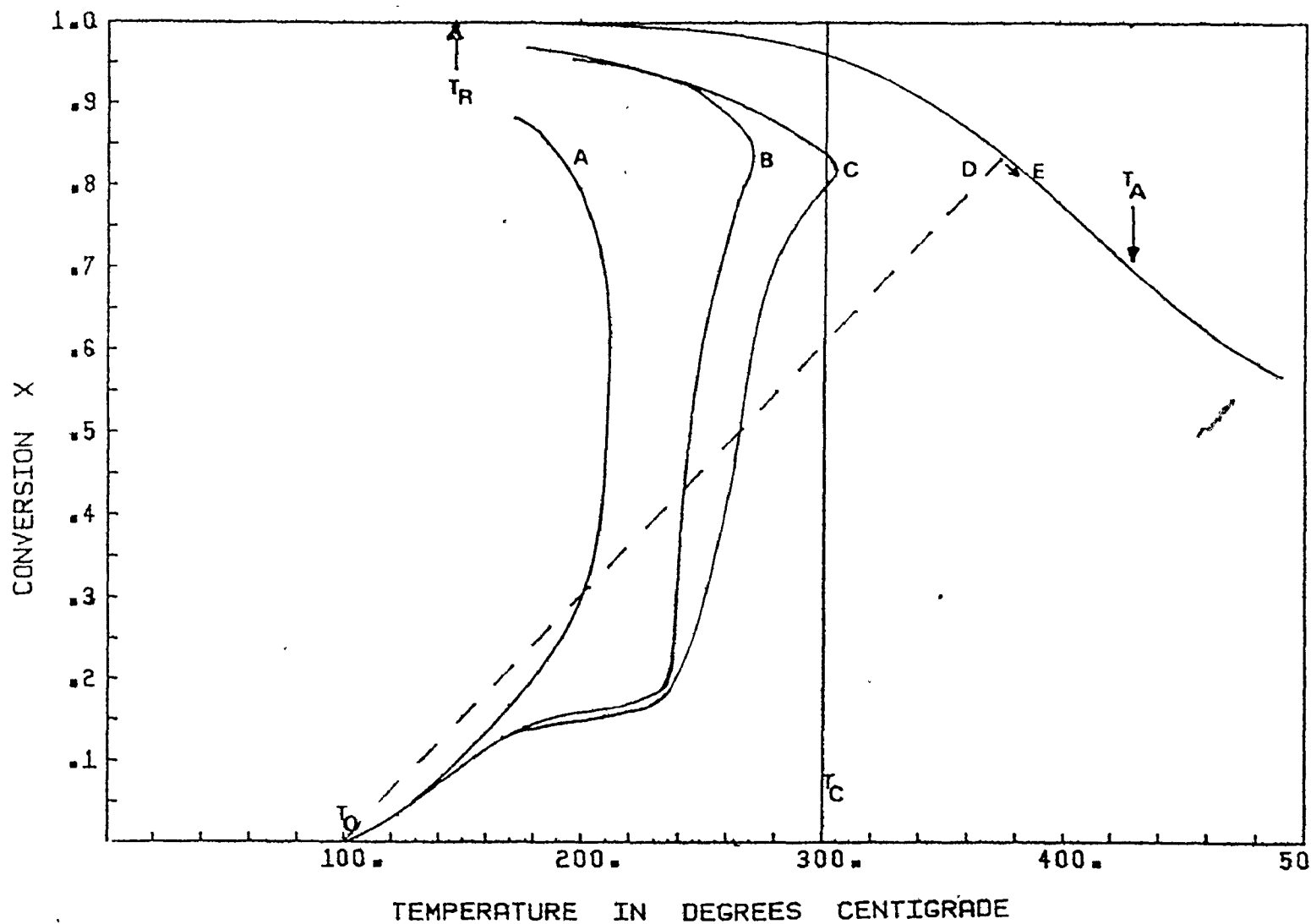


Figure 2.2 : Conversion vs. Temperature. Reaction Paths.

- A  $P_0 = 0$  psig
- B  $P_0 = 50$  psig
- C  $P_0 = 100$  psig
- D Adiabatic path
- E Equilibrium conversion
- $T_A$  Maximum adiabatic temperature
- $T_C$  Ceiling temperature
- $T_R$  Temperature of the oil bath
- $T_0$  Initial temperature.

The changes of  $\Delta G^0$  with respect to temperature and pressure are in opposite directions.

$\Delta V$  can be expressed as:

$$\Delta V = \Delta V_p^* - \Delta V_{dp}^* \quad (32)$$

where  $\Delta V_p^*$  is the same as  $\Delta V^*$  defined in section 2.5.1.  $\Delta V_{dp}^*$  contributes the most to  $\Delta V$ , because the volume change in the depropagation reaction is very small, and can be considered that  $\Delta V = \Delta V_p^*$ . Differentiation of equation (19.b) with respect to temperature, taking the limit when  $T \rightarrow T_c$ , where  $k_p[m] = k_{dp}$ , leads to an equation similar to the liquid-vapor equilibrium reaction isochore from which Dainton and Ivin<sup>(31)</sup> originally derived equation 26.

### 2.5.3 Thermodynamics of Polymer Solutions

There are several distinct ways in which it is possible to obtain expressions for calculating the equilibrium properties of polymers in solution. For a complete description, the readers are referred to the excellent review by Bonner<sup>(39)</sup>. It is indicated that, in general, the Huggins formulation is a good approximation for concentrated polymer solutions. We will deal here only with binary solutions containing a low molecular weight substance, a solvent, in this case styrene and a high molecular weight substance, a polymer, in this case polystyrene.

It is to be stated that the use of mole fraction is inadequate in polymer solution calculations, because the high molecular weight of polymer (and its distribution) results in a low mole fraction of polymer, even if the weight fraction of polymer is near unity. Three concentration scales are widely used. The volume fraction  $\phi_j$  was chosen, which can be expressed as a function of conversion ( $x$ ) and volume contraction ( $\epsilon$ ):

$$\phi_p = \frac{x(1 + \epsilon)}{1 + \epsilon x} \quad (33)$$

where  $\epsilon$  can be calculated assuming that volume varies linearly with respect to conversion through polymerization<sup>(46)</sup>.

$$V = V_0 (1 + \epsilon x) \quad (34)$$

where  $\epsilon = \frac{(V)_{x=1} - (V)_{x=0}}{(V)_{x=0}} \quad (a)$

$$\epsilon = \frac{1/\rho_p - 1/\rho_m}{1/\rho_m} \quad (b) \quad (35)$$

$$\epsilon = \frac{\rho_m}{\rho_p} - 1 \quad (c)$$

$$\text{and } \phi_m = 1 - \phi_p \quad (36)$$

Flory (loc. cit 39) suggested that the Gibbs energy of mixing of a polymer solution can be calculated by adding an empirical mixing term to the entropy of athermal mixing.

$$\Delta G^M = \Delta H^M - T\Delta S^M \quad (37)$$

The Gibbs energy of mixing  $n_1$  moles of monomer with  $n_2$  moles of polymer is given by the so-called Flory-Huggins expression:

$$\frac{\Delta G^M}{RT} = \chi n_1 \phi_p + [n_1 \ln \phi_m + n_2 \ln \phi_p] \quad (38)$$

$\chi$  is an empirical parameter called the interaction parameter. It is a function only of temperature and independent of  $\phi_i$ . It can be calculated using the solubility parameter criterion of Hildebrand<sup>(47)</sup>. It is a free energy parameter, hence it should contain the contributions of enthalpy and entropy:

$$\chi = \chi_S + \chi_H \quad (39)$$

A safe value for  $\chi_S$  is 0.34<sup>(48)</sup>, and

$$\chi_H = \frac{v_1}{RT} (\delta_p - \delta_M)^2 \quad (40)$$

$\delta_p$  and  $\delta_M$  are the solubility parameters for polymer and monomer.  $v_1$  is the molar volume of styrene. The solubility parameter of monomer is obtained from its enthalpy of vaporization  $\Delta H_V$ :

$$\delta_M = \left( \frac{\Delta H_v - RT}{v_1} \right)^{1/2} \quad (41)$$

The polymer solubility parameter is estimated from a group contribution method proposed by Small<sup>(49)</sup>.

$$\delta_p^2 = \delta_d^2 + \delta_{DS}^2 + \delta_H^2 \quad (42)$$

where the symbols stand for:

$p$  = polymer solubility parameter

$d$  = contribution from dispersion forces

$DS$  = contribution from polar forces

$H$  = contribution from hydrogen bonding forces.

Extensive compilation of values may be found elsewhere<sup>(51)</sup>.

The chemical potential of monomer can be obtained by differentiating equation (38), holding  $x$  constant:

$$[\mu_M(p,T) - \mu_M^0(p,T)]/RT = \ln \phi_M + (1 - v_1/v_2) \phi_p + x \phi_p^2 \quad (43)$$

where  $\mu_1^0$  is the chemical potential of pure monomer. The activity of the solvent is therefore:

$$\ln a_M(p,T) = \ln \phi_M + (1 - v_1/v_2) \phi_p + x \phi_p^2 \quad (44)$$

For the purpose of calculating the partial pressure of styrene in a styrene-polystyrene solution and neglecting  $v_1/v_2$  as very small compared to unit; equation (44) can be expressed more conveniently as:

$$\ln \left( \frac{P_S}{P_S^0} \right) = \ln \phi_M + (1 - \phi_M) + x (1 - \phi_M)^2 \quad (45)$$

Of course, the total pressure will be given by



$$P_T + P_S + P_{PS} + P_I \quad (46)$$

where  $P_I$  is the partial pressure of any inerts in the system. In this study it will be the partial pressure of nitrogen. In the ranges of temperature and pressure used, nitrogen behaves as an ideal gas.  $P_{PS}$  would be the partial pressure of polystyrene and will have a value of zero. Frenkel<sup>(45)</sup> showed that it is impossible to vaporize a polymeric chain. It will rather break (degrade) than vaporize. This author states that the vapor phase could contain components whose chain lengths are equal or less than the ratio of energy required to break a carbon-carbon bond (in polystyrene,  $\Delta H = 62$ ) to the enthalpy of evaporation of styrene. This ratio is approximately 7; hence it could be expected to have up to heptamers in the vapor phase. There is evidence that it is possible to evaporate even pentamers, but the level of energy required is too large and cannot be reached under the present experimental conditions. No attempt to account for the possible partial pressure of oligomers will be done in this study.

### 3. MATHEMATIC MODEL DEVELOPMENT

In this chapter, the different free radical reactions, their rates and rate constants will be considered and an expression for the overall rate of polymerization ( $R_p$ ) will be obtained. From such an expression the conversion-time history, the molecular weights and the molecular weight distribution can be calculated. The complete equations that describe the behavior of a non-isothermal polymerization will also be derived.

#### 3.1 Reactions

The different free radical reactions are summarized in Table 3.1 where only the significant reactions in styrene polymerization are included.

TABLE 3.1 Free Radical Reactions and Rates

<u>Reaction</u>		<u>Rate expression</u>
A) Thermal Initiation	$M + M \xrightarrow{k_i} 2M\cdot$	$R_{IT} = 2k_i [M]^3$
B) Chemical Initiation	$I \xrightarrow{k_d} 2R\cdot$	$R_{IC} = 2f k_d [I]$
C) Propagation	$R_m\cdot + M \xrightarrow{k_p} R_{m+1}\cdot$	$k_p [M] [R\cdot]$
D) Depropagation	$R_{m+1}\cdot \xrightarrow{k_{dp}} R_m\cdot + M$	$k_{dp} [R\cdot]$
E) Chain transfer to monomer	$R_m\cdot + M \xrightarrow{k_{fm}} P_m + M\cdot$	$k_{fm} [R\cdot] [M]$
F) Termination	$R_m\cdot + R_n\cdot \xrightarrow{k_{tc}} P_{m+n}$	$k_{tc} [R\cdot]^2$

For further details on thermal initiation, the readers are referred to the works of Hui and Hamielec<sup>(53)</sup> and of Husain<sup>(23)</sup>. Hui and Hamielec demonstrated that thermal initiation follows a third order reaction.

For equation B the initiator concentration  $[I]$  is given by equation (6). The term  $f$  denotes efficiency, estimated by the ratio of initiator decomposed to polymer chains formed. This efficiency is introduced to account for the radicals formed by equation B that do not initiate polymeric chains, either by fast recombination, by reaction with a free radical scavenger or, during the viscous stage, by being immobilized and unable to diffuse. (Cage effect). The efficiency of an initiator is, in general, within the 0.5 - 1.0 range. Hui<sup>(22)</sup> showed that the efficiency of a catalyst decreases with conversion and initial concentration of initiator, and, as expected, increases with temperature.. In this work a constant value is to be used. The calculated efficiencies for AIBN and DTBP are 0.64 and 0.58 respectively<sup>(71)</sup>.

When several  $n$ -initiators are used, for whatever purpose, i.e. shortening the time of reaction, wanting to obtain certain molecular weights, wishing to optimize the heat removal capacity of a reactor, etc. the rate of chemical initiation becomes:

$$R_{IC} = 2 \sum_{i=1}^n f_i k_{d_i} [I]_i \quad (47)$$

The total rate of initiation then becomes:

$$R_I = 2 \sum_{i=1}^n f_i k_{d_i} [I]_i + 2 \bar{k}_i [M]^3 \quad (48)$$

For equations C and D, the terms  $[R\cdot]$  are a representation of  $\sum_r [R_r\cdot]$  and  $\sum_{r \neq 1} [R_r\cdot]$  for which, by assumption, the rate constants are independent; hence  $[R\cdot]$  represents the concentration in number of free radicals, regardless of length..

### 3.2 Rate of Polymerization

Differential equations describing the variation of polymer radical concentration follow:

$$\frac{1}{V} \frac{dN_{\cdot 1}}{dt} = R_I + (k_{f_m} [M]) \sum_{r=1}^{\infty} [R_{\cdot r}] + k_{d_p} R_{\cdot 2} - R_{\cdot 1} [k_p [M] + k_{f_m} [M] + k_t R_{\cdot}] \quad (49)$$

for  $r = 1$

$$\frac{1}{V} \frac{dN_{\cdot r}}{dt} = k_p [M] (R_{\cdot r-1} - R_{\cdot r}) + k_{d_p} (R_{\cdot r+1} - R_{\cdot r}) - R_{\cdot r} [k_{f_m} [M] + k_t R_{\cdot}] \quad (50)$$

for  $r \geq 2$

Adding equations (49) and (50) with respect to  $r$ :

$$\frac{1}{V} \frac{d(\sum_{r=1}^{\infty} N_{\cdot r})}{dt} = R_I - k_t [R_{\cdot}]^2 \quad (51)$$

Application of S.S.H. yields:

$$[R_{\cdot}] = \left( \frac{R_I}{k_t} \right)^{1/2} \quad (52)$$

This expression is consistent, as it expresses that the only reactions that affect the free radical population are the initiation and termination ones. Biesenberger and Capinpin<sup>(50)</sup> showed that the Steady State Hypothesis (S.S.H.) is valid for non-isothermal polymerizations. It seems that the only restriction to this hypothesis occurs when the gel-effect is extreme.

From equation (19a) and considering the volume shrinkage, we obtain the following expression:

$$-\frac{d[M]}{dt} = [k_p [M] - k_{d_p}] \left(\frac{R_I}{k_t}\right)^{\frac{1}{2}} + \frac{[M]}{V} \frac{dV}{dt} \quad (53)$$

due to volume contraction:

$$[M] = \frac{[M]_0 (1 - x)}{(1 + \epsilon x)} \quad (54)$$

$$\text{or } x = \frac{[M]_0 - [M]}{[M]_0 + [M]_\epsilon} \quad (55)$$

$$\text{and } \frac{1}{V} \frac{dV}{dt} = - \left( \frac{\epsilon}{[M]_0 + [M]_\epsilon} \right) \frac{dM}{dt} \quad (56)$$

substituting (56) into (53) and rearranging:

$$\frac{d[M]}{dt} = \frac{(k_p [M] - k_{d_p}) \left(\frac{R_I}{k_t}\right)^{\frac{1}{2}}}{\frac{\epsilon [M]}{[M]_0 + \epsilon [M]} - 1} \quad (57)$$

Remember that  $R_I$  is also a function of the monomer concentration  $[M]$ .

Equations (55) and (57) describe the conversion-time history for a batch, bulk, isothermal polymerization. The following Arrhenius equations are available in the literature<sup>(58)</sup> and are the ones used in this study.

$$\left. \begin{aligned} k_p &= 1.051 \times 10^7 \exp(-3557/T) \\ k_{f_m} &= 2.31 \times 10^6 \exp(-6377/T) \\ k_t &= 1.255 \times 10^9 \exp(-844/T) \\ k_i &= 2.19 \times 10^5 \exp(-13810/T) \\ k_{d_p} &= 10^{13} \exp(-11379/T) \end{aligned} \right\} \begin{array}{l} \text{lt/g mol-sec} \\ \text{lt}^2/\text{g mol}^2\text{sec}^{(53)} \\ \text{1/sec}^{(31)} \end{array}$$

### 3.3 Rate of Heat Generation

For a batch non-isothermal reactor the energy equation becomes:

$$\rho C_p \frac{dT}{dt} = (-\Delta H)R_p - \frac{UA}{V} (T - T_R) - \frac{A_s \Delta H_v R_v}{V} \quad (58)$$

the term  $A_s \Delta H_v R_v / V$  represents the heat removed due to evaporation of monomer. A method for evaluating  $R_v$ , the rate of evaporation is presented in Arnold's paper<sup>(56)</sup>. However, this conventional method of evaluating the rate  $R_v$  does not account for the increasing viscosity or, in other ways, the increasing resistance for molecular motion. In the experiments held in this study, it was found that the amount of styrene vaporized is negligible, as most of the experimentation was done under pressure to avoid boiling of the monomer, and therefore will not be considered.

$$\text{Hence: } \rho C_p \frac{dT}{dt} = (-\Delta H)R_p - \frac{VA}{V} (T - T_R) \quad (59)$$

Equations (57) and (59), bearing in mind that  $R_p = \frac{1}{V} \frac{dN_M}{dt}$ , describe completely the system and must be solved simultaneously.

### 3.4 Corrections for Gel-effect

The gel effect acts to reduce the termination reaction rate constant and its reduction will be given by an empirical correction after Hui and Hamielec<sup>(53)</sup>. They developed an empirical correction which depends on the conversion. The use of conversion as a parametric variable would contain the viscosity implicitly. Attempts have been made to include the viscosity as an explicit parameter<sup>(17)</sup>, but as it is a function of the molecular weight and concentration, such attempts have been fruitless.

The Hui and Hamielec<sup>(53)</sup> correction is as follows:

$$k_t/k_{t_0} = \exp(-2. (Bx + Cx^2 + Dx^3)) \quad (60)$$

where B, C and D are linear functions of temperature.

$$B = 2.57 - 5.05 \times 10^{-3} T \quad (a)$$

$$C = 9.56 - 1.76 \times 10^{-2} T \quad (b) \quad (61)$$

$$D = -3.03 + 7.85 \times 10^{-3} T \quad (c)$$

This correction has been found to fit adequately the conversion and molecular weights in the range 100-230°C<sup>(23,53)</sup>.



### 3.5 Molecular Weights and Molecular Weight Distribution (MWD)

The instantaneous chain length averages are given by:

$$\bar{r}_n = \frac{1}{\tau + \beta/2} \quad (62)$$

$$\bar{r}_w = \frac{2\tau + 3\beta}{(\tau + \beta)^2} \quad (63)$$

and the instantaneous MWD by

$$w(r) = (\tau + \beta)(\tau + \frac{1}{2}\beta (\tau + \beta) r) r \exp(-(\tau + \beta)r) \quad (64)$$

where  $\tau = \frac{k_{fm}}{k_p} + B_1 x$  (65)

and  $\beta = \frac{k_t R_p}{k_p^2 [M]^2}$  (66)

$B_1$  is a correction for the suggested transfer reaction to the Diels-Alder adduct (equation 7a)<sup>(23)</sup>. Although the steady state concentration of this specie is very small, its transfer reaction is so large that it dominates the term  $\tau$  in equation (65).  $B_1$  is a function of temperature. Hui and Hamielec<sup>(53)</sup> allowed it to take the form

$$B_1 = -1.013 \times 10^3 \log_{10} \left( \frac{473.12 - T}{202.5} \right) \quad (67)$$

This is limited to an upper limit of 200°C. Husain and Hamielec<sup>(52)</sup> extended its range from 200°C upwards as:

$$B_1 = \frac{E_1 \times 10^{-2}}{1 + 2E_1} \quad (68)$$

where:  $E_1 = 0.9755 \exp \left\{ -12180 \left( \frac{1}{T} - \frac{1}{473} \right) \right\}$  (69)

$B_1 x$  can be thought as equal to  $\frac{k_{fAH}}{k_p} \frac{[AH]}{[M]}$ .

In this study, equations (67) and (68) were used. However, when the temperature exceeded 240°C, a higher value for  $B_1$  was used in order to compensate for the possible transfer reaction to oligomers and degradation byproducts.

The cumulative chain length averages and MWD are expressed as:

$$\bar{r}_n \text{ cum} = \frac{x}{\int_0^x \frac{1}{\bar{r}_n} dx} \quad (70)$$

$$\bar{r}_w \text{ cum} = \frac{1}{x} \int_0^x \bar{r}_w dx \quad (71)$$

$$w(r) \text{ cum} = \frac{1}{x} \int_0^x w(r) dx \quad (72)$$

The variance of the number chain length distribution is given by

$$\sigma_N^2 = \bar{r}_N^2 \left( \frac{\bar{r}_w}{\bar{r}_N} - 1 \right) \quad (73)$$

The average molecular weights are given by

$$\bar{M}_i = M_m \bar{r}_i \quad (74)$$

where  $M_m$  is the molecular weight of the monomer, equal to 104.14 g/g-mol.

## 4. EXPERIMENTAL

### 4.1 Description of the Reactor

The reactor consists of a steel shell that contains a wood jacket, intended to provide insulation, and inside this jacket there is a glass cylinder, where the reaction actually takes place. The glass cylinder is sealed with a wood cap, provided with four holes for the measurements of pressure and temperature and injection of monomer, initiators and nitrogen. On top of this cap comes the flange of the shell which is held with screws and sealed by means of a Teflon annular seal.

The reactor is equipped with a pressure transducer. The range of this instrument is 0 - 350 p.s.i.g. and was calibrated for use in the range 0 - 200 p.s.i.g. Two chromel-alumel thermocouples were used for measurements of temperatures in different points of the reactor. The thermocouples can be used either one or both simultaneously.

The reactor also has a nitrogen line, which provides an inert atmosphere and also some degassing of the monomer (more properly, removes some of the dissolved oxygen). The reactor is equipped with a venting quick-open valve and with a rupture disc as a safety device. The rupture disc is designed to break at 300 p.s.i.a. This rupture disc was overdesigned, due to misinterpretation of a recent paper<sup>(12)</sup>. Actual industrial rupture discs for bulk polymerization reactors usually break with an increment of 30 - 40 p. s.i.g.

The entire apparatus is immersed in an oil bath, which can provide control up to  $\pm 1^\circ\text{C}$ . The purpose of the oil bath is twofold: it is used to provide heating to the reaction medium initially, which takes a long time and reduces the temperature gradient between the locus of the reaction and the surroundings. This reduces the heat losses and would avoid excessive thermal shocks and stresses on the materials.

A diagram of the reactor is shown in Figure 4-1. The recordings of temperature(s) and pressure were made by means of a two-pen recorder. The monomer and initiators were injected using a 50 ml syringe.

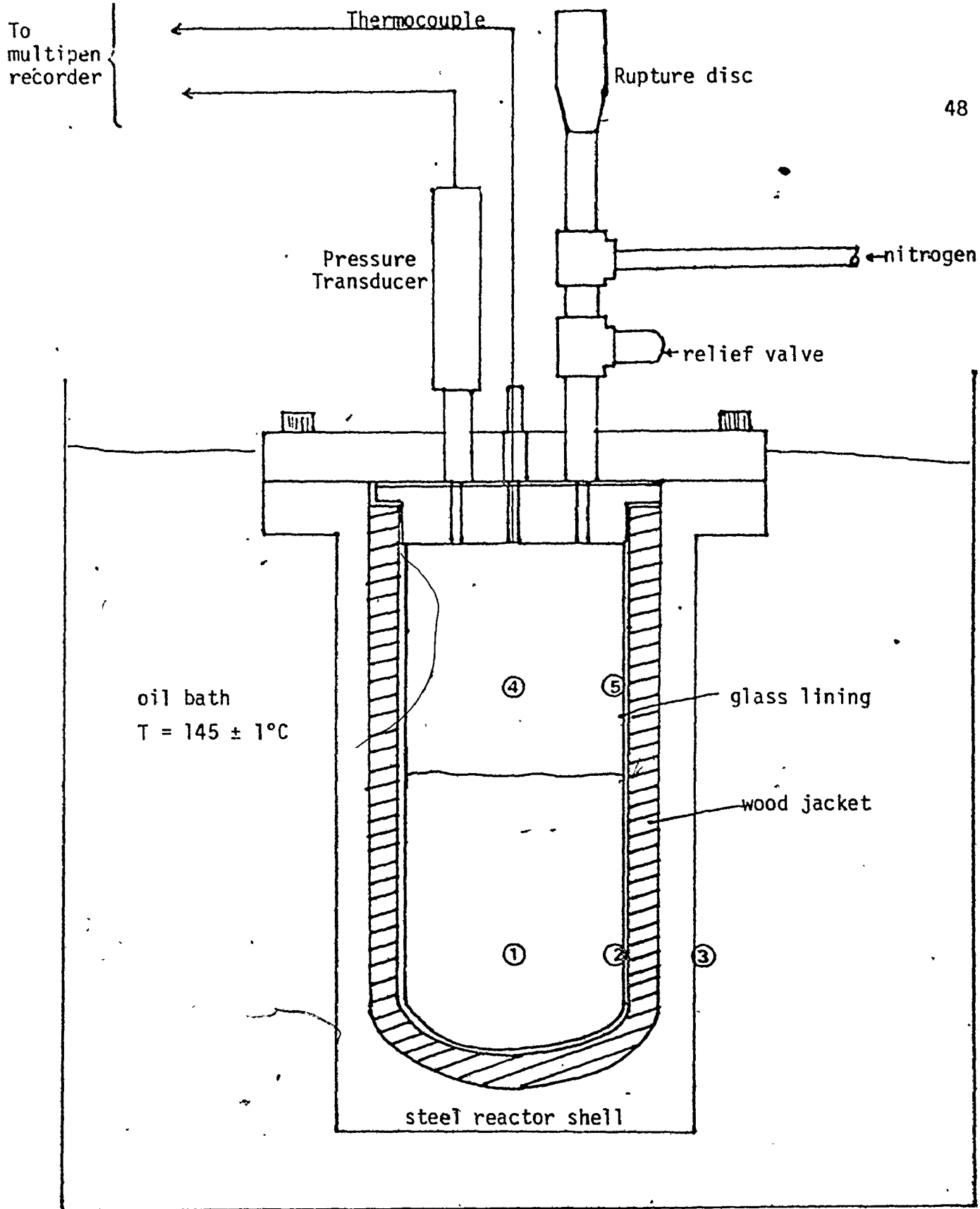


Figure 4.1 : Reactor for non-isothermal Polymerizations.  
(not drawn to scale)

#### 4.2 Reactants and Choice of Polymerization Conditions

Commercial polymerizations of styrene are done mainly in the 100 - 200°C range, mostly around 100°C. Therefore it was decided to initiate the runaway reactions at 100°C. As a temperature gradient was needed to heat the reactant mixture, it was decided to set the oil bath at 150°C, a misadjustment in the thermostat set the temperature at 145°C, this only has effect on the heating time.

The monomer used in this study was provided by Monsanto Company and it is inhibited with approximately 10p.p.m of hydroquinone. Some experiments were performed using distilled monomer (under vacuum at 40°C). No difference between undistilled and distilled monomer was noted. Usually the amount of inhibitor has no effect over 120°C. It should be noted that in all the study the reactions were initiated chemically. Although the reaction can runaway thermally, the rate of thermal initiation at 100°C is very slow.

Three different initiators were used, either alone or in several combinations. These initiators are listed in Table 4-1, where some additional data is also provided.

As commercial polymerizations are done with a wide range of initiator concentrations, sometimes up to 1%, an arbitrary concentration of 0.25% wt. with respect to monomer was selected and used in most of the study. An 'a posteriori' justification is discussed later.

TABLE 4.1 Data for Initiators

Initiator		Molecular Weight	Frequency Factor (sec <sup>-1</sup> )	Energy of Activation/R (°K)
Azobis-IsoButynoNitrile (AIBN)	a	164.21	2.013 x 10 <sup>14</sup>	14879
Di-Tert Butyl Peroxide (DTBP)	b	146.23	6.506 x 10 <sup>12</sup>	14954
Benzoyl Peroxide. (BEPO)	c	242.22	3.333 x 10 <sup>15</sup>	17673

a Eastman Organic Chemicals.  
b Chinook Chemicals Corp. Ltd.,  
c Eastern Chemical Corp.

Nitrogen was used with three purposes in mind: i) As an inert atmosphere; ii) As a degassing medium, it was passed continuously through the reactor during the heat-up period. This was supposed to help in removing the dissolved oxygen from the styrene, which is known to be an inhibitor to the polymerization at low temperatures. However, as shown elsewhere<sup>(23)(34)</sup>, this same oxygen acts as an accelerator at high temperatures. This effect has been discussed earlier in Section 2-1; nevertheless, its presence cannot be accounted for quantitatively and therefore it is undesirable. Some attempts were made to degas the styrene following the degassing procedure used by Hui<sup>(22)</sup> and Balke<sup>(20)</sup>, using a 150 ml vacuum flask. The problems associated with the expansion-contraction of solid styrene and the impossibility of transferring the monomer

to the reactor without having contact with air, made the idea impractical and it was decided to proceed as described above; and iii) As a pressurizing medium. Since styrene has a boiling point of  $145^{\circ}\text{C}$ , in order to avoid an 'artificial isotherm' due to the removal of latent heat during boiling, most of the experiments were done under pressure, provided by nitrogen. The experiments were conducted at 0, 50 and 100 p.s.i.g. The response of the pressure transducer was calibrated putting pressure in the reactor, recording the signal from the transducer in the chart recorder and measuring the pressure in the reactor with a manometer. Three different manometers of different ranges were used. In addition two gauges were used on the nitrogen cylinder. The procedure was repeated until a satisfactory average was obtained at each pressure setting. This procedure was repeated at several temperatures. The instrument has a calibration procedure for electric adjustment, which was checked several times. It should be indicated that the reactor was tested under 1000 p.s.i.g. without showing any leaking or indication of possible mechanical failure.

The temperature recordings were calibrated following an analogous procedure. That is, the thermocouples were immersed in glycerin at different temperatures, measuring the response of the thermocouples in millivolts (with a voltmeter) and the temperature of the liquid with a mercury thermometer. All the calibration procedure was tested several times during the research and no deviations were found.

All the joints were sealed with Teflon tape and tested for leaks.



### 4.3 Experimental Techniques

The following procedure was adopted in order to achieve a fast runaway reaction and at the same time to ensure a zero initial conversion before chemical initiation takes place.

- a) The reactor was assembled, sealed and tested for leaks. Then it was immersed in the cold oil bath. This was done to ensure the absence of thermal shocks in the materials. Nevertheless, it was impossible to avoid them. For example, the insulating jackets broke constantly, due to excessive temperature gradients and differences in the expansion coefficients of the different materials.
- b) The oil bath was set on and a gradual heating took place. It took at least three hours for the oil bath and the whole reactor to reach a stable temperature. This temperature was  $145^{\circ}\text{C} \pm 1$ .
- c) When the temperature at the centre of the reactor had stabilized, the thermocouple was removed. It should be noted that initially only one thermocouple was used, later on provisions were made to have a second one at the wall. 80 ml of styrene at room temperature were injected to the reactor using a 50 ml syringe. The thermocouple was installed again. During all the procedure nitrogen was kept passing through the reactor.
- d) When the temperature of the mass of styrene reached  $105^{\circ}\text{C}$ , the thermocouple was removed and a solution of initiator or initiators

in 20 ml of styrene were injected to the reactor. The solution was prepared as follows:

- (i) determine the mass of styrene to be used, if 100 ml are to be injected. This calculation is done at room temperature.
- (ii) Calculate the weight percent of total initiator to be used. Determine the relative percentage of each initiator to be used and weigh the respective amounts.
- (iii) Dissolve each initiator in a separate volume of styrene, which total is to be 20 ml.
- (iv) The several initiator solutions are maintained in ice and isolated from each other until the initiators are to be injected.

After injection of the solution of initiators, the reactor was re-assembled by installing the thermocouple.

- e) Proper adjustments of the partial pressure of nitrogen were made, in order to have a fixed initial total pressure.
- f) The reaction proceeded by itself once it was initiated. During the polymerization continuous records of pressure and temperature were kept.
- g) After the temperature reached a maximum and started decreasing, usually after 25-40 minutes, the reactor was opened (temperature approximately 190°C) and samples of the polymer mixture were obtained using glass pipettes. As the viscosity was very high, the mixture was forced up by increasing the pressure of nitrogen. These samples were quenched either in liquid nitrogen or in ice and stored for analysis of conversion and molecular weight data.

h) The reactor was disassembled and the cleaning procedure began; this consisted of scratching and dissolving the polymer. This procedure took an average 2-3 days. When something went wrong the reactor was down for a week or so.

Several experiments were made in order to find the best conditions for the experiment, these were the first 18 experiments and are reported in Table 5-1, and no further comment will be made on these experiments.

Experiment A-24 was done to check for the homogeneity of the reaction mixture temperature. The experimental procedure was as described above. Two thermocouples were used, one at the centre of the reaction mass and the other at the wall (points 1 and 2 respectively, Figure 4-1). The corresponding temperature profile is presented in Figure 4-2. Although a difference of about 12°C can be observed at the maximum temperature, this represents an approximate maximum variation of 7%. This variation is detected at the peak of the heat generation rate and also at the end of the reaction, when the reaction medium is very viscous and therefore the heat removal mechanism is mainly by conduction. The thermal conductivity of styrene has a very low value. This result will permit the use of a lumped parameter system of equations, instead of the distributed mass and energy balances

$$\frac{\partial T}{\partial t} = \alpha \nabla^2 T + Q_g - Q_r \quad (75)$$

$$\frac{\partial c}{\partial t} = D_{ab} \nabla^2 c + R_p \quad (76)$$

REACTION TEMPERATURE IN DEGREES CENTIGRADE  
AS FUNCTION OF REACTION TIME IN MINUTES

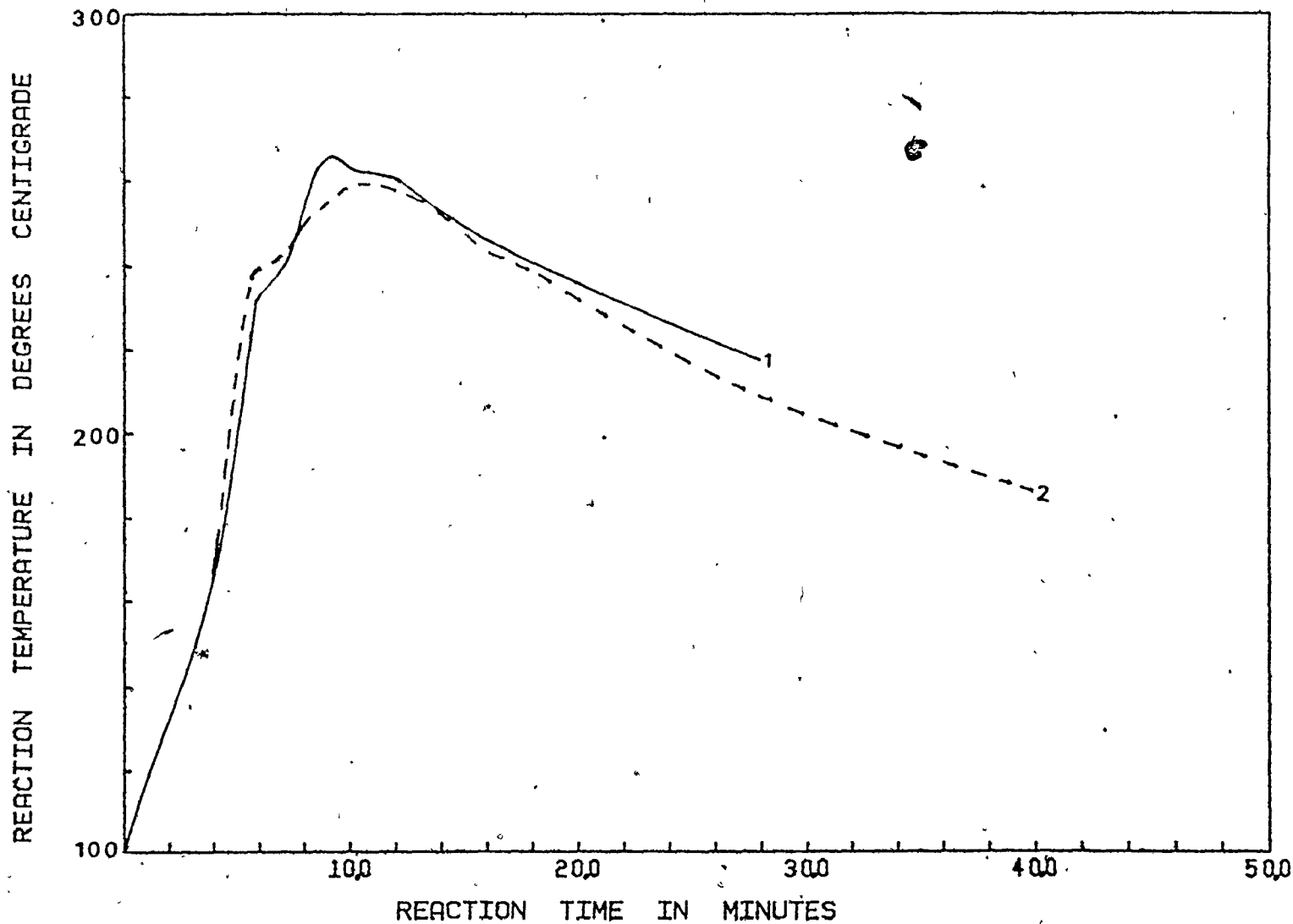


Figure 4.2 : Temperature profiles. Thermocouples at points 1 and 2.

One experiment was done to determine the value of UA (heat transfer coefficient times wetted area available for heat transfer). This was done by using one thermocouple at the inside of the wall and the other at the outside of the wall (points 2 and 3, Figure 4-1). The calculation of UA from this data is outlined in Appendix A4. The corresponding temperature profiles are presented in Figure 4-3.

REACTION TEMPERATURE IN DEGREES CENTIGRADE  
AS FUNCTION OF REACTION TIME IN MINUTES

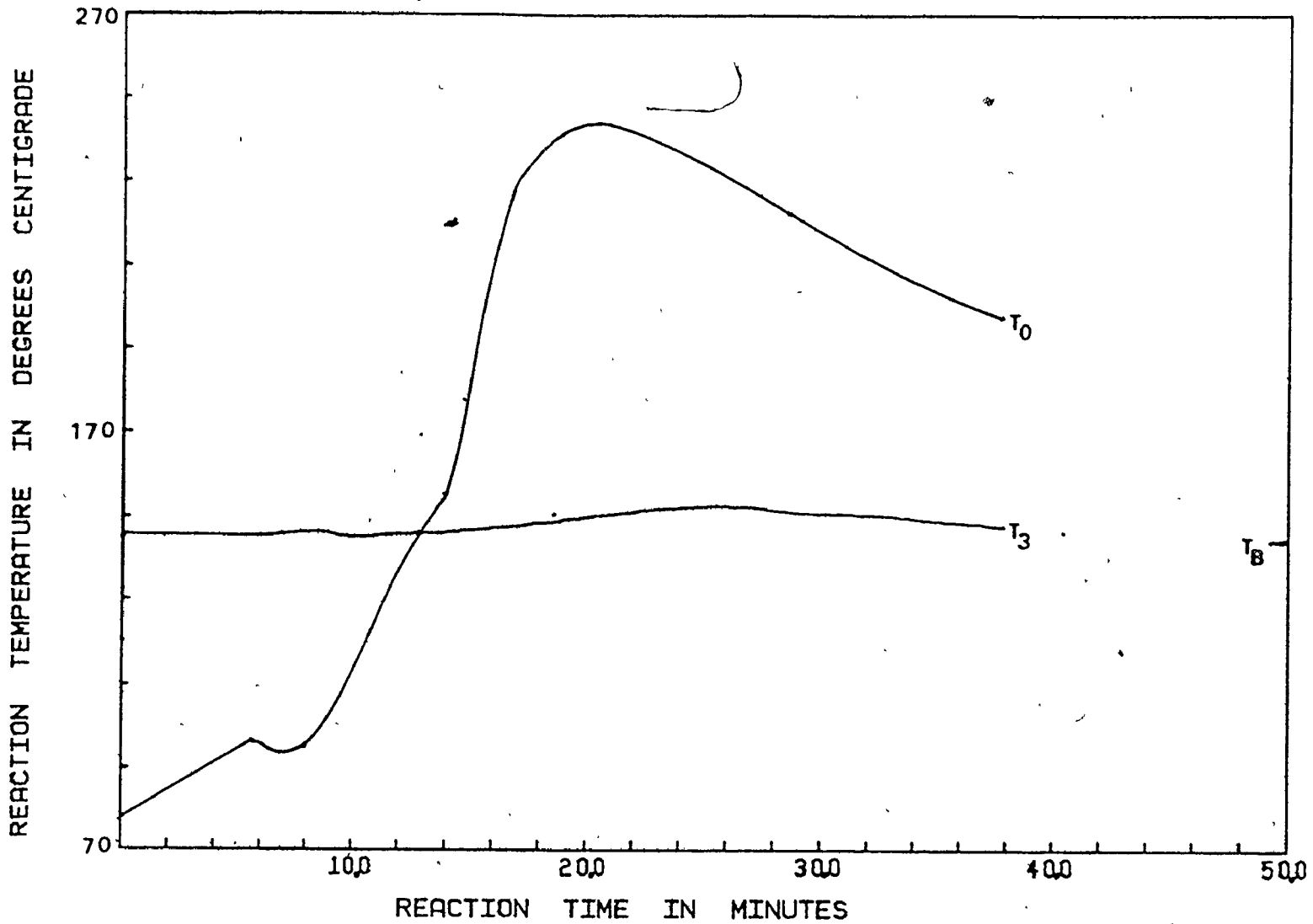


Figure 4.3 : Temperature profiles for heat transfer coefficient determination.

$T_0$ ,  $T_3$ ,  $T_B$  as described in Figure A3.1.

#### 4.4 Analysis

The samples mentioned before (4.3g) were analyzed for conversion and for molecular weights. The conversion was analyzed both by gravimetry and by gel-permeation chromatography (GPC). The gravimetric procedure is as follows:

- a) A sample of approximately 0.1 g was weighed and dissolved in 10 ml of THF.
- b) This solution was poured drop by drop into 100 ml of methanol, precipitating the polymer.
- c) The resultant slurry was filtrated, washed with methanol and dried overnight at 60°C under vacuum.
- d) The precipitated polymer was then weighed and the conversion estimated by difference.

The analysis by GPC was intended to provide the molecular weights  $\bar{M}_n$  and  $\bar{M}_w$  and the molecular weight distribution (MWD). It is possible to measure the conversion knowing that the area under each peak (polymer and monomer peaks) is proportional to its concentration. The GPC work was done using an array of columns similar to Husain's<sup>(23)</sup>. See Table 4-2.

A calibration curve using narrow standards was obtained and is reported in Table 4-3 and presented in Figure 4-4. The interpretation of the chromatographs was done by means of a non-linear calibration curve algorithm, which used the real calibration curve. The molecular weights calculated by this algorithm were subsequently corrected for axial dis-

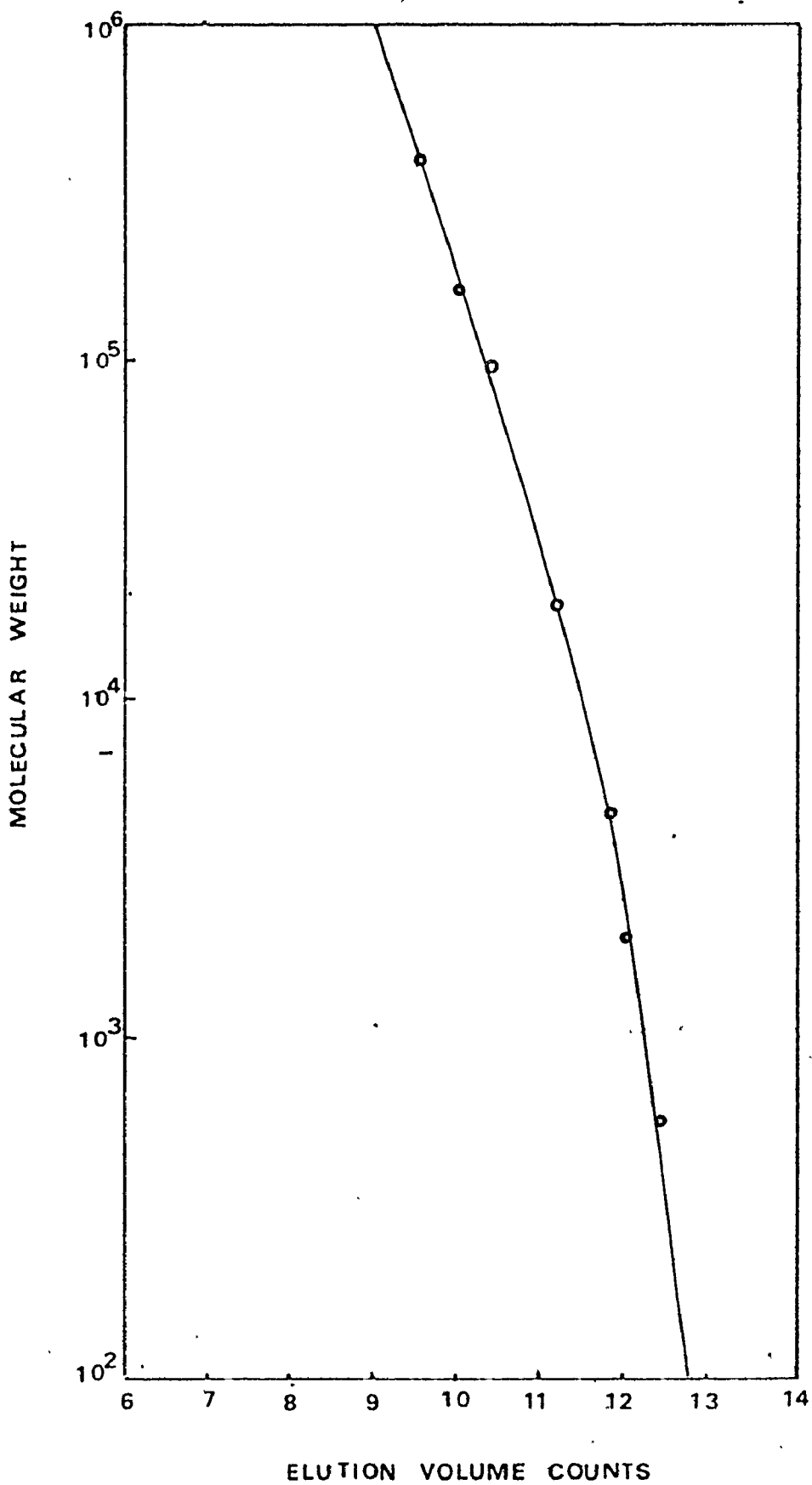


Figure 4.4 : GPC calibration curve.



persion and skewing. The equations for these corrections are<sup>(59)</sup>:

$$M_n(t) = M_n(\infty) (1 + sk) \exp(D_2^2/4h) \quad (77)$$

$$M_w(t) = \frac{M_w(\infty)}{(1-sk)} \exp(-D_2^2/4h) \quad (78)$$

where  $h$  = axial dispersion factor

$sk$  = correction for skewing

$M_i(t)$  = true molecular weight

$M_i(\infty)$  = uncorrected molecular weight

$i = n$  for number average

$= w$  for weight average

TABLE 4.2. Columns used in GPC Analysis

<u>Type</u>	<u>Pore Size (Å)</u>
μ-Styragel	100
μ-Styragel	500
CPG	2500

Carrier Solvent flow 2.75 ml/min.

TABLE 4.3 Standards used for GPC Calibration Curve.

$\bar{M}_n$	$\bar{M}_w$	$M_p$	<u>Elution Volume at peak</u>	$\bar{M}_{n\infty}$	$\bar{M}_{w\infty}$	SK	h
600	-	600	12.4				
1950	2100	2025	12	1130	6620	.6894	28.10
4600	5000	4200	11.8	1550	8900	.6817	1.05
9700	10300	10000	11.4	2750	23270	.7770	.87
19650	19850	19750	11.2	7530	39700	.6784	1.35
96200	98200	97200	10.4	10960	101310	.8011	.38
164000	173000	171000	10	32700	267200	.7713	.57
39200	411000	402000	9.5	276600	546050	.3063	7.31

## 5. RESULTS AND DISCUSSION

### 5.1 Temperature

The conditions under which the experiments were conducted are shown in Table 5.1.

Experiments 1 to 18 were made looking for the best conditions to perform the polymerization; understanding that the aim was to obtain the highest rise in temperature possible in the shortest time. For example, see Figure 5.1 where the behaviour of the system using different initiators is illustrated. It can be seen in this graph that although AIBN provokes a good rise in temperature, it is slow over 150°C, whereas DTBP does not give a very high rise in temperature but is very fast in generating polymer chains at 150°-200°C. Therefore a combination of AIBN/DTBP was chosen for the rest of the experimentation. With this combination of initiators, several experiments performed under initial pressures of 0, 50 and 100 psig were done to determine the best pressure conditions. At 0 psig, the system boils at some temperature-pressure combination level, resulting in a plateau in temperature, see for example Figure 5.3; and in massive evaporation causing measurement and cleaning problems. The highest rise in temperature was achieved under 100 psig but at these conditions  $P \approx 130$  psig,  $T \approx 310^\circ\text{C}$ ) the Teflon seals are far beyond the distortion conditions and near the melting points (Teflon has two melting points, one reversible at 327°C and a degradative one at 345°C; both under atmospheric pressure<sup>(51)</sup>).

TABLE 5.1 Experimental Conditions

Experiment	Initiators	$[I]_0$ g-mol $lt^{-1} \times 10^3$	Initial pressure (psig)	Notes
7	AIBN	13.78	0	Determination of best conditions
8	AIBN	13.78	0	
9	AIBN	13.78	50	
10	DTBP	15.88	50	"
11	AIBN	6.89	60	"
	DTBP	7.74		
12	AIBN	6.89	100	"
	DTBP	7.74		
13	AIBN	6.89	100	"
	DTBP	7.74		
14	AIBN	6.89	50	"
	DTBP	7.74		
15	BEPO	9.34	50	"
16	BEPO	4.67	50	"
	DTBP	7.74		
17	AIBN	4.59	50	"
	BEPO	3.11		
	DTBP	5.15		
18	DTBP	15.48	50	"
19	AIBN	6.89	50	Main replicate site
	DTBP	7.74		
20	AIBN	6.89	50	"
	DTBP	7.74		
21	AIBN	6.89	50	"
	DTBP	7.74		
22	AIBN	6.89	50	"
	DTBP	7.74		

/cont.....

Table 5.1 (Continued)

23	AIBN	6.89	50	Main replicate site, thermocouple at wall.
	DTBP	7.74		
24	AIBN	6.89	50	" "
	DTBP	7.74		Two thermocouples, in- jection at wall.
25	AIBN	6.89	50	" "
	DTBP	7.74		Two thermocouples, in- jection at centre.
26	AIBN	8.93	50	Determination of the eff- ect of amount of initia- tors.
	DTBP	23.41		
27	AIBN	6.89	50	Determination of VA
	DTBP	7.74		
28	AIBN	6.89	100	
	DTBP	7.74		
29	AIBN	6.89	50	two thermocouples ① ⑤
	DTBP	7.74		
30	AIBN	6.89	0	two thermocouples ② ④
	DTBP	7.74		
32	AIBN	6.89	50	two thermocouples ② ④
	DTBP	7.74		
35	AIBN	6.89	0	
	DTBP	7.74		

REACTION TEMPERATURE IN DEGREES CENTIGRADE  
AS FUNCTION OF REACTION TIME IN MINUTES

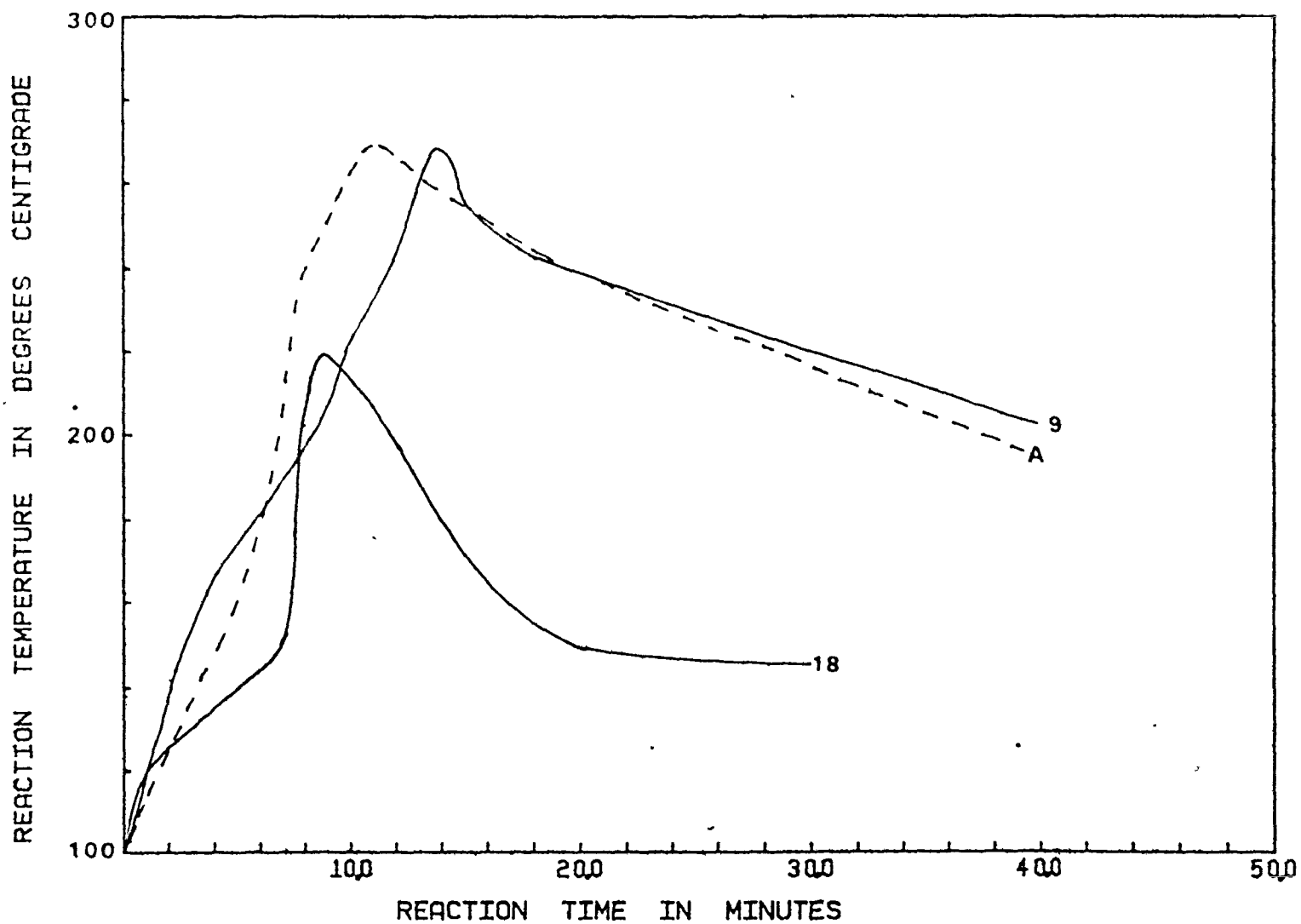


Figure 5.1 : Effect of different initiators on the temperature profile.

9 AIBN  
18 DTBP  
A AIBN:DTBP, 1:1

REACTION TEMPERATURE IN DEGREES CENTIGRADE  
AS FUNCTION OF REACTION TIME IN MINUTES

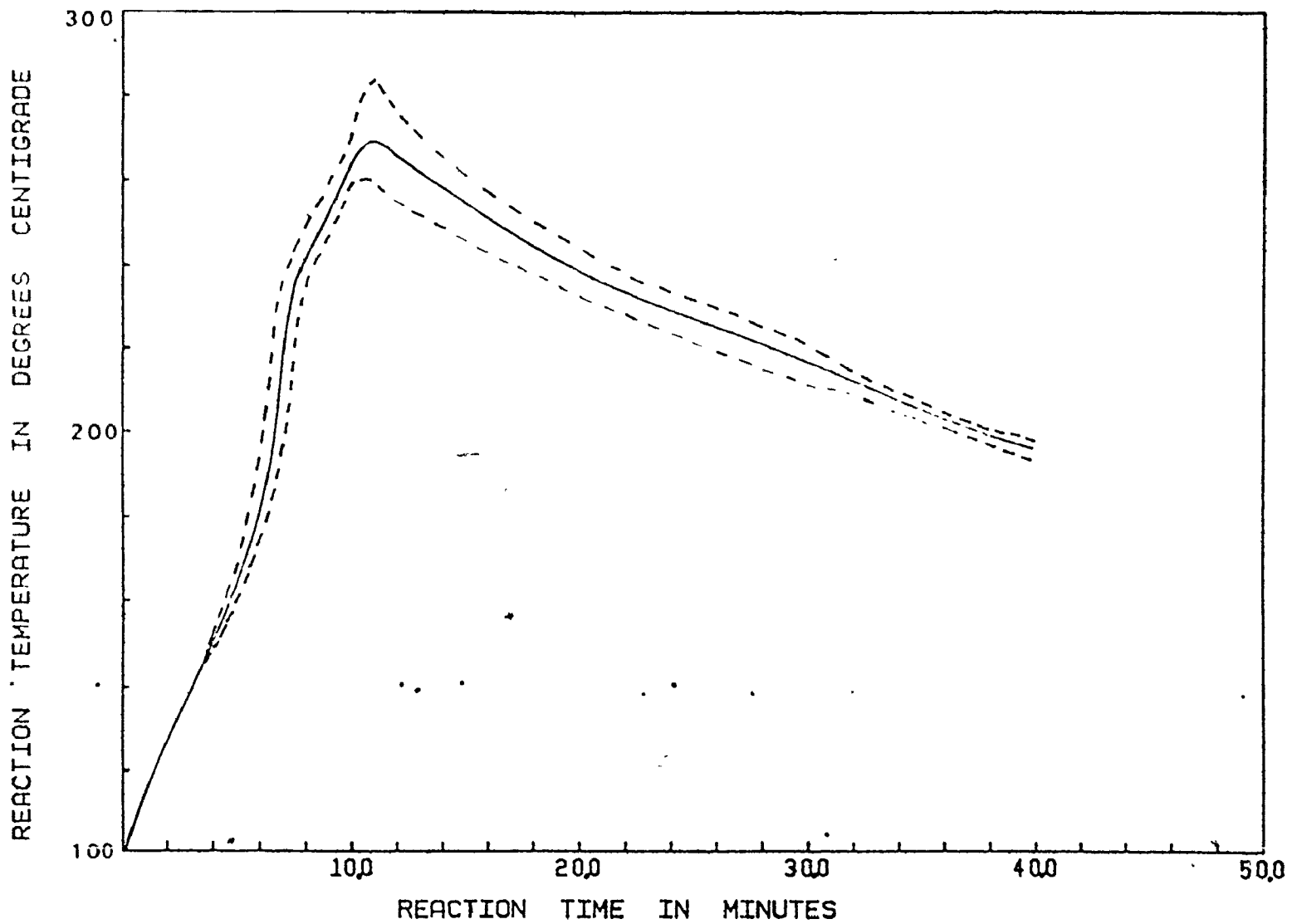


Figure 5.2 : Average temperature profile and its 95% confidence intervals.  $P_i = 50$  psig.

REACTION TEMPERATURE IN DEGREES CENTIGRADE  
AS FUNCTION OF REACTION TIME IN MINUTES

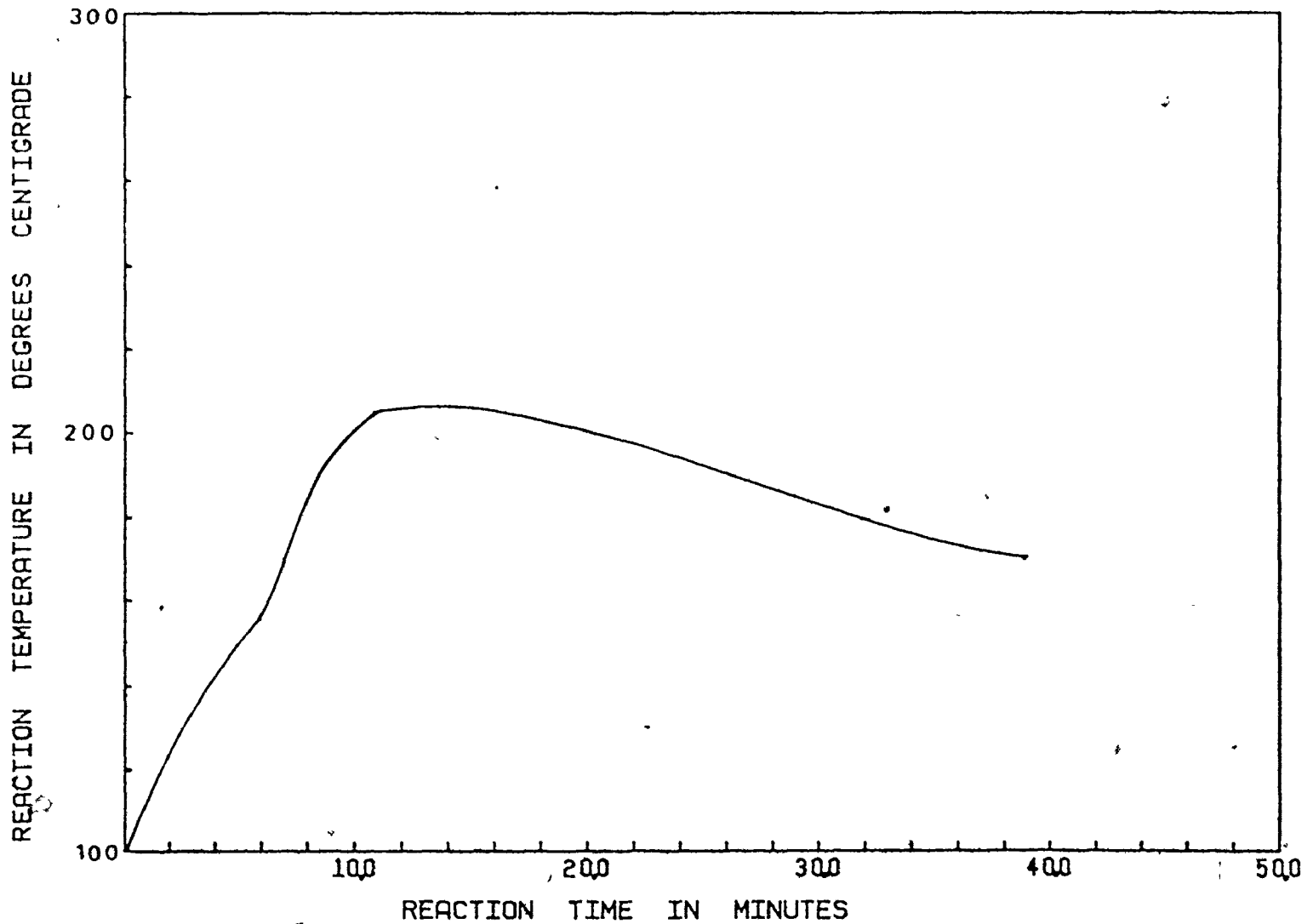


Figure 5.3 : Temperature profile for  $P_i = 0$  psig



Consequently the sealing of the system does not hold any longer and the reactor starts leaking. The reproducibility at these conditions is very poor. In Figure 5.4. an average temperature profile for these experiments can be seen.

It was found then that the best conditions for experimentation are: 0.25% of initiator, using AIBN/DTBP in 1:1 proportion, starting at 100°C with zero conversion and under an initial pressure of 50 psig.

Experiments 11, 19, 20, 21, 22, 23, 24, 25, 26 and 32 were made to obtain replicates at those conditions. Figure 5.2 shows the temperature profiles for the average or "most probable" temperature profile and its 95% confidence intervals. The reproducibility was found to be good, as the average error is about 4%. The error in reading temperatures was estimated to be  $\pm 2^\circ\text{C}$ . The difference in conversion is less than 0.15%.

In experiments, 23, 24, 25, 27, 29, 30 and 32, the temperature was measured at two different points in the reactor, for different purposes. It was found, for example, in experiment 30, that the temperature at the centre of the reacting mass was totally different from the temperature at the centre of the gas phase. This phenomenon was more dramatic in experiment 29 where the initial pressure was 50 psig. Temperature profiles for these two experiments are presented in Figures 5.5. and 5.6. respectively. An explanation can be offered recalling that the geometry of the reactor is different in the upper section and that it is semi-exposed to the environment; even as efforts to insulate it were done, the heat transfer coefficient for this section is totally different and impossible to de-

REACTION TEMPERATURE IN DEGREES CENTIGRADE  
AS FUNCTION OF REACTION TIME IN MINUTES

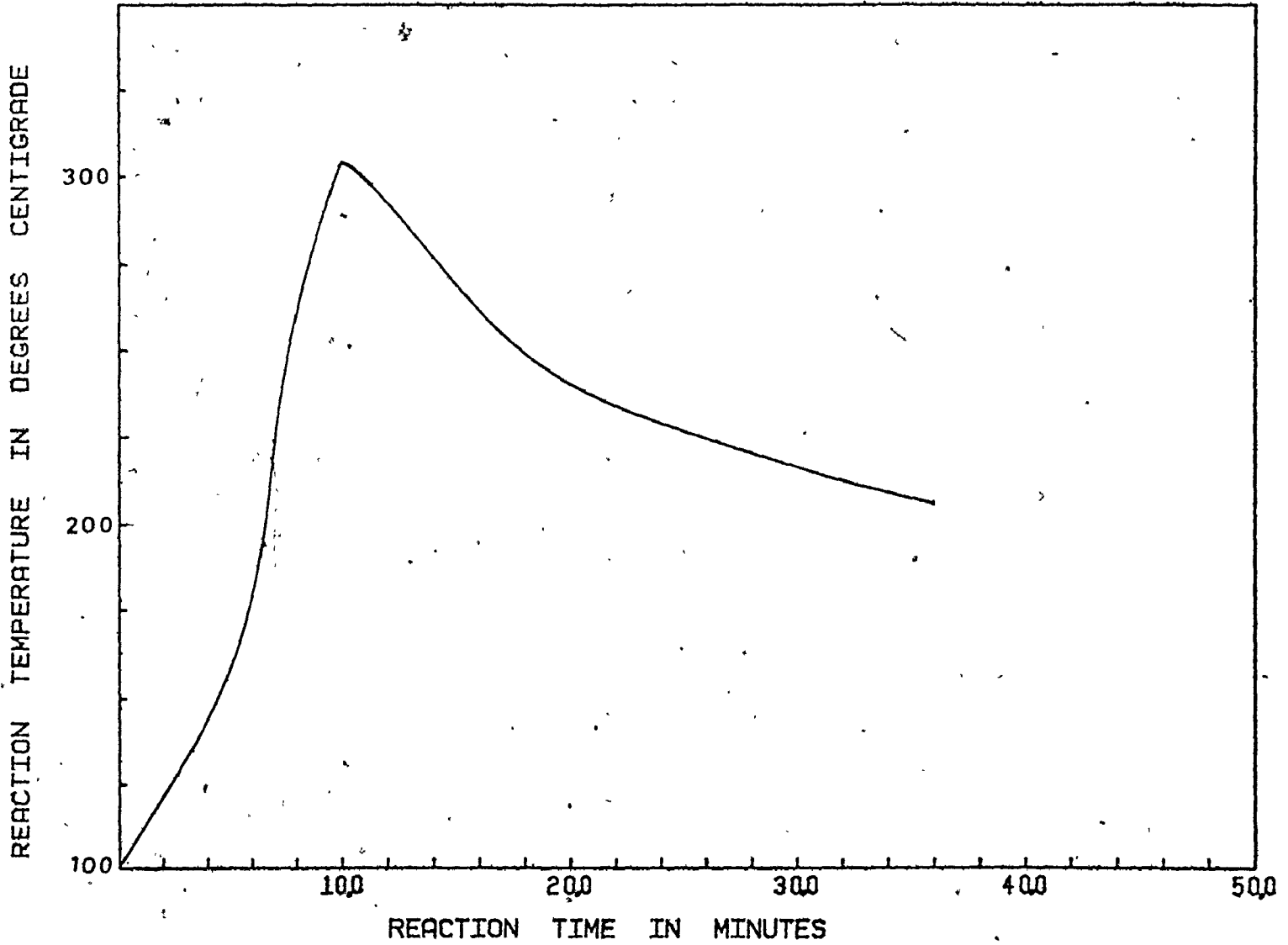


Figure 5.4 : Temperature profile for  $P_i = 100$  psig

REACTION TEMPERATURE IN DEGREE'S CENTIGRADE  
AS FUNCTION OF REACTION TIME IN MINUTES

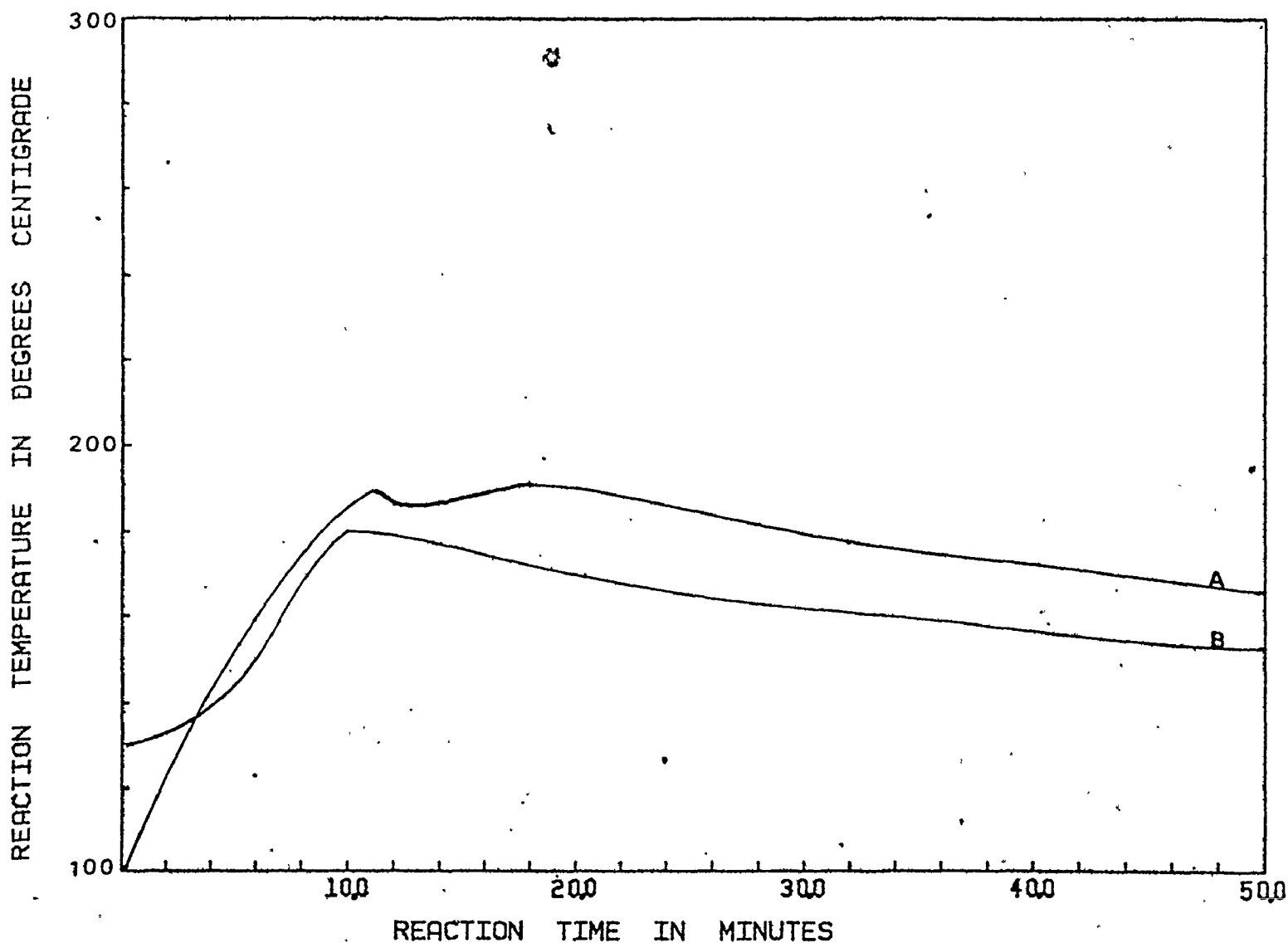


Figure 5.5 : Temperature profile for Points ② and ④  $P_i = 0$  psig. Experiment 30

A point ②

B point ④

REACTION TEMPERATURE IN DEGREES CENTIGRADE  
AS FUNCTION OF REACTION TIME IN MINUTES

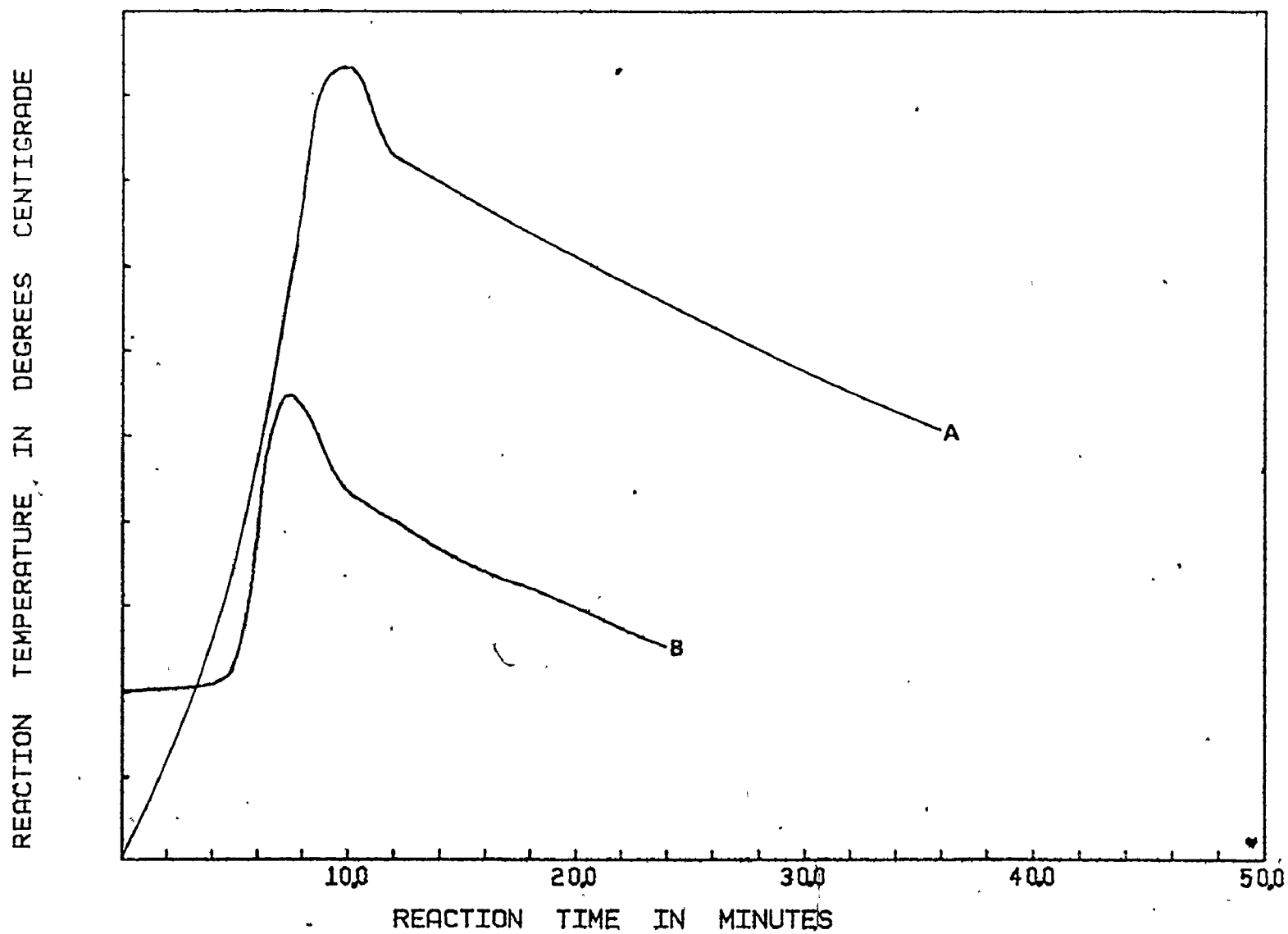


Figure 5.6 : Temperature profiles for points ① and ⑤.  $P_i = 50$  psig. Experiment 29

A point ①

B point ⑤

termine. In addition, the nitrogen was fed from a cylinder at room temperature and the room temperature varied considerably. This will not affect the conversion history but will have an effect on the pressure determinations.

It is compulsory to indicate the maximum temperature obtainable in an adiabatic system. Consider equation (59), if the reactor is perfectly adiabatic and no heat losses would occur, equation (59) transforms to

$$\rho C_p \frac{dT}{dt} = (-\Delta H_p) R_p \quad (79)$$

Assuming for a moment that  $\rho$ ,  $C_p$  and  $(-\Delta H)$  are independent of temperature, this expression can be expressed as:

$$dT = \frac{(-\Delta H_p)}{\rho C_p} R_p dt \quad (80)$$

$$\text{Recalling that } R_p = -\frac{1}{V} \frac{dN_M}{dt} \quad (81)$$

and substituting (81) into (80) and integrating

$$T = T_0 + \frac{(-\Delta H_p)}{\rho C_p} ([M]_0 - [M]) \quad (82)$$

and when complete conversion has been achieved

$$T_A = T_0 + \frac{(-\Delta H_p)}{\rho C_p} [M]_0 \quad (83)$$

Now, remember that  $(-\Delta H)$ ,  $\rho$ , and  $C_p$  are functions of temperature. Make  $T_0 = 100^\circ\text{C}$  and apply a Newton-Raphson procedure to determine  $T_A$ , the maximum adiabatic temperature obtainable. A value of  $430^\circ\text{C}$  was calculated. A path for an adiabatic polymerization is represented by the dotted line in Figure 2.2. Notice that this path goes through the ceiling

temperature and arrives to an equilibrium point where the conversion of monomer is around 70%. The temperature gradients mentioned in Section 4.3, and presented in Figure 4.2, were neglected when dealing with conversion and molecular weight calculations. This can be justified by the fact that the polymer samples were taken at the same spot at which the thermocouple was set. However, when dealing with pressure this approach might not be valid, as a 10°C variation in temperature could result in a 20 psig variation in pressure. As the pressure is an intensive property, its values could be specified at each point of a system. Such property does not require any specification of the quantity of the referred substance and is not additive. Trying to calculate the vapor pressure in such a way would lead to an intractable scheme, as it is impossible to assign a value for pressure to a fixed point since a liquid-vapor interphase is involved. Natural convection and diffusion cannot be disregarded. It would seem logical to suggest the use of a temperature average, biased toward the wall temperature. Provisions for a stirred reactor must be made. It should be pointed out that these variations appeared only when the polymerizations were made under pressure.

## 5.2 Conversion

The simultaneous equations (57) and (59) that describe the system, present serious problems in their solutions. All the rate constants  $k_p$ ,  $k_{d_p}$ ,  $k_t$ ,  $\bar{k}_i$  and  $k_{d_i}$ , the densities  $\rho_m$  and  $\rho_p$ , the heat of polymerization ( $-\Delta H_p$ ), the heat capacity  $C_p$ , the volume contraction etc., are functions of temperature, and some are functions of conversion. The two equations that describe the system become very stiff at the point of the "heat-kick", meaning by stiffness that the slopes of the temperature and conversion histories approach a large value, near infinity. An increase in temperature causes an increase in conversion, which in turn causes a larger increase in temperature and so on. Even the use of Gear's method<sup>(60)</sup> for solving stiff differential equations proved inadequate, unless very short intervals of time were used. As this would require very large computation time, it is impractical. An approximation was used to represent the system. The approximation involves considering the polymerization as being isothermal over a short period of time and integrating equation (57) over this interval. Different intervals were used, selecting the longest one for which the variation from the shorter period was negligible. In other words, the system was solved by isothermal steps. The resulting conversion profiles, using this approach, for the different experimental temperature profiles (Figures 5.2, 5.3 and 5.4) are shown in Figures 5.7, 5.8 and 5.9 respectively.

The conversion of the polymeric samples analyzed by gravimetry and by gel permeation chromatography seemed to be lower than predicted

CONVERSION X

AS

75

FUNCTION OF REACTION TIME IN MINUTES

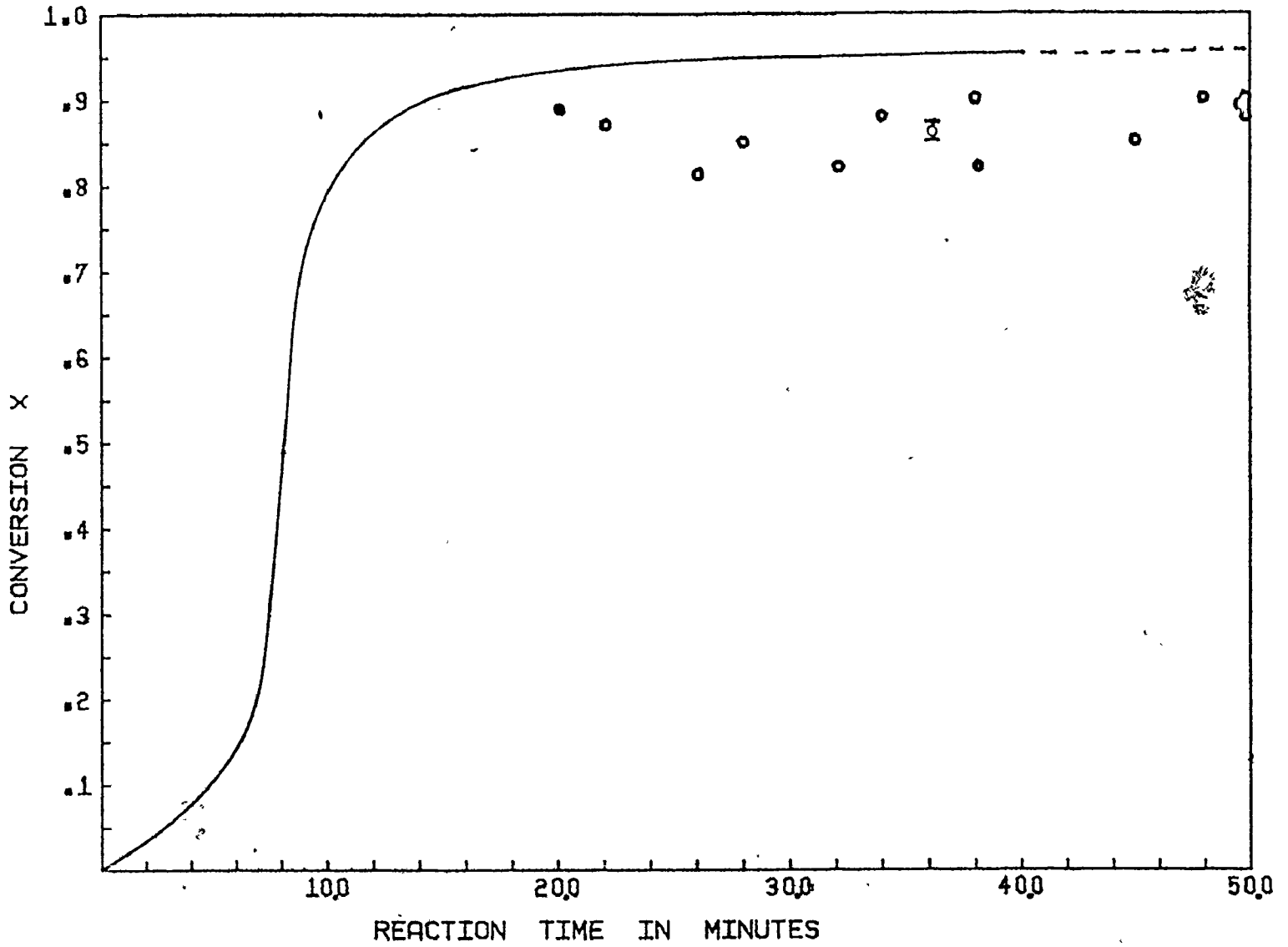


Figure 5.7 : Conversion versus time for average temperature profile at  $P_i = 50$  psig



CONVERSION X

AS

76

FUNCTION OF REACTION TIME IN MINUTES

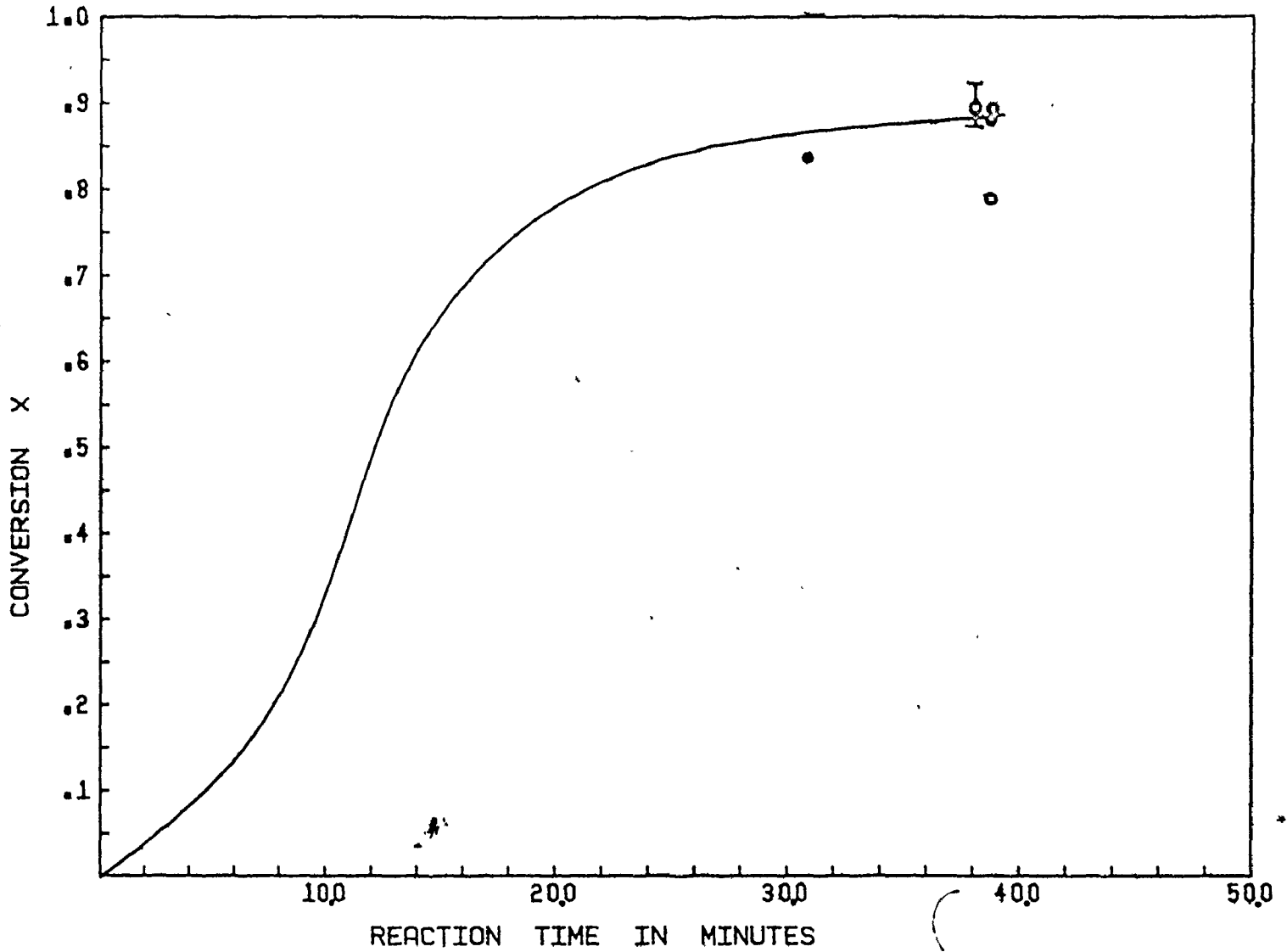
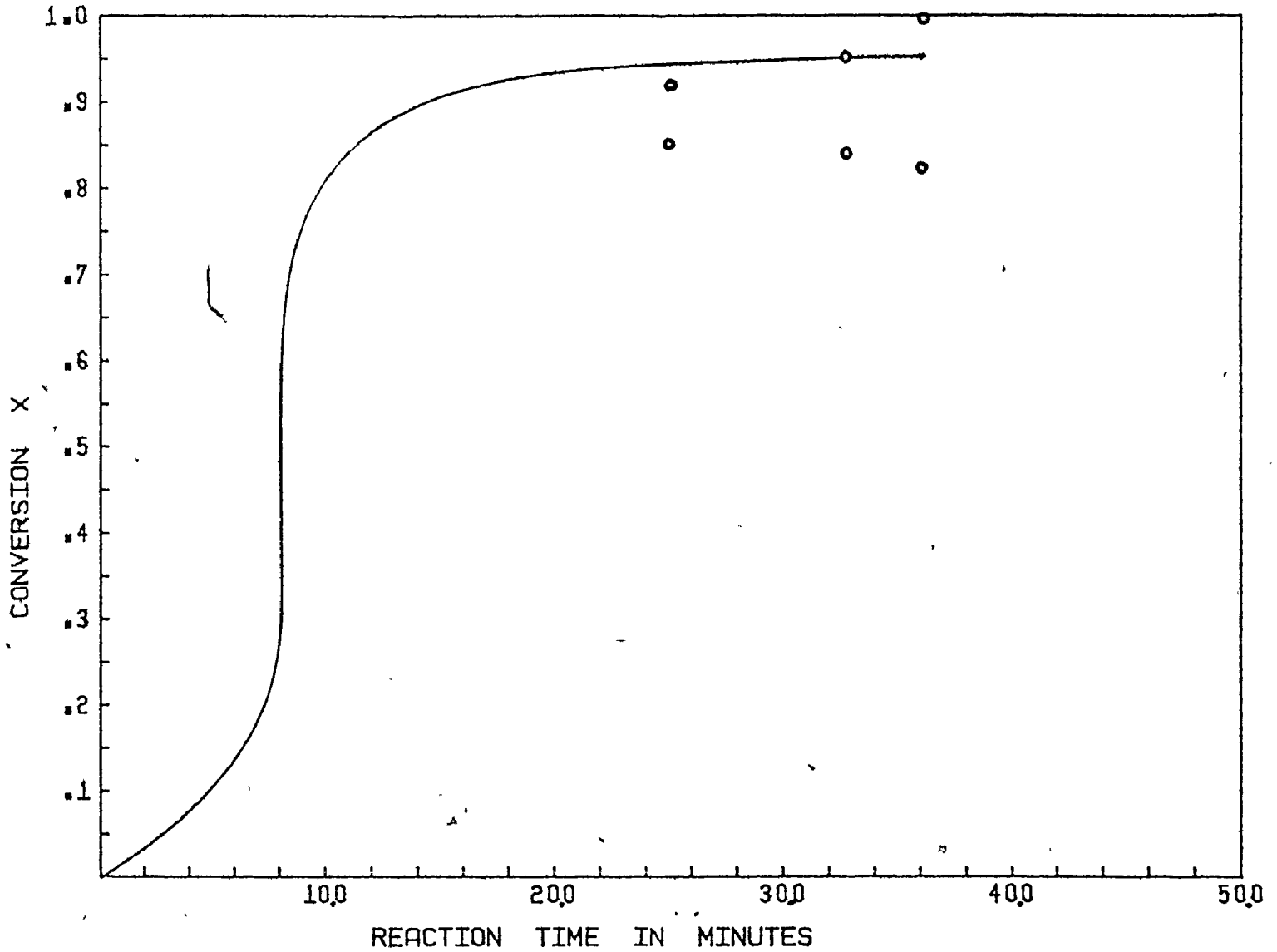


Figure 5.8 : Conversion versus time,  $P_1 = 0$  psig

## FUNCTION OF REACTION TIME IN MINUTES

Figure 5.9 : Conversion versus time,  $P_i = 100$  psig

by the model. Both methods failed to detect the presence of oligomers and degradation byproducts. The presence of small molecule byproducts was detected by the color of the final polymer, from yellowish when the polymerization was done at 0 psig, to deep orange for the polymerizations done under 100 psig. The color disappeared when the polymer was dissolved and reprecipitated, indicating that the molecules responsible for the coloration are small and remain dissolved. In gravimetry, as outlined above, the dimers and trimers and others remain dissolved in the non-solvent. In GPC the oligomers remain masked between the tail of the polymer peak and the monomer peak.

According to Husain and Hamielec<sup>(52)</sup>, the average content of oligomers, when styrene is polymerized at 200-220°C is 4%.

It should be borne in mind that conversion is defined with respect to a monomer basis, therefore the oligomer fraction must be added to the polymer fraction before calculations can be made. This means that for the particular system of this study, the real conversions should be 4-6%, or maybe more, higher than the values determined.

The experimental determinations for conversion are shown in Figures 5.7, 5.8 and 5.9 as dots. The reproducibility of these determinations lies within 1%.

Objections may be made to the sites of the conversion measurements to the effect that almost any curve could pass through these points; however, the measurements of pressure will provide an independent proof of the adequacy of the model. It must be pointed out that

the nature of the system prevented sampling early in the reaction.

The doubts that can be raised about the adequacy of including a depropagation or other degradative reaction in the model must be dissipated by (1) the appearance of color in the polymer, and (2) the experimental conversion-temperature paths. The latter are shown in Figure 2.2, where it can be seen that the paths go near the ceiling temperature and for polymerizations at 100 psig, the path goes over  $T_c$ . Readers must have care in the interpretation of this graph. Time is not included explicitly and final conversion for each path was obtained in the same time, which means that for the longest path, the reaction was faster. Figure 2.1 can help clarify this phenomenon; as the temperature moves near  $T_c$ , the equilibrium constant  $K_e$  approaches 1.

On the other hand, the degradation reaction for a dead polymer chain is too complicated and so far no acceptable scheme and/or data are available for a degradation-polymerization system. Therefore, this reaction will not be considered.

### 5.3 Molecular Weight Development

The molecular weights measured by gel-permeation chromatography (GPC) are plagued with the same illness as the conversion. That is, there is an overlapping of polymer and monomer peaks, masking the oligomer fraction in such a way that it is impossible to evaluate it. Putting extra columns for separating low molecular fractions was not practical, as the resulting huge increases in pressure drop and axial dispersion were not worth the small resolution gained.

Several samples were purified of low molecular fractions. For these samples the molecular weights  $\bar{M}_n$  and  $\bar{M}_w$  were consistently higher than for the unpurified samples, and the polydispersity was somewhat lower.

The molecular weights obtained after using equations (70) and (71) are shown in Figures 5.10 and 5.11. The experimental values corrected by equations (77) and (78) are shown in the same graphs. The experimental molecular weights are lower than the predicted ones. This is explained by two separate facts: (1) The real conversions are higher, so that the points should actually be shifted to the right, and (2) the transfer reactions<sup>(52)</sup> became more and more important at higher temperatures. These reactions include transfer to monomer, transfer to the Diels-Alder adduct (equation 7) and possible transfer to all the oligomer species and degradation byproducts identified by Staudinger<sup>(24)</sup>.

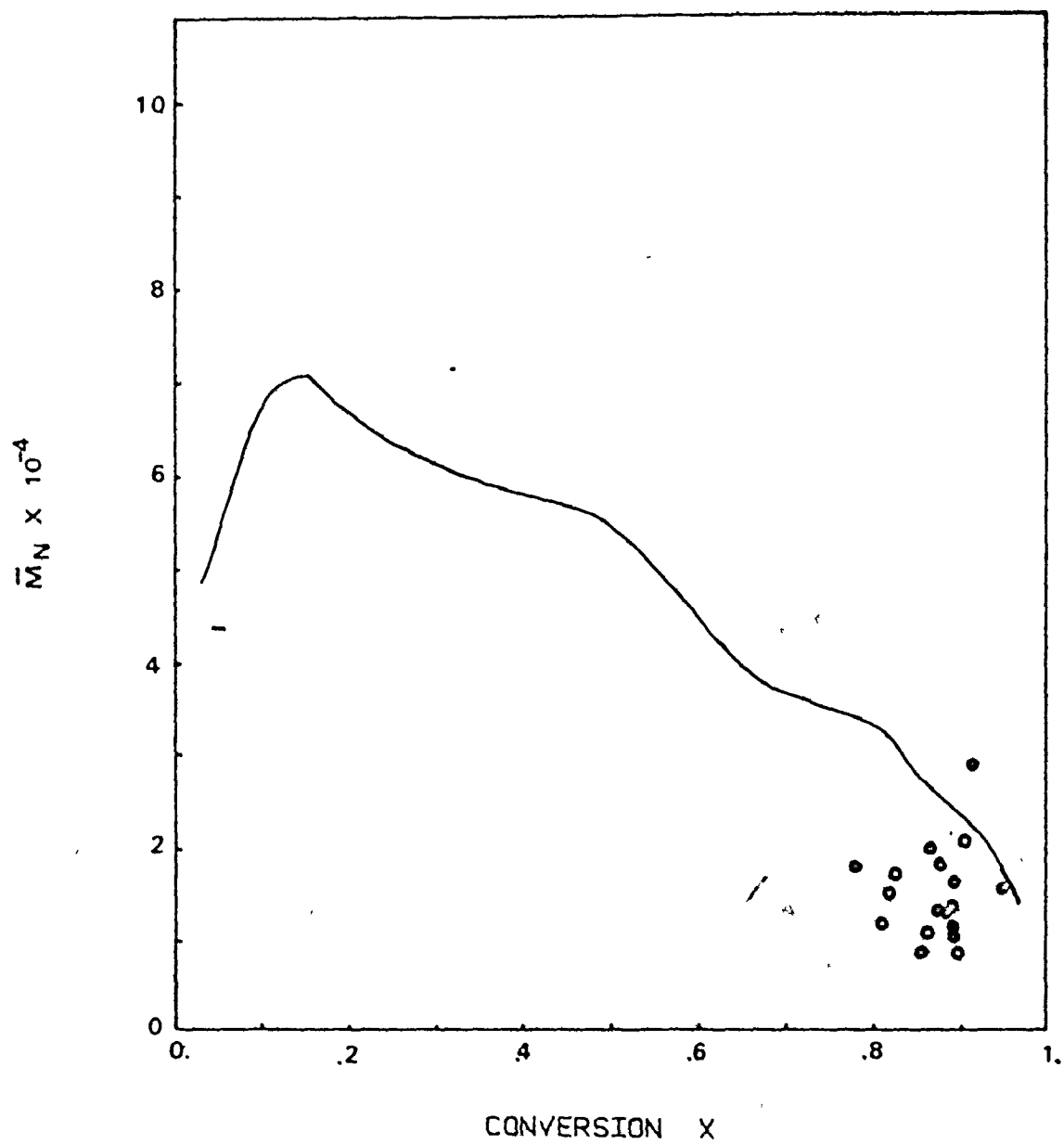


Figure 5.10 : Average number molecular weight versus conversion

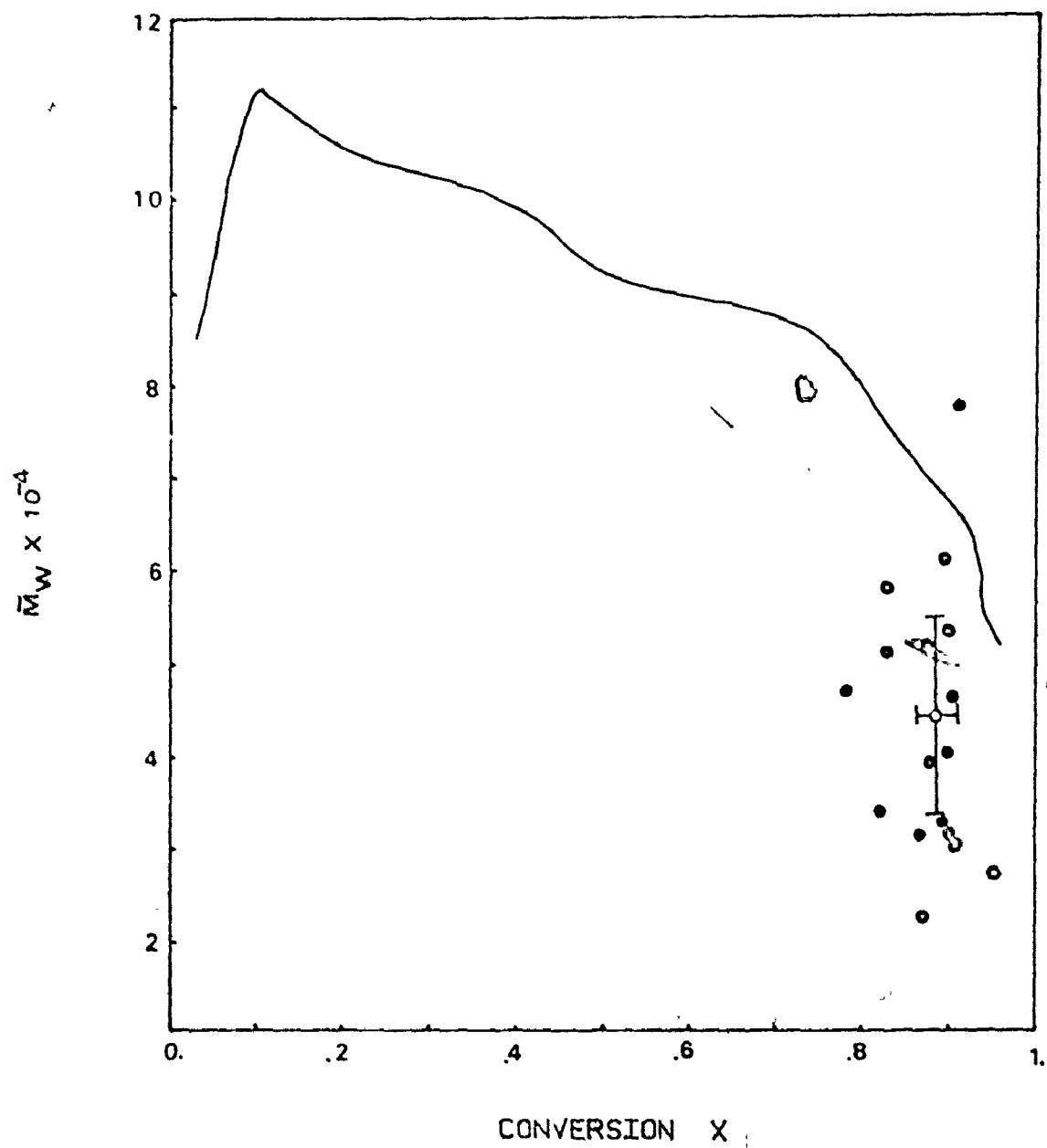


Figure 5.11 : Average weight molecular weight versus conversion

All these possible transfer reactions will increase the value of the parameter  $\tau$  causing a decrease in both molecular weights. The corrections after Hamielec and coworkers<sup>(52,53)</sup> have proven valid up to 230°C, the extrapolation of equation (68) upwards cannot be assumed to be valid. Therefore, the predicted molecular weights should actually be lower, mainly in the region from conversion equal to 0.4 and higher.

Biesenberger and Capinpin<sup>(17)</sup> established that the behaviour of the cumulative number average molecular weight  $\bar{M}_n$  with respect to conversion will determine the mechanism that dominates the polymerization under runaway conditions. The predictions from the model used in this study present a mixed behaviour, there are oscillations.

At low conversions (< 20%) the system undergoes polymerization in a mixed dead end-gel effect fashion. That is, the reaction medium is becoming viscous and the initiators are being consumed very fast. This can be assumed as a pure mild gel-effect polymerization during which the molecular weight increases. Remember the temperature and the rate of polymerization are increasing as well.

After the "heat-kick", the molecular weight  $\bar{M}_n$  decreases, but continues oscillating; this is a mixed behaviour between a pure conventional polymerization and a mild gel-effect. This is supported by the behaviour of  $k_t/k_{t_0}$ , which is presented in Figure 5.12, compared with the  $k_t/k_{t_0}$  ratio for several of Hui's<sup>(22)</sup> experiments. Near the end of the reaction, as the temperature decreased, the growing influence of the gel effect was again noticed. Similar behaviour was observed for the instantaneous number molecular weight.



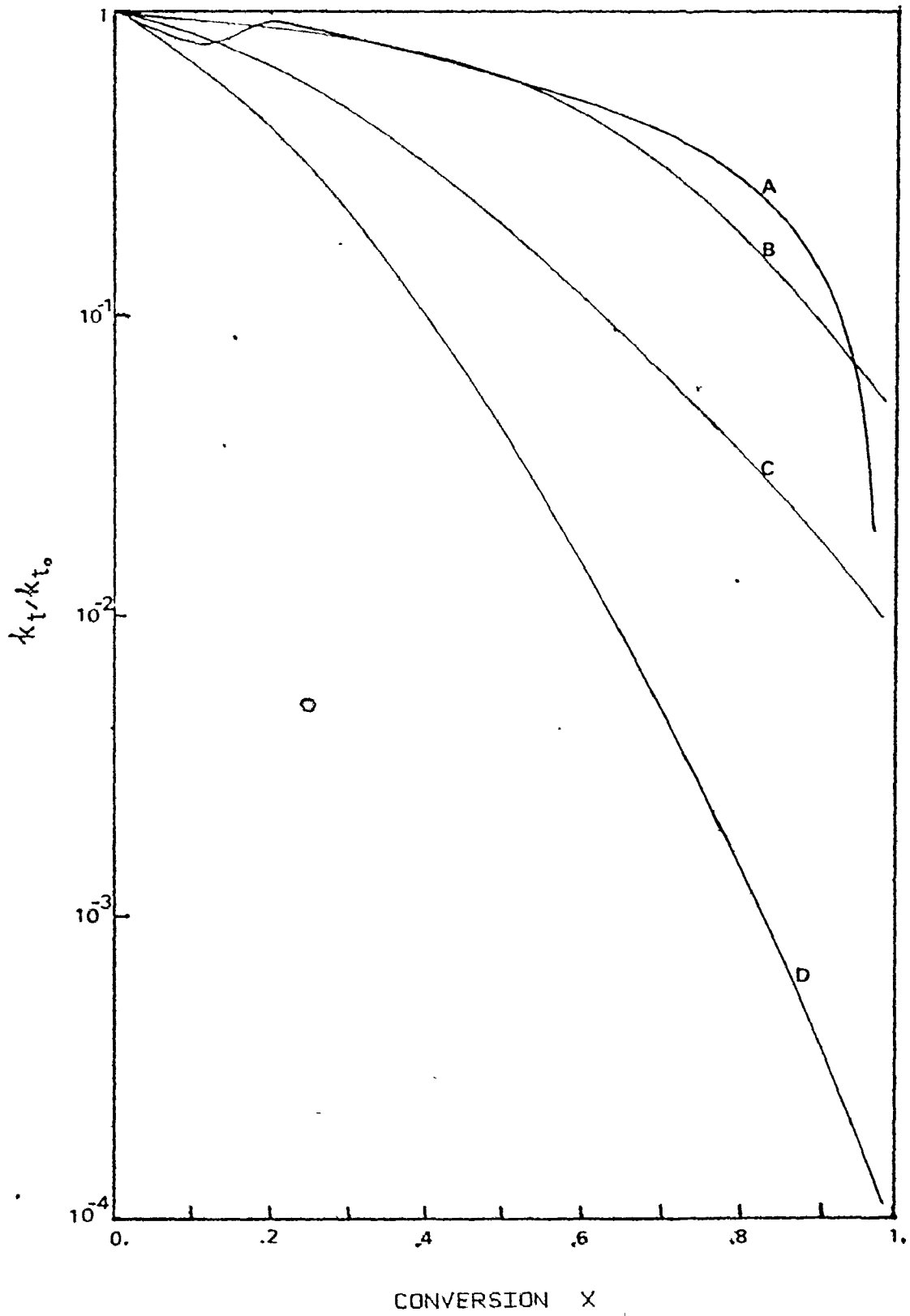


Figure 5.12 :  $k_t/k_{t_0}$  versus conversion

- A. Average Temperature Profile this study (see Figure 5.2)
- B.  $T = 240^\circ\text{C}$  (23)
- C. Experiment 6 (22)
- D. Experiment 7 (22)

The above description and the results from experiment 26 where a larger amount of initiator was used, producing the same temperature rise as the other experiments where less initiator was used (Figure 5.13), indicate that there is no dead end polymerization for styrene and all polymers are able to polymerize thermally. Remember the dead end polymerization was defined as one in which the reaction stops short of completion when the initiator is depleted.

Figure 5.14 shows that for a runaway reaction, no matter how much initiator is put in, the initiator will be completely depleted within seven minutes, or less; and the polymerization continues exclusively due to thermal initiation.

A more accurate measurement of molecular weights is desirable. The different polymer samples give skewed chromatograms and require large skewing corrections. Although the skewing factor (SK) appears to be fairly constant, the dispersion factor ( $h$ ) does not have a clear correlation with respect to volume peak elution (22,23). See, for example, Table 4.3. The skewing factor is extremely sensitive to experimental variation. In addition, as a true calibration curve was used in the GPC determinations, the slope of the calibration curve ( $D_2$ ) was not constant. Although  $D_2$  was estimated locally at peak elution volume for each sample, new improved equations must be developed to supersede equations (77) and (78).

REACTION TEMPERATURE IN DEGREES CENTIGRADE  
AS FUNCTION OF REACTION TIME IN MINUTES

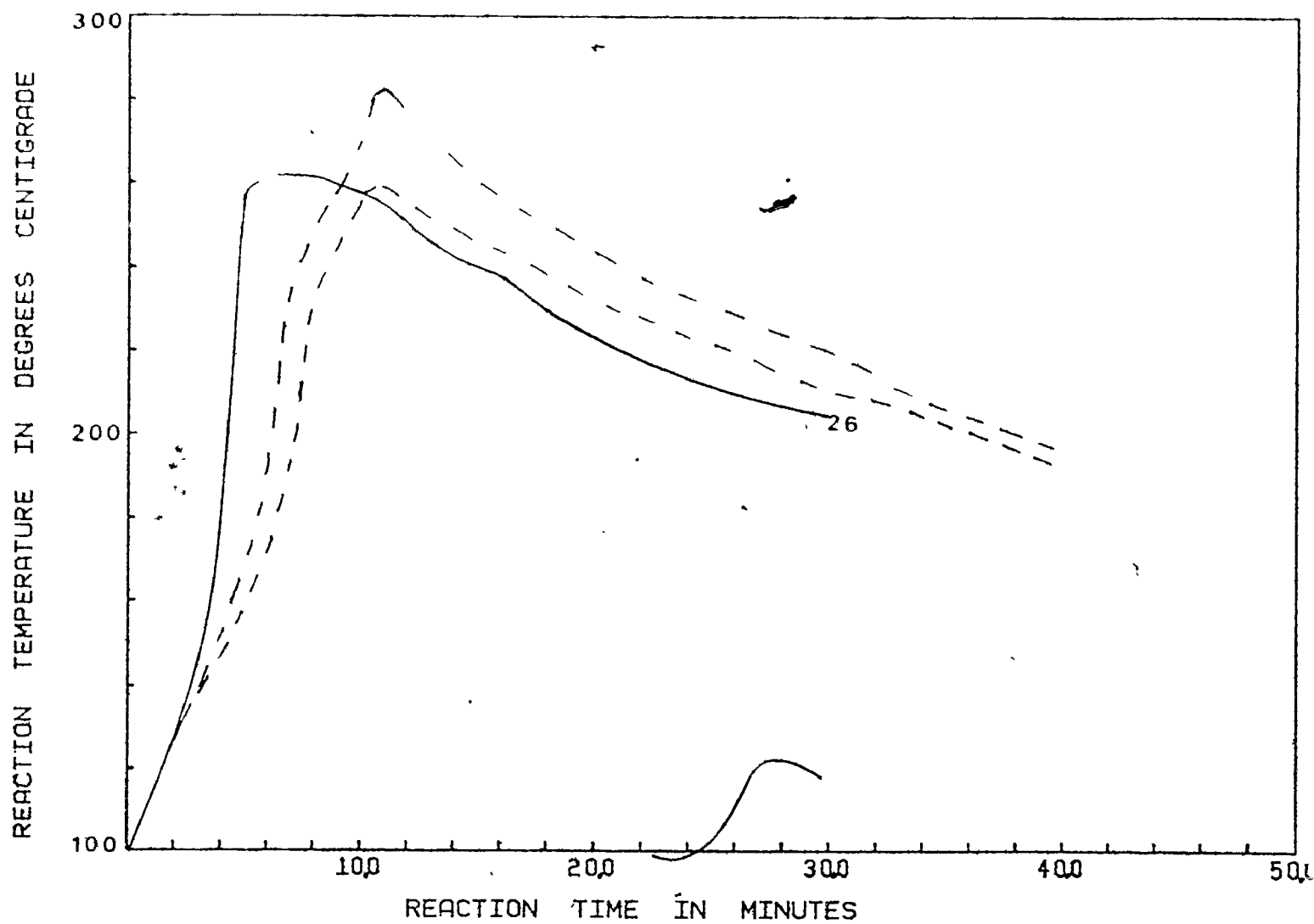


Figure 5.13 : Effect of amount of initiator on the temperature profile

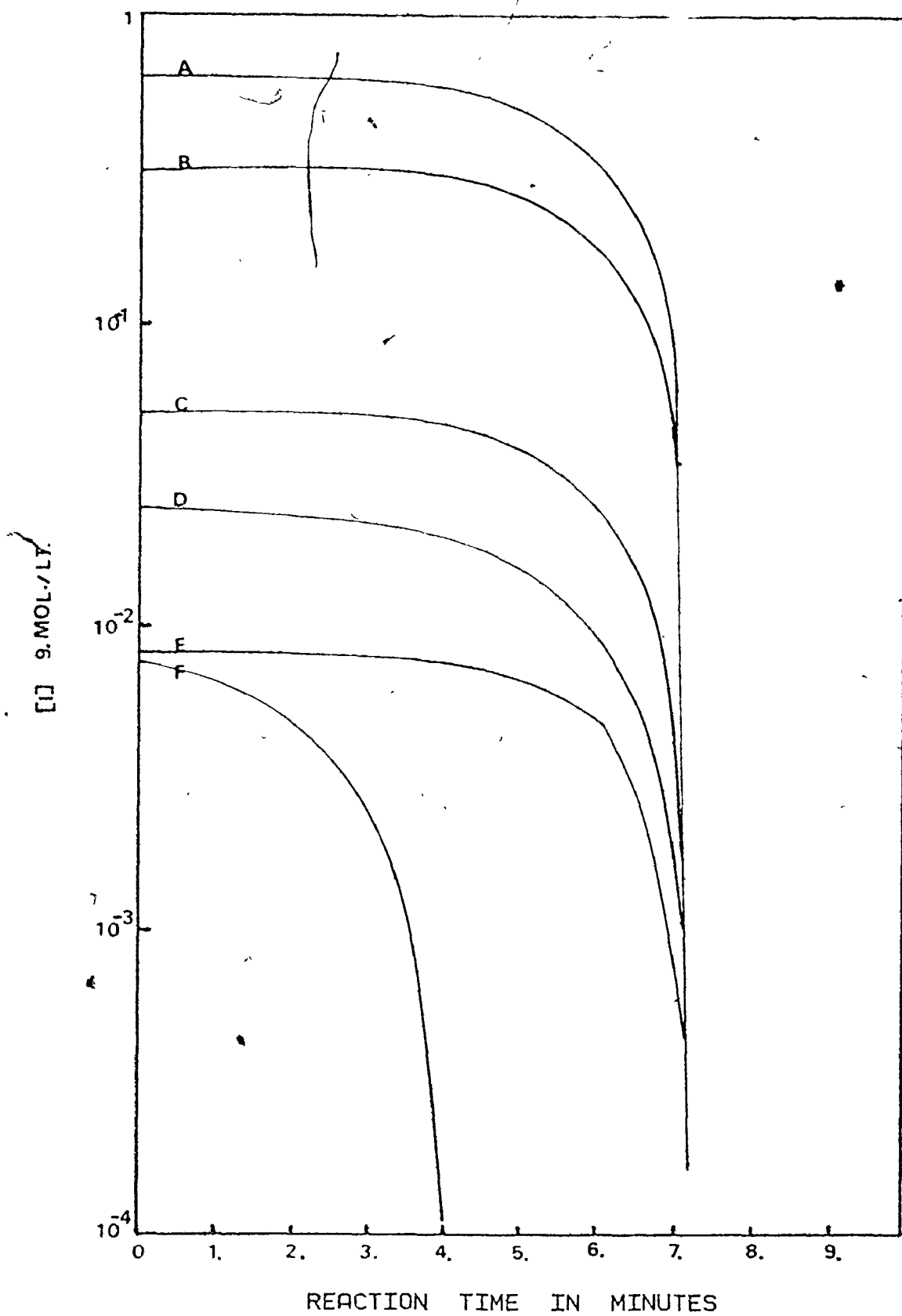


Figure 5.14 : Initiator concentration versus reaction time

A	10% DTBP	D	0.37% DTBP
B	5% DTBP	E	0.12% DTBP
C	1% DTBP	F	0.12% AIBN

(The corresponding temperature profile is shown in Fig.5.13)

#### 5.4 Pressure Development

The vapor pressure of styrene was predicted by using a regression curve for data reported in the literature<sup>(61)(62)</sup>. This approach gave a better fit than the use of Antoine's equation. Both expressions are presented in Appendix A1.

As the reaction mass undergoes a volume contraction, the void volume in the reactor increases. The total predicted pressure was corrected for this effect as well as for the changing temperatures in the vapor phase.

As before, the experimental and predicted profiles are presented for the three settings of experimental conditions at 0, 50 and 100 psig, in figures 5.15, 5.16 and 5.17 respectively. A good fit was obtained for the experiments in which no nitrogen was used as a pressurizing medium., while the experiments using nitrogen presented increasing deviations with the increasing partial pressure of nitrogen. Although the heat capacity of nitrogen is small compared to the one of the liquid mass, as the nitrogen was fed cold, it must be responsible to some extent for the deviations. Figure 5.18 shows the temperature profiles for experiment 32, in which one thermocouple was set in the reaction mass and the other in the centre of the vapor phase. It can be observed that it took six minutes for the gas phase to reach 145°C, the temperature of the walls, while in the same lapse of time the temperature of the fluid mass was already 200°C. The corresponding predicted and experimental pressure pro-

# PRESSURE

89

AS FUNCTION OF REACTION TIME IN MINUTES

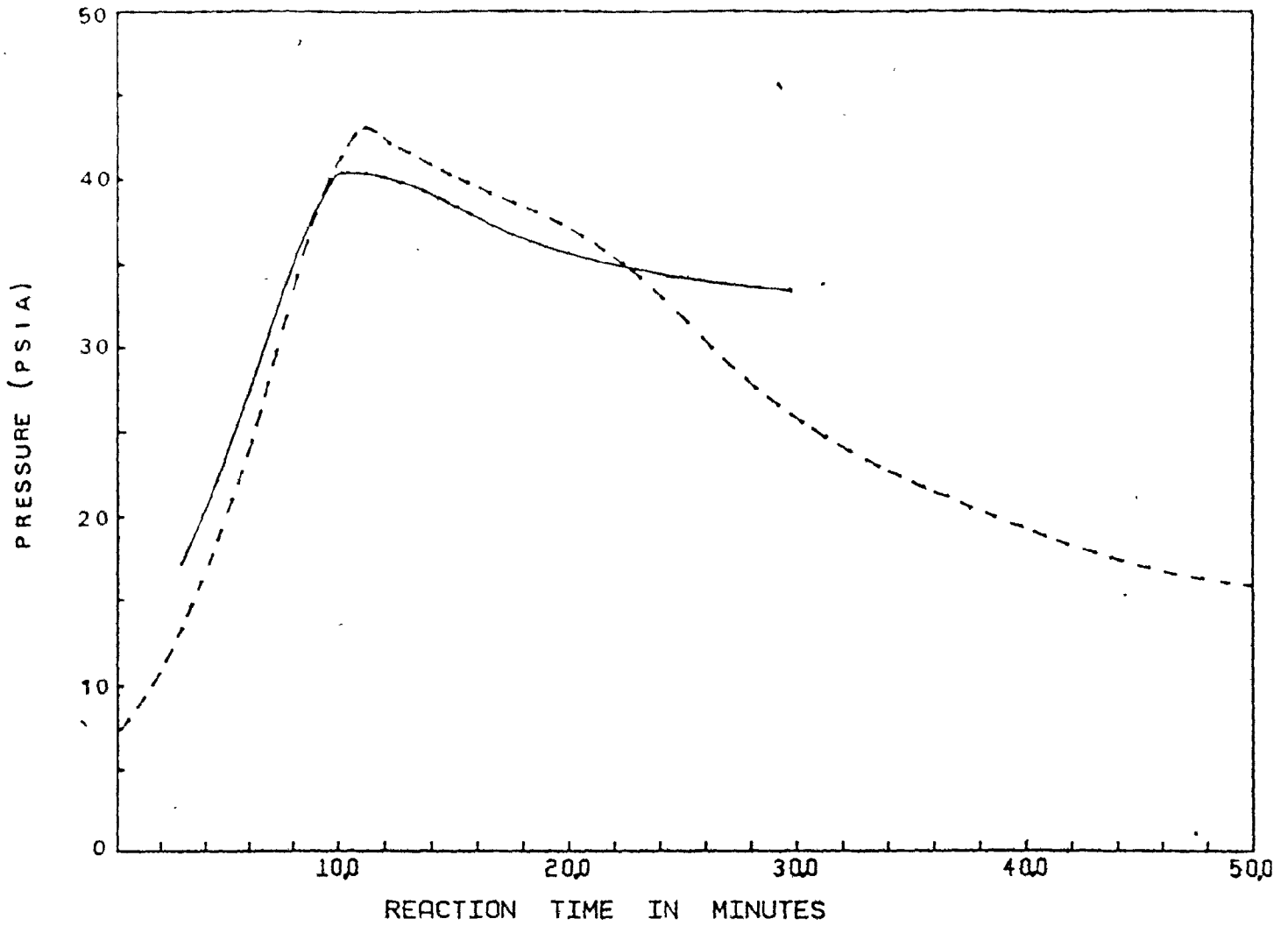


Figure 5.15 : Pressure versus time,  $P_i = 0$  psig

————— Experimental  
----- Predicted

# PRESSURE

90

AS FUNCTION OF REACTION TIME IN MINUTES

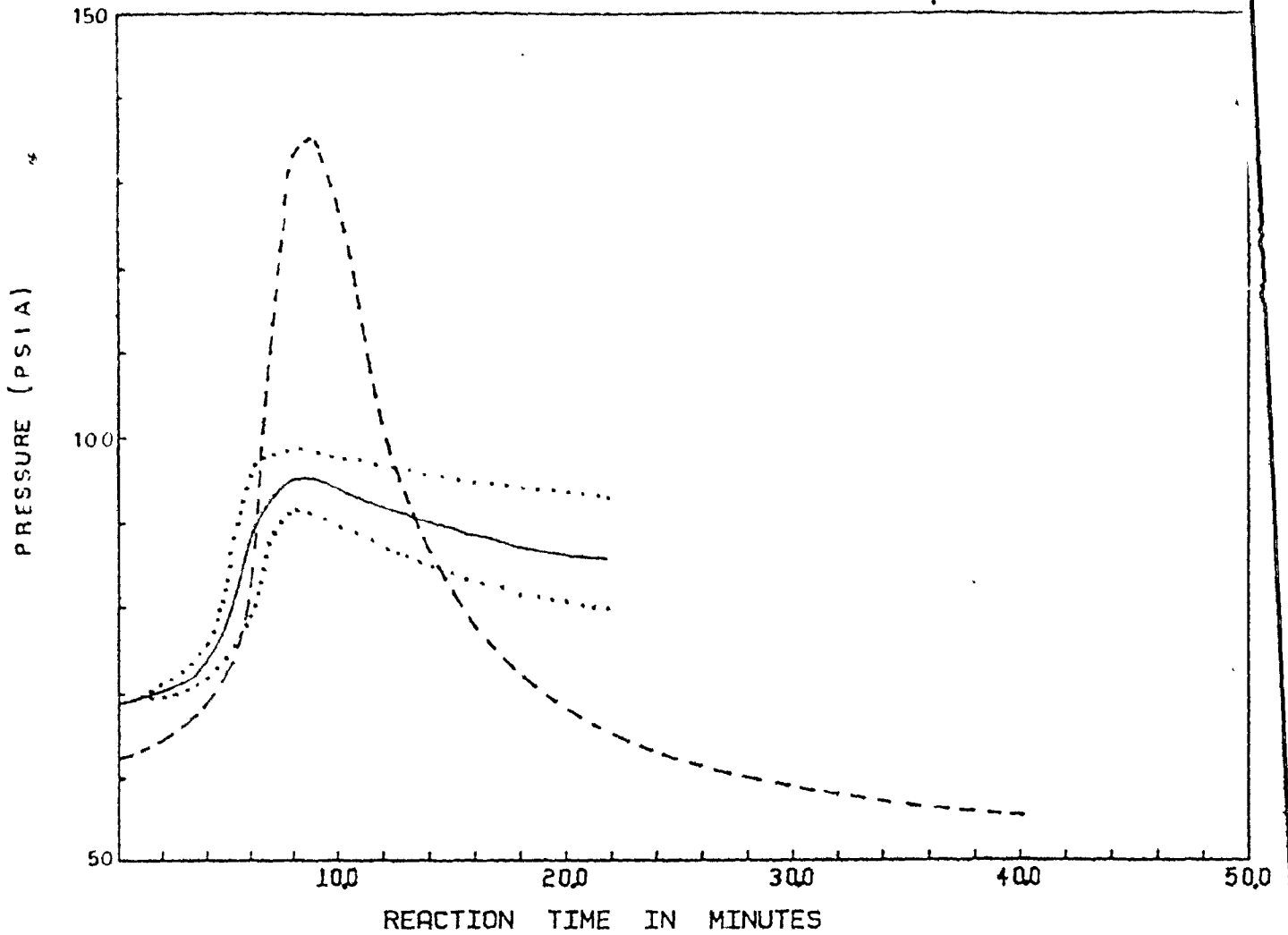


Figure 5.16 : Pressure versus time,  $P_i = 50$  psig

————— Experimental  
----- Predicted

# PRESSURE

91

AS FUNCTION OF REACTION TIME IN MINUTES

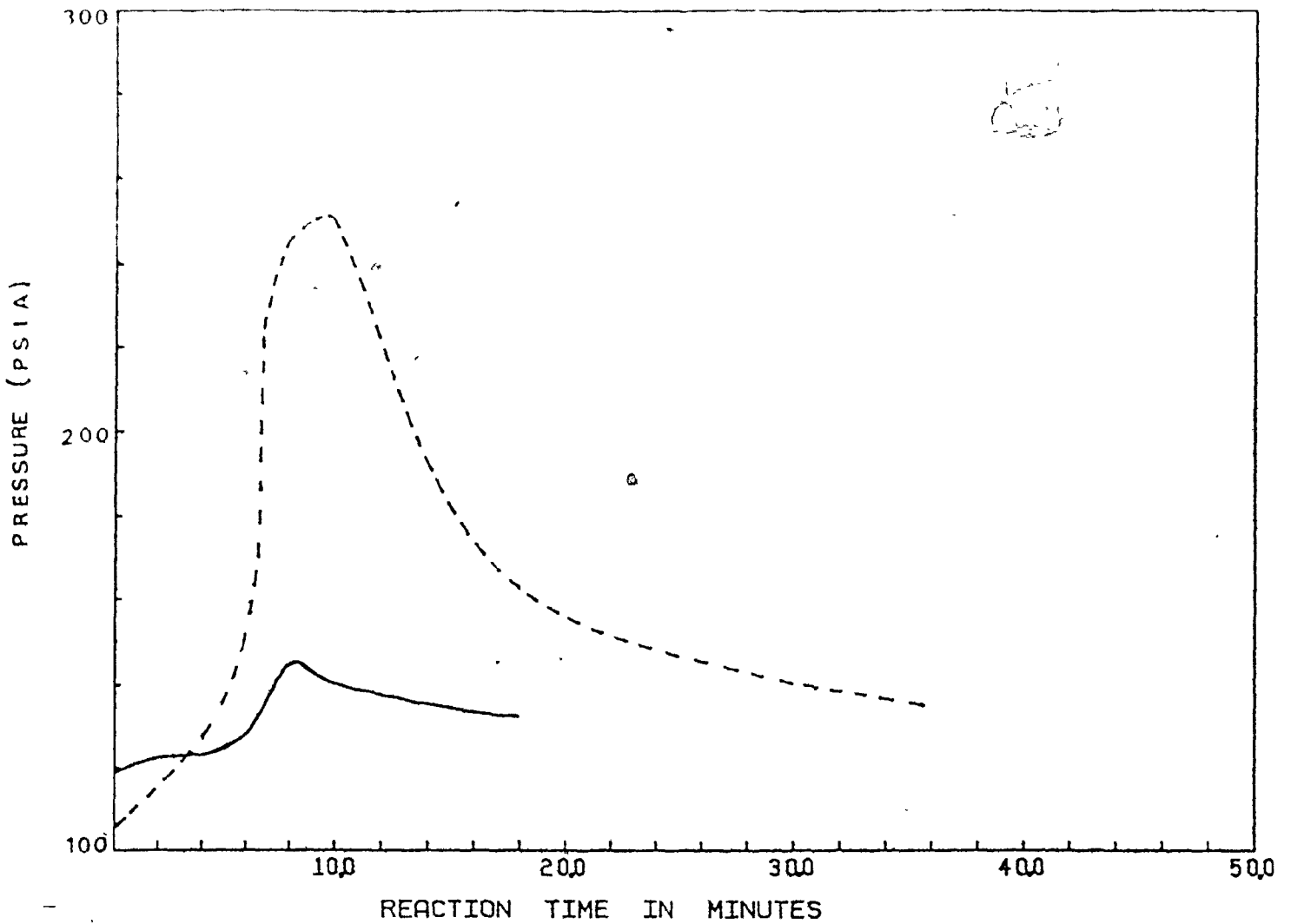


Figure 5.17 : Pressure versus time,  $P_i = 100$  psig

————— Experimental  
----- Predicted



REACTION TEMPERATURE IN DEGREES CENTIGRADE  
AS FUNCTION OF REACTION TIME IN MINUTES

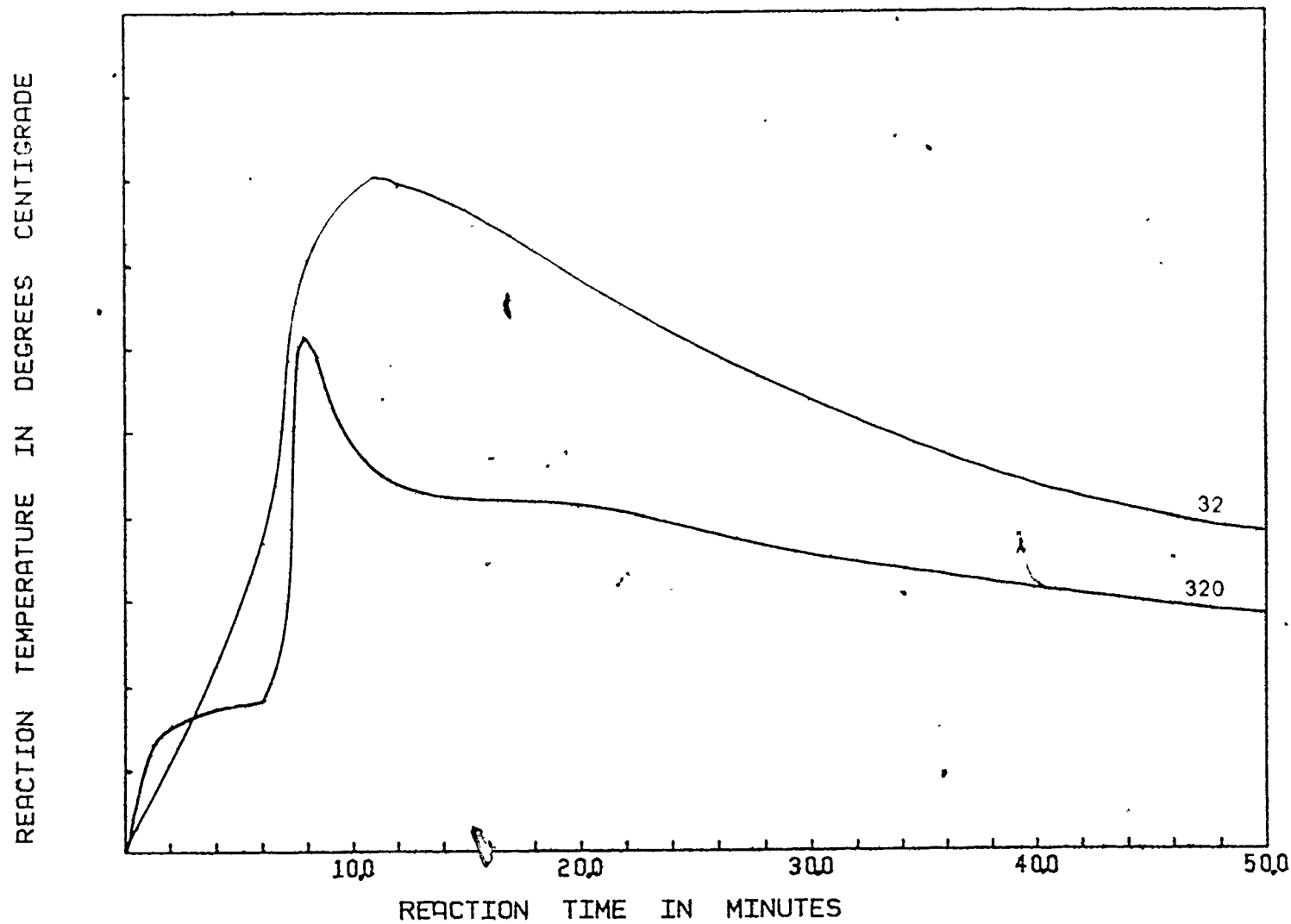


Figure 5.18 : Temperature profiles, experiment 32.

32 Thermocouple at point ②

320 Thermocouple at point ④

files can be found in Figure 5.19. It can be seen that the total pressure of the system is greatly affected by the partial pressure of nitrogen. This is supported by the fact that nitrogen prevented vaporization of styrene to a large extent; whenever the reactor was vented with the intention of flashing the system, an almost undetectable amount of styrene came out. This styrene was collected in a glass cylinder immersed in chilled water and the amount collected was just enough to wet the walls. Therefore, the variations in temperature in the liquid phase are not the same as the variations in the vapor phase, causing the discrepancy reported. The use of devices for injection and sampling under pressure without having to open the reactor would greatly improve the results and predictions. If the temperature of both phases were in equilibrium, as in the experiments done at 0 psig, the pressure could be predicted adequately. A locii for the dependence of pressure on temperature and conversion is presented in Figure 5.20.

The solubility of nitrogen in styrene was determined using Osburn and Markovic's<sup>(64)</sup> method. It was found that even under the most severe conditions, the amount of nitrogen dissolved in styrene is less than 0.01 mole fraction. This cannot by itself explain the discrepancy between prediction and experiments and therefore was not considered.

# PRESSURE

94

AS FUNCTION OF REACTION TIME IN MINUTES

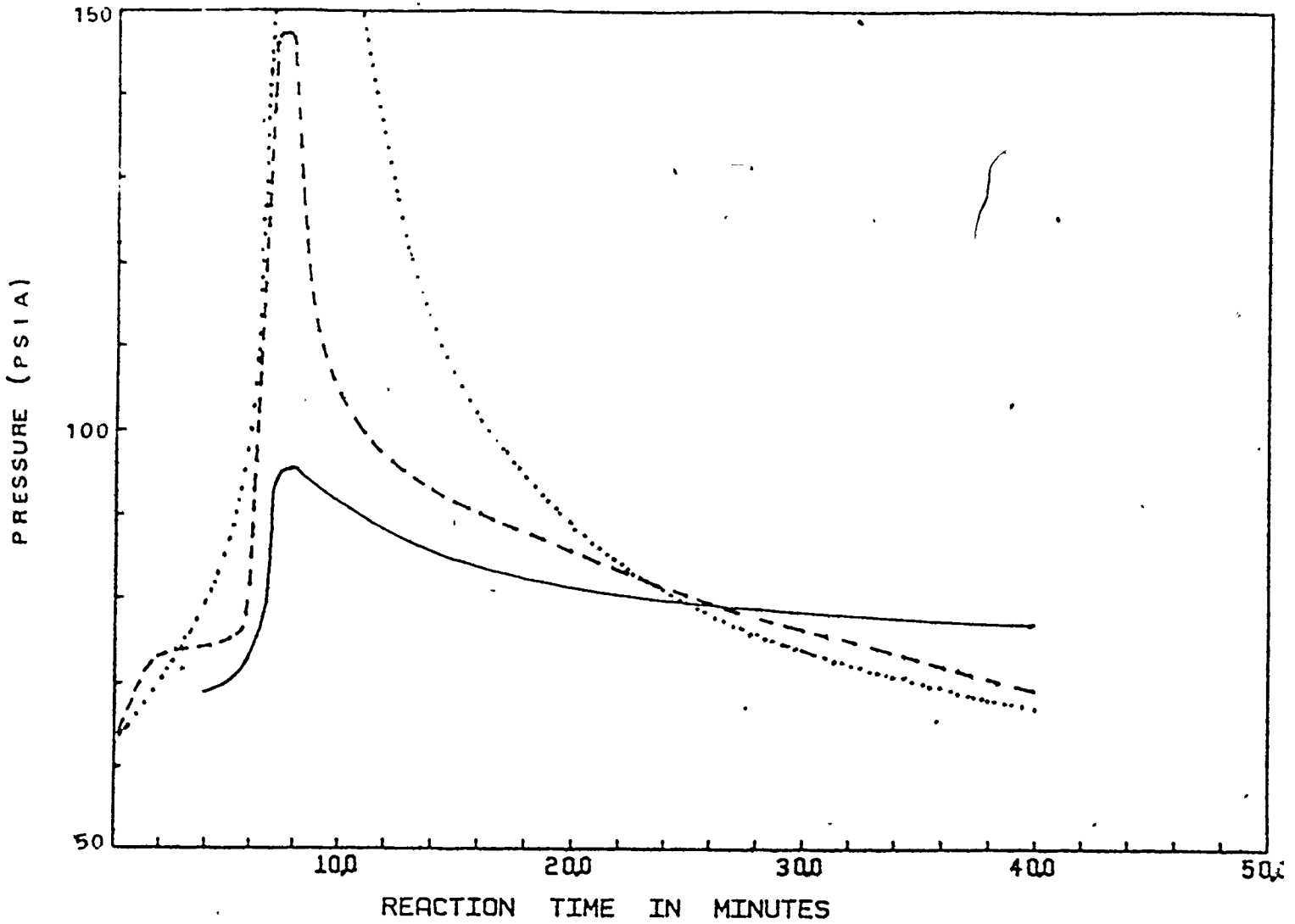


Figure 5.19 : Pressure profiles, experiment 32

- Experimental
- - - - - Predicted by temperature profile 320
- ..... Predicted by temperature profile 32

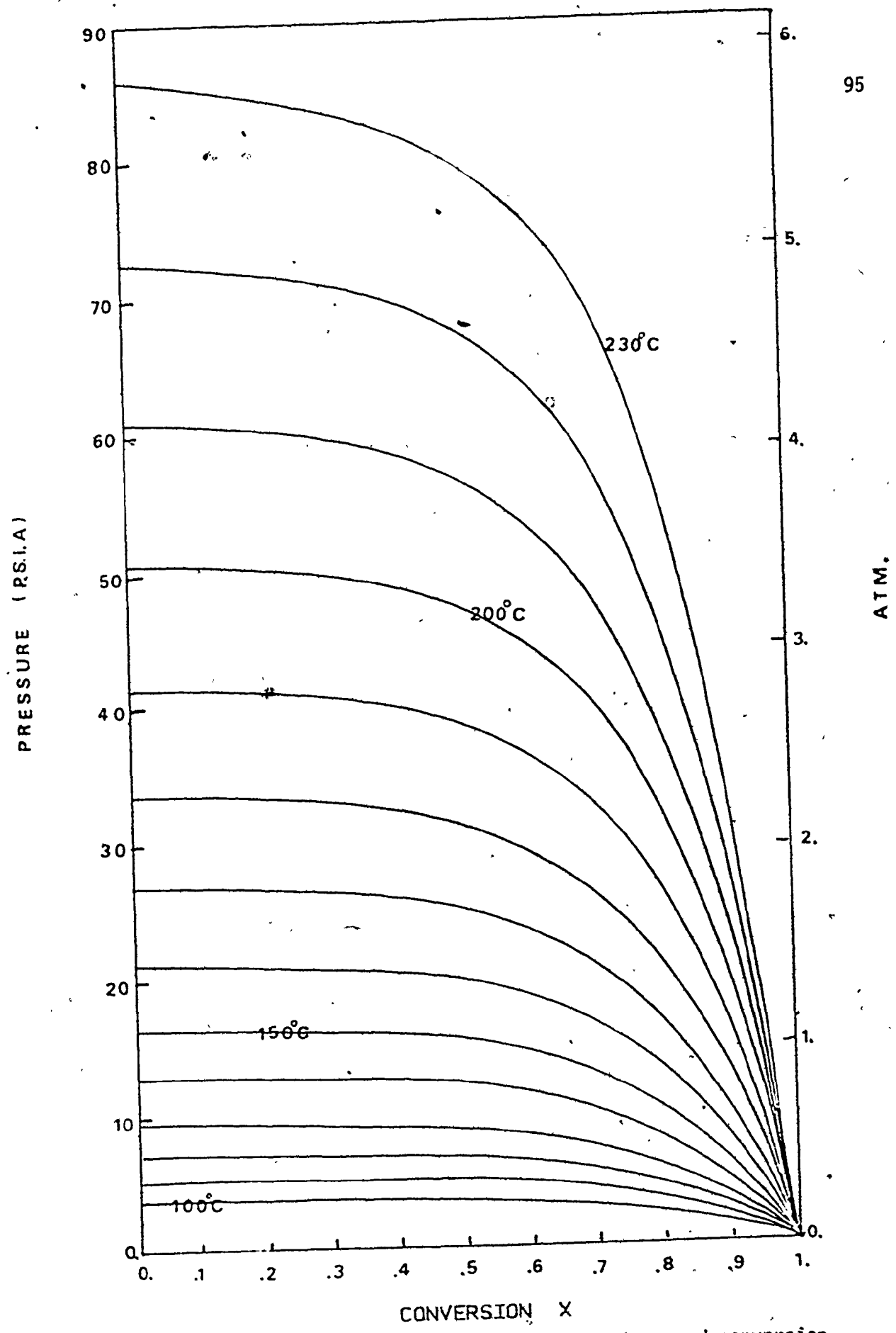


Figure 5.20 : Pressure as function of temperature and conversion

## 6. CONCLUSIONS

1. It must be obvious, after analysis of the foregoing material, that Gordon's assumptions 3(a) and 3(b) are not valid as there are physical changes, i.e. changes in density, in heat capacity, in viscosity and in evaporation of monomer, and chemical changes such as depropagation, degradation and transfer reactions which affect the kinetics of the system. In addition, the main mechanism of the reaction is affected by temperature, the gel-effect is very sensitive to it. Hence, Gordon's assumptions provide an idealization; a more realistic approach can be used nowadays, taking into account all the deviations already discussed and solving the system in a numerical form.
2. The kinetic model of Hui and Hamielec<sup>(53)</sup> and the extension by Husain and Hamielec<sup>(52)</sup> can be extrapolated up to temperatures of 310°C, provided that a term for the depropagation reaction is included. Such a term was included in the present work. All polymerizations made above 260°C must include this reaction. This model is able to predict conversion, molecular weights and pressure as functions of time.
3. Pressure measurements can be used to follow the conversion of monomer during polymerization, made either in isothermal or non-isothermal mode. The partial pressure of inerts must be adequately accounted for.

4. A runaway reaction will go near to complete conversion in a short time, being limited only by the amount of oligomers and degradation by-products, which may be non-reactives, produced. The only limitation is that the monomer must be capable of undergoing thermal polymerization, otherwise dead end polymerization will occur.

5. No dead end polymerization exists for styrene, it will take time but eventually complete conversion of monomer will be obtained.

6. The molecular weights of polymer produced in non-isothermal polymerization are low; the number average between 9000 and 30000 and the weight average between 20000 and 70000. However, the polydispersity (2.0 - 2.5) is lower than for high temperature isothermal polymerizations. This could be due to thermal degradation which tends to narrow the molecular weight distribution if the chains break near their centre.

Therefore, polymers with desired molecular weights and polydispersities can be produced by non-isothermal polymerizations, either by runaway reactions or by temperature-programmed polymerizations.

APPENDIX A1Physical Properties of Styrene and Polystyrene

The expressions for the following properties were either obtained from the literature or adjusted using a non-linear least squares regression algorithm. In the latter case they are marked with an asterisk(\*). In all cases references are indicated.

A1.1 StyreneDensity

$$\rho_m = 924. - 0.918 (T - 273) \text{ g/l} \quad (65)$$

Heat Capacity

$$C_p = 41.85 - 0.0664 (T - 273) + 0.0003069 (T - 273)^2 \text{ cal/g mol } ^\circ\text{C} \quad (66)$$

Vapor Pressure

$$\text{a) } \log_{10} P = -1.7135 + (29.045644 - 3300/T - 6.97343 \log_{10} T) \text{ lb/in}^2 \quad (61)^*$$

b) Antoine's Equation

$$\log_{10} P = 7.21947 - \left(\frac{1627}{T-4.3}\right) \text{ mm Hg} \quad (67)$$

Solubility Parameter

$$\delta_s = 9.3306 \left(\frac{\text{cal}}{\text{cm}^3}\right)^{1/2} \quad (51)$$

Boiling Point

$$T_{b/1 \text{ atm}} = 145.2 \text{ } ^\circ\text{C}$$

Heat of vaporization, viscosity, surface tension and thermal conductivity data can be found elsewhere<sup>(61)</sup>.

## A1.2 Polystyrene

### Density

$$\rho_p = 1084.8 - 0.605 (T - 273) \text{ g/lit} \quad (65)$$

### Heat Capacity

$$C_p = 27.5 + 0.05 T \frac{\text{cal}}{\text{g-mol } ^\circ\text{K}} \quad (51)^*$$

### Heat of Polymerization

$$(-\Delta H_p) = 11.01 + 0.026 T - 0.239 \times 10^{-4} T^2 \frac{\text{k cal}}{\text{g mol}} \quad (9)^*$$

### Entropy of Polymerization

$$(-\Delta S^\circ) = 8.229 + 0.0825 T - 7.909 \times 10^{-5} T^2 \frac{\text{cal}}{\text{g mol } ^\circ\text{K}} \quad \begin{matrix} (9) \\ (32) \\ (43)^* \end{matrix}$$

### Glass Transition Temperature

$$T_g = (373 - 10^5/\bar{M}_v) = 80 - 100^\circ\text{C} \quad (51)$$

### Solubility Parameter

$$\delta_p = 9.0139 \left(\frac{\text{cal}}{\text{cm}^3}\right)^{1/2} \quad (51)$$

### Melting point

$$T_m = 240 - 250^\circ\text{C} \quad (51)$$

### Ceiling Temperature

$$T_c = 300^\circ\text{C} \quad (34)$$

### Thermal Conductivity

$$k = 0.128 [\text{W m}^{-1} \text{K}^{-1}] \quad (51)$$

Additional thermal and mechanical data can be found elsewhere<sup>(51)</sup>.



## APPENDIX A2

### Review of Pressure Relief Systems.

In the event of occurrence of a runaway reaction, the main concern in industry is the resulting pressure build-up. Two approaches are commonly used:

1. Design the vessel to withstand the maximum pressure expected. This has the limitations that (a) the heat transfer capacity of the reactor would be somewhat reduced, (b) the estimation of pressure can be unreliable, and (c) if the polymer is infusible or difficult to dissolve, the reactor will be down for a lengthy period of time.
2. Design the reactor for a lower pressure and provide vent equipment to relieve any over-pressure. This is accomplished by using safety rupture discs designed to break at a determined pressure. The length and diameter of the venting line are critical.

Remember that the reaction mixture will be in a runaway condition, which means that it will be at high temperature and conversion and that the vent discharge will be a very viscous two-phase gas-liquid mixture, whose flow properties would be hard to estimate.

#### A2.1 Empirical Methods

The most commonly used is the Factory Insurance Association method,

based on the exothermicity, i.e. the heat released per unit volume of reacting mass. A series of graphs are available<sup>(15)</sup>.

Another method was indicated by Schlegel<sup>(68)</sup>. He suggested that the diameter of the venting line must be at least 0.0012 sq.in per gallon of reactor capacity. Both methods are very primitive and lead to a great over design.

#### A2.2 Semi-theoretical Method

This method was first proposed by Boyle<sup>(13)</sup> and it is based on the fact that the vent discharge mixture will be a liquid or a vapor-liquid mixture. The basic assumption is that vent flowrate could offset the rate of vaporization. However, the author assumed that the vent discharge would be a liquid and, more important, used an extremely simple approximation for the kinetics of the system. Under different conditions this approach could result in undersized relief systems.

#### A2.3 Theoretical Method

Huff<sup>(54)</sup> presented a more sophisticated treatment, including the two-phase flow, the non-Newtonian behaviour of the mixture and the pressure rise using the Flory-Huggins expression. In spite of not using a sound kinetic model, his approach is so far the best one available. A flow diagram for this method is presented in Figures A2-1 and A2-2.

In conclusion, no accurate method exists and the design data obtained by any of the above methods should be multiplied by a safety factor.

The inclusion of a kinetic model as the one tested in this study may improve the reliability of these designs.

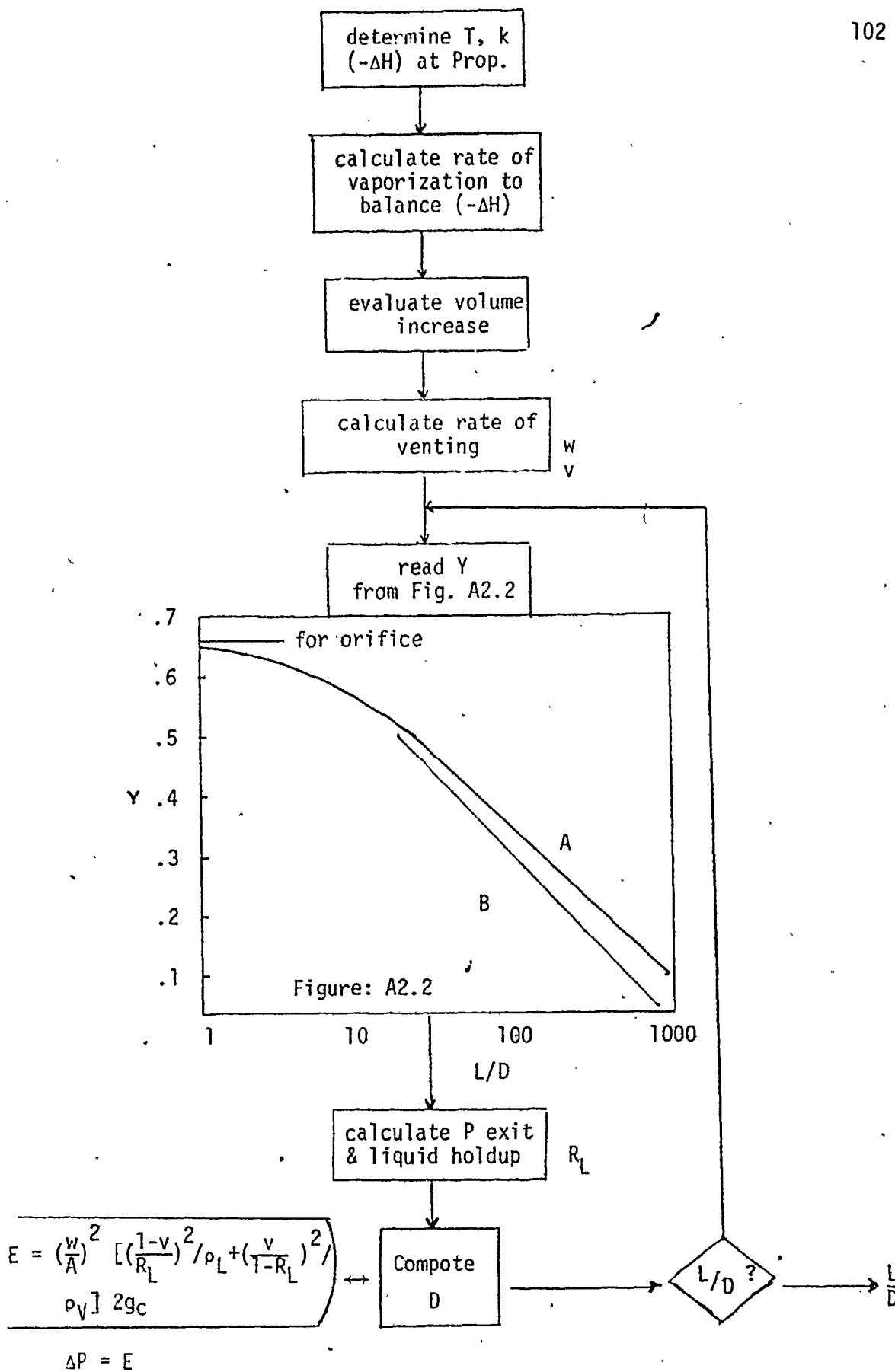


Figure A2.1 Huff's Algorithm.

APPENDIX A3Estimation of Heat Transfer Coefficient for Reactor

The following analysis follows Bird et al.<sup>(63)</sup>. Having a system as represented by Figure A3-1, with the values of the different radii and thermal conductivities as given in Table A3-1, the application of the equation of energy in cylindrical coordinates gives:

$$r_o q_o = -k_1 r \frac{dT}{dr}^{01} \quad (a)$$

$$r_o q_o = -k_2 r \frac{dT}{dr}^{12} \quad (b)$$

$$r_o q_o = -k_3 r \frac{dT}{dr}^{23} \quad (c)$$

where the superscripts 01, 12 and 23 represent the interval of variation; integration of these equations, assuming constant thermal conductivities gives:

$$T_o - T_1 = r_o q_o \left( \frac{\ln r_1/r_o}{k_1} \right) \quad (d)$$

$$T_1 - T_2 = r_o q_o \left( \frac{\ln r_2/r_1}{k_2} \right) \quad (e)$$

$$T_2 - T_3 = r_o q_o \left( \frac{\ln r_3/r_2}{k_3} \right) \quad (f)$$

at the two liquid-solid interfaces:

$$T_F - T_o = q_o/h_o \quad (g)$$

$$T_3 - T_B = q_3/h_3 = q_o r_o/h_3 r_3 \quad (h)$$

Adding equations d, e, f, g and h, we can obtain an expression for  $(T_F - T_B)$  which when solved for  $q_0$ :

$$Q_0 = 2\pi L r_0 q_0 = \frac{2\pi L (T_F - T_B)}{\left(\frac{1}{r_0 h_0} + K + \frac{1}{r_3 h_3}\right)} \quad (i)$$

$$\text{where } K = \sum_{i=1}^3 \frac{\ln r_i / r_{i-1}}{k_i} \quad (j)$$

Defining an overall heat transfer coefficient based on the inner surface:

$$Q_0 = U_0 (2\pi r_0 L)(T_F - T_B) \quad (k)$$

Combination of equations i and k gives:

$$U_0 = \frac{1}{r_0 \left(\frac{1}{r_0 h_0} + K + \frac{1}{r_3 h_3}\right)} \quad (l)$$

$$\text{where } h_0 = \frac{T_0 - T_3}{r_0 K (T_F - T_0)} \quad (m)$$

$$h_3 = \frac{T_0 - T_3}{r_3 K (T_3 - T_B)} \quad (n)$$

For the reactor used in this system the volume was  $100 \text{ cm}^3$  and the inner wetted surface equal to  $90.9 \text{ cm}^2$ . Table A3-2 shows the values for  $T_0$ ,  $T_3$  and  $T_F$  obtained from experiment 27 and the corresponding values of UA at each temperature.

No correlation of UA with respect to temperature  $T_F$  was detected. An average value of  $0.0044 \text{ cal/sec } ^\circ\text{K}$  with a standard deviation of  $0.0003$  was obtained.

TABLE A3-1. Radii and Thermal Conductivities for the Different Materials that Constitute the Reactor.

<u>Index</u>	<u>Material</u>	<u>Radius (cm)</u>	<u>Thermal conductivity<sup>(69)</sup> g.cal/(Sec cm<sup>2</sup>)(°C/cm)</u>
0	-	2.2	
1	glass	2.35	0.0025835
2	wood	3.25	0.0000379
3	steel	3.75	0.1240096

TABLE A3-2

Temperatures for Estimation of UA.

$T_0$ (°C)	$T_3$ (°C)	$T_F$ (°C)	$UA \times 10^3$ ( $\frac{\text{Cal}(\text{cm}^2)}{\text{Sec}^\circ\text{k}(\text{cm}^2)}$ )
124	145	125	4.815
136	146	138	5.350
155	146	158	3.939
183	146.5	190	4.135
212	147	230	3.816
229	147.5	240	4.288
236	148	255	3.997
242	148.5	250	4.479
244	149.5	251	4.527
244	150	250	4.571
243	150	254	4.347
240	151	245	4.608
239	152	245	4.553
236	152	243	4.494
233	152	240	4.483
229	152	238	4.361
225	151	233	4.399
222	151	232	4.273
219	151	229	4.252
216	151	225	4.287
213	151	220	4.390
210	151	218	4.304
207	149.5	216	4.227
201	149	214	3.912
203	149	211	4.262
200	149	209	4.162
198	148	204	4.377

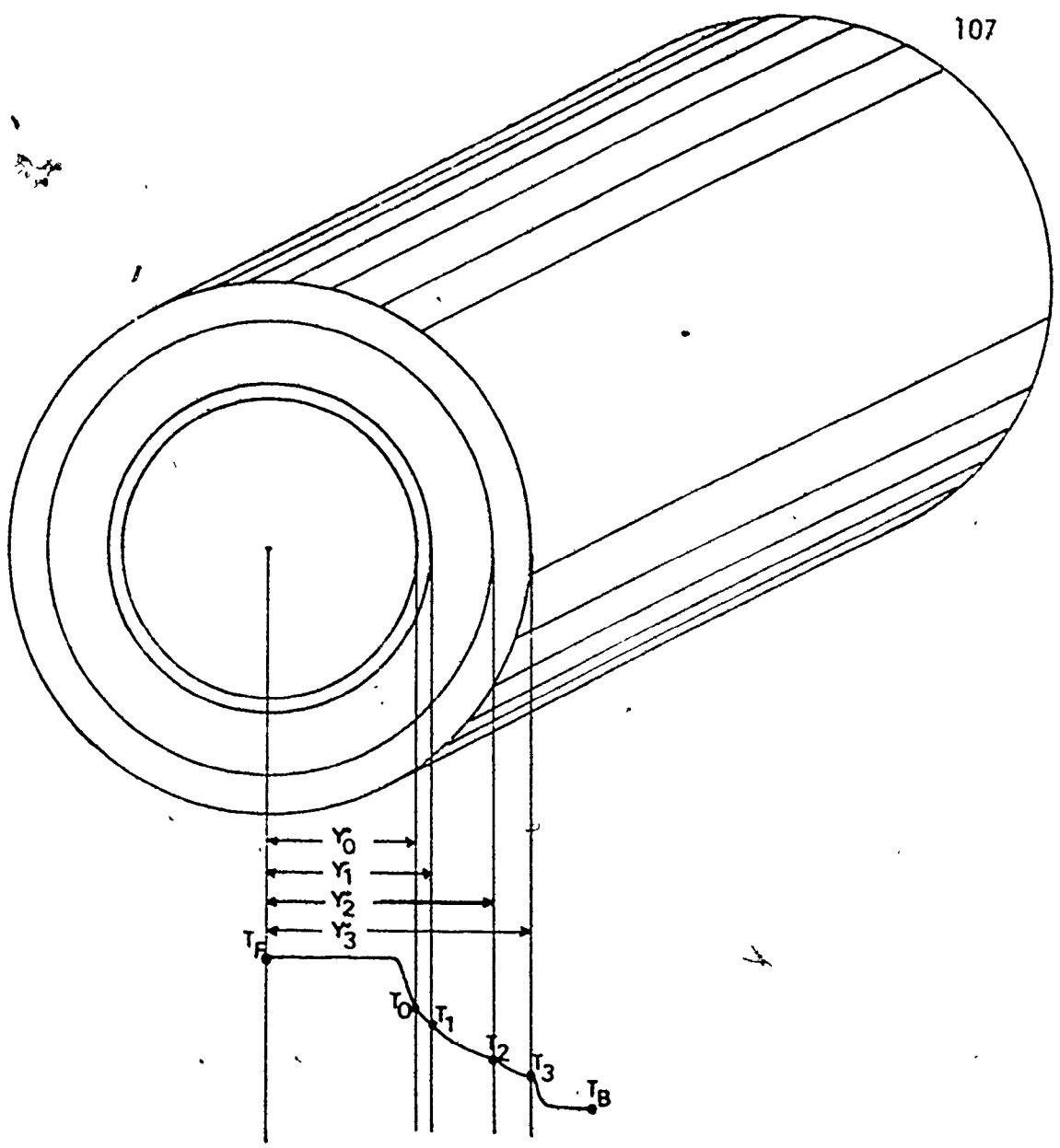


Figure A3.1 : Reactor's composite walls



APPENDIX A4Limiting Conversion as Function of  $T_g$ 

The following treatment follows Horie et al.<sup>(28)</sup> and is presented by Balke and Hamielec<sup>(46)</sup>. It is based on the "Free Volume" theory. Two important relationships involve the effect of the molecular weight on its glass transition temperature,  $T_g$ :

$$T_g = T_{g\infty} - \frac{2\rho_p N \Theta}{\alpha_p \bar{M}_v} \quad (a)$$

and the glass transition temperature of the polymer solution:

$$T_{g_s} = \frac{\{\alpha_p \phi_p T_g + \alpha_m (1 - \phi_p) T_{g_m}\}}{\{\alpha_p \phi_p + \alpha_m (1 - \phi_p)\}} \quad (b)$$

The final volume of the mixture, calculated as:

$$V_f = V_{f_p} \phi_p + V_{f_m} \phi_m \quad (c)$$

$$= [0.025 + \alpha_p (T - T_g)] \phi_p + [0.025 + \alpha_m (T - T_{g_m})] \phi_m \quad (d)$$

At glass transition temperature  $T = T_{g_s}$

$$\frac{dx}{dt} = 0 \quad (e)$$

and  $V_f = 0.025$ , then:

$$\phi_{p \text{ limiting}} = \frac{-\alpha_m (T - T_{g_m})}{[\alpha_p (T - T_g) - \alpha_m (T - T_{g_m})]} \quad (f)$$

and

$$\frac{\phi_p}{1 + \epsilon(1 - \phi_p)} = X \quad (g)$$

Figure A4-1 shows this effect<sup>(70)</sup> for several polymers. No complete conversion can be reached when polymerization is done under the glass

transition temperature of polymer,  $T_g$ .

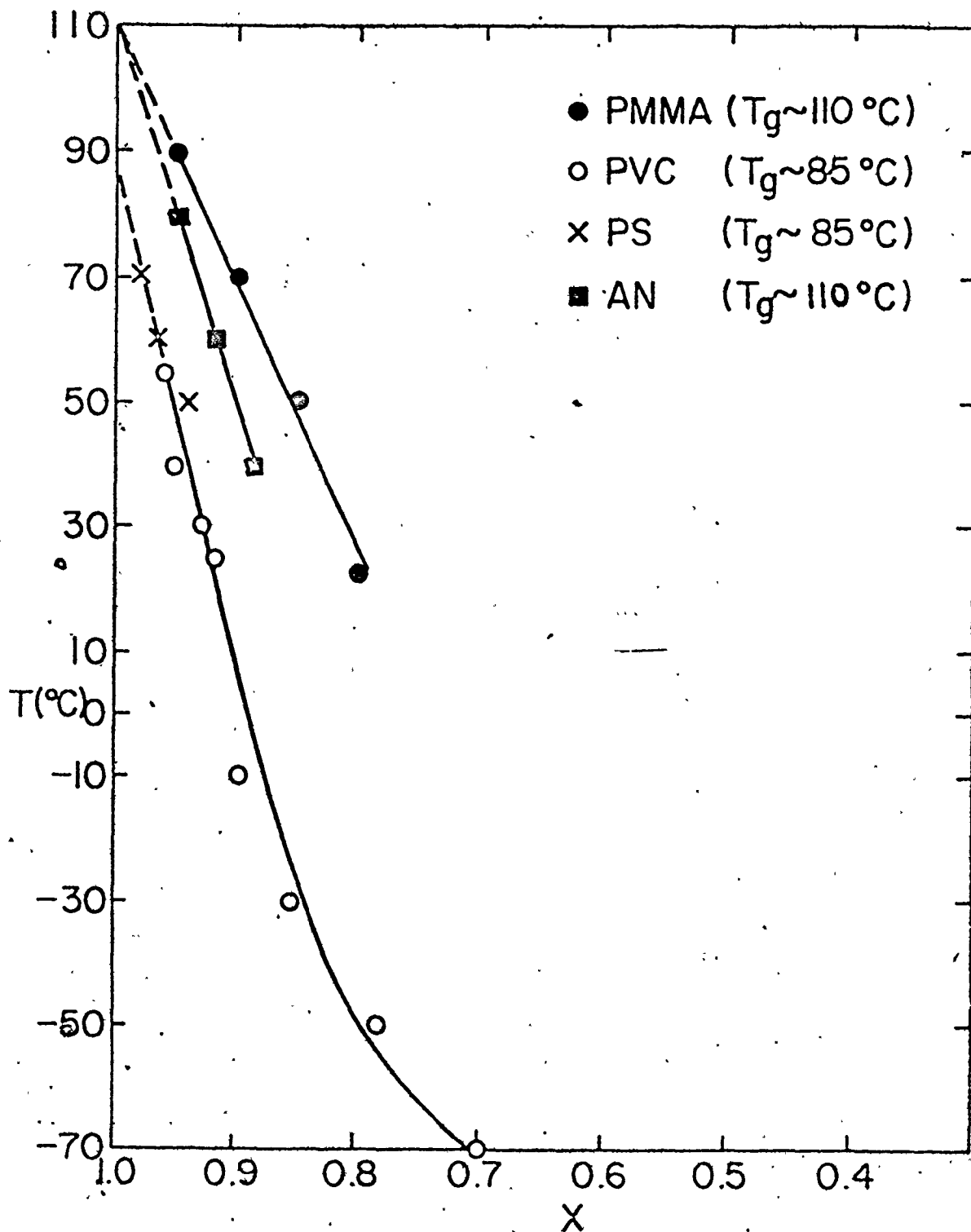


Figure A4.1 : Polymerization Temperature versus limiting conversion for different monomer-polymer systems.

## BIBLIOGRAPHY

1. L.F. Albright, "Processes for Major Addition-type Plastics and their Monomers", McGraw-Hill, 1974.
2. G. Beckmann, Chem. Tech. 3 (5), 304 (1973).
3. J.S. Shastry, L.T. Fan, L.E. Erickson, J. Appl. Polym. Sci. 17, 3101 (1973).
4. V.D. Yenalyev and V.I. Melnichenko, 169th Meeting A.C.S. (1975).
5. R.G. Gleizer, G.I. Faidel, I.A. Khanukayeva and F.A. Shatkhan, Vysokomol. Soed. 16 (9), 1967 (1974).
6. M.E. Sacks, S.I. Lee and J.A. Biesenberger, Chem. Eng. Sci. 28, 241 (1973).
7. L. Miramontes-Vidal and A.E. Hamielec. Unpublished data.
8. R.B. Bishop, "Practical Polymerization for Styrene", Cahners Books, 1971.
9. R.H. Boundy and R.F. Boyer, "Styrene, its Polymers, Copolymers and Derivatives", Hafner Publishing Co., 1970.
10. D.C. Chappellear and R.H. Simon, Polymer Reaction Engineering. Course notes, McMaster University 1976.
11. N. Platzer, I.E.C. 62(1) 6 (1970).
12. W.C. Brassie, Chem. Eng. Progr. 58 (1) 45 (1962).
13. W.J. Boyle, Chem. Eng. Progr. 63 (8) 61 (1967).
14. G.W. Harmon and H.A. Martin, Loss. Prev. 4, 95 (1970).
15. H.A. Duxbury, A.I.Ch.E. 81st Meeting, 1976.
16. J.A. Biesenberger, R. Capinpin and D. Sebastian, Appl. Poly. Symp. 26, 211 (1975).
17. J.A. Biesenberger and R. Capinpin, Polym. Eng. Sci. 14 (11) 738 (1974).
18. J.A. Biesenberger, R. Capinpin and J.C. Yang, Polym. Eng. Sci. 16 (2); 101 (1976).

19. D.H. Sebastian and J.A. Biesenberger, Polym. Eng. Sci. 16, 2 (1976).
20. S.T. Balke; Ph.D. Thesis, McMaster University, 1972.
21. M.H. George, Kin. Mech. Polym. 1 (1) 140 (1967).
22. A.W.T. Hui; Ph.D. Thesis, McMaster University, 1970.
23. A. Husain; M. Eng. Thesis, McMaster University, 1976.
24. H. Staudinger, M. Brunner, K. Frey, P. Goresch, R. Singer and S. Wherli, Ber. 62B, 241 (1929).
25. H. Staudinger and A. Steinhofner, Ann. 571, 35 (1935):
26. Z. Seha and J. Svab, Collect. Czech. Chem. Commun. 32, 4055 (1967).
27. J.N. Cardenas; Ph.D. Thesis, University of Waterloo, 1975.
28. K. Horie, I. Mita and H. Kambe, J. Polym. Sci. A1, 6, 2663 (1968).
29. A.V. Tobolsky, J. Am. Chem. Soc. 80, 5927 (1958).
30. A. V. Tobolsky, C.E. Rogers and R.D. Brickman, J. Am. Chem. Soc. 82, 1277 (1960).
31. F.S. Dainton and K.J. Ivin, Quart. Rev. 12, 61 (1958).
32. K.F. O'Driscoll and P.J. White, Polymer Letters 1, 597 (1963).
33. Z. Tadmor and J.A. Biesenberger, Polymer Letters 3, 753 (1965).
34. S.L. Mardosky, "Thermal Degradation of Organic Polymers", Interscience Publishers, 1964.
35. H.H.G. Jellinek, "Degradation of Vinyl Polymers", Academic Press, 1955.
36. L. Reich and S.S. Stivala, "Elements of Polymer Degradation", McGraw-Hill, 1971.
37. K.E. Weale, Quart. Rev. 16, 267 (1962).
38. M.G. Evans and M. Polanyi, Trans. Faraday Soc. 31, 875 (1935).
39. D.C. Bonner, J. Macromol. Sci. Rev. Macromol. Chem. C 13 (2), 263 (1975).
40. A.A. Zhanov, A.L. Berlin and N.S. Enikolopyan, J. Polym. Sci. C 16, 2313 (1967)

41. F.M. Merret and R.G.W. Norrish, Proc. Roy. Soc. A206, 309 (1951).
42. A.E. Nicholson and R.G.W. Norrish, Discuss. Faraday Soc. 22, 97 (1956).
43. R.M. Joshi and B.J. Zwolinski, Kinet. Mech. Polym. 1(8), 445 (1967).
44. K.J. Ivin, "Macromolecular Chemistry", Butterworth, 1962.
45. J. Frenkel, "Kinetic Theory of Liquids", Dover Publishing Inc., 1955.
46. S.T. Balke and A.E. Hamielec, J. Appl. Polym. Sci. 17, 905 (1973).
47. J.H. Hildebrand and R.L. Scott, "The Solubility of Non-Electrolytes", Dover Publishing Inc., 1964.
48. R.F. Blanks, Chem. Tech. 6 (6) 396 (1976).
49. P.A. Small, J. Appl. Chem. 3, 71 (1953).
50. J.A. Biesenberger and R. Capinpin, J. Appl. Polym. Sci. 16, 695 (1972).
51. J. Brandup and E.H. Immergut, "Polymer Handbook", 2nd ed., John Wiley and Sons, 1975.
52. A. Husain and A.E. Hamielec, in press J. Applied Poly Sci. (1977).
53. A.W.T. Hui and A.E. Hamielec, J. Appl. Polym. Sci. 16, 749 (1972).
54. J.E. Huff, Paper 59d. AIChE Meeting, 1972.
55. A.O. Tonoyan, A.D. Leikin, S.P. Davtyan, B.A. Rozenberg and N.S. Enikolopyan, Vysokomol. Soed. Ser. A16 (8) 1847 (1973).
56. J.H. Arnold, Trans. AIChE 40, 361 (1944).
57. M. Gordon, Trans, Faraday Soc. 44, 196 (1948).
58. J.H. Duerksen, A.E. Hamielec and J.W. Hodgins, AIChE J. 13, 1081 (1967).
59. N. Friis and A.E. Hamielec, Advan. Chrom. 13, 41 (1975).
60. C.W. Gear, Comm. A.C.M. 14, 179 (1971).
61. R.W. Gallant, Hydrocarbon Processing 49, (2) 112 (1970).
62. S. Bywater, J. Polym. Sci. 9, 417 (1952).

63. R.B. Bird, W.E. Stewart and E.N. Lightfoot, "Transport Phenomena", Wiley-Toppan 1960.
64. J.O. Osburn and P.L. Markovic, Chem. Eng. 76,(18) 105 (1969).
65. W. Patnode and W.J. Scriber, J. Am. Chem. Soc. 61, 3449 (1939).
66. K.S. Pitzer, L. Guttman and E.F. Westrum, J. Am. Chem. Soc. 68, 2209 (1946).
67. R.R. Dreibach, "P-V-T Relationships of Organic Compounds", Handbook Press 1952.
68. W.F. Schlegel, Chem. Eng. 88 (March 20, 1972).
69. R.H. Perry and C.H. Chilton, "Chemical Engineers' Handbook", 5th Ed. 1973. McGraw-Hill Book Co.
70. A.E. Hamielec and N. Friis, Polymer Reaction Engineering. Course Notes, McMaster University, 1976.
71. H. Sasaki and M. Nagayama, J. Appl. Polm. Sci. 11, 2097 (1967).